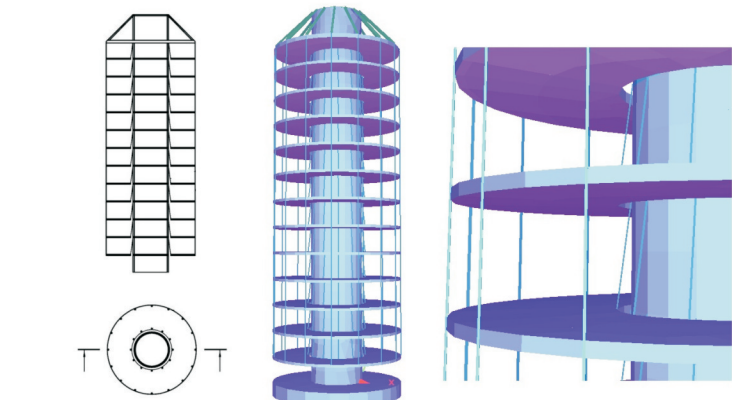


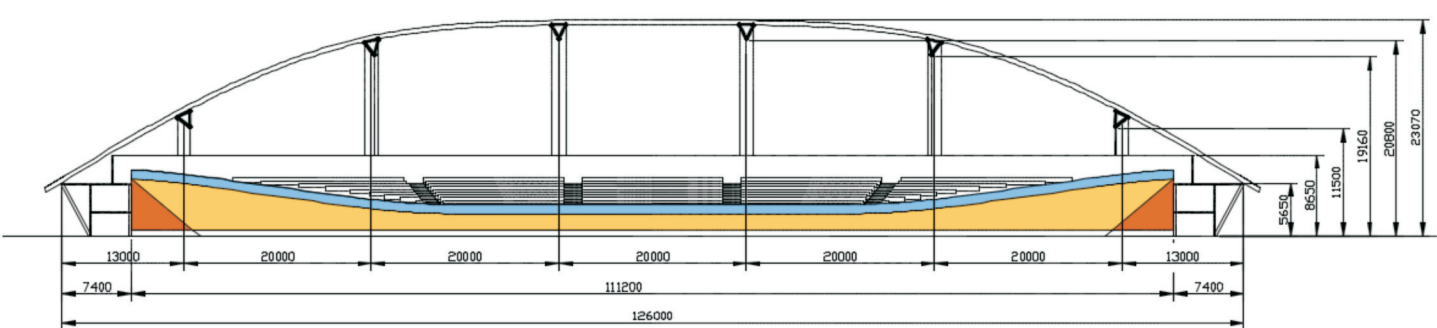
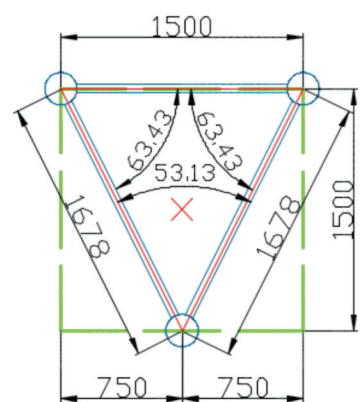
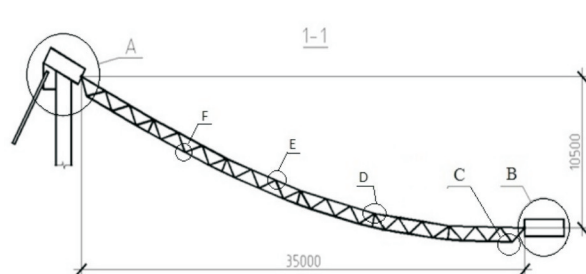
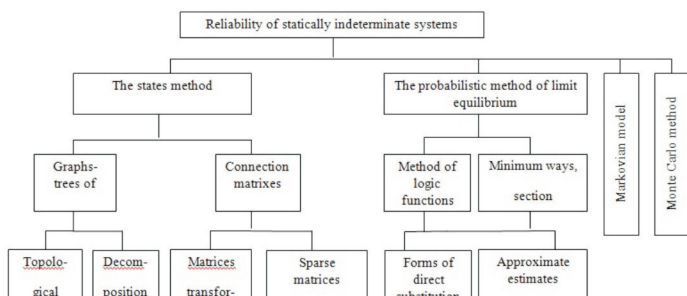
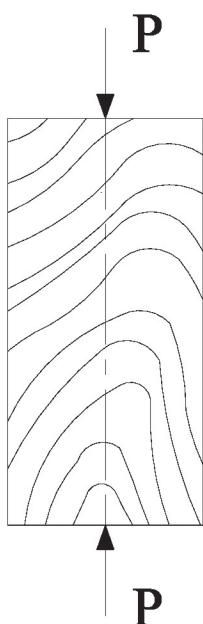
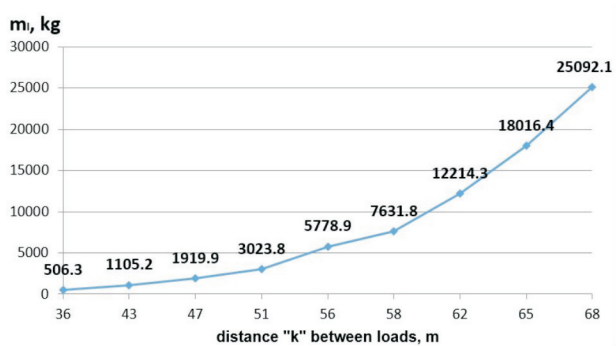


№5(65) 2016

КОНСТРУКЦИИ



МАТЕРИАЛЫ





ПОЛИТЕХ

Санкт-Петербургский
политехнический университет
Петра Великого

**Инженерно-строительный институт
Центр дополнительных профессиональных программ**
**195251, г. Санкт-Петербург, Политехническая ул., 29,
тел/факс: 552-94-60, www.stroikursi.spbstu.ru,
stroikursi@mail.ru**

**Приглашает специалистов организаций, вступающих в СРО,
на курсы повышения квалификации (72 часа)**

Код	Наименование программы	Виды работ*
Курсы по строительству		
БС-01-04	«Безопасность и качество выполнения общестроительных работ»	п.1,2, 3, 5, 6, 7, 9, 10, 11, 12, 13, 14
БС-01	«Безопасность и качество выполнения геодезических, подготовительных и земляных работ, устройства оснований и фундаментов»	1,2,3,5
БС-02	«Безопасность и качество возведения бетонных и железобетонных конструкций»	6,7
БС-03	«Безопасность и качество возведения металлических, каменных и деревянных конструкций»	9,10,11
БС-04	«Безопасность и качество выполнения фасадных работ, устройства кровель, защиты строительных конструкций, трубопроводов и оборудования»	12,13,14
БС-05	«Безопасность и качество устройства инженерных сетей и систем»	15,16,17,18,19
БС-06	«Безопасность и качество устройства электрических сетей и линий связи»	20,21
БС-08	«Безопасность и качество выполнения монтажных и пусконаладочных работ»	23,24
БС-12	«Безопасность и качество устройства мостов, эстакад и путепроводов»	29
БС-13	«Безопасность и качество выполнения гидротехнических, водолазных работ»	30
БС-14	«Безопасность и качество устройства промышленных печей и дымовых труб»	31
БС-15	«Осуществление строительного контроля»	32
БС-16	«Организация строительства, реконструкции и капитального ремонта. Выполнение функций технического заказчика и генерального подрядчика»	33
Курсы по проектированию		
БП-01	«Разработка схемы планировочной организации земельного участка, архитектурных решений, мероприятий по обеспечению доступа маломобильных групп населения»	1,2,11
БП-02	«Разработка конструктивных и объемно-планировочных решений зданий и сооружений»	3
БП-03	«Проектирование внутренних сетей инженерно-технического обеспечения»	4
БП-04	«Проектирование наружных сетей инженерно-технического обеспечения»	5
БП-05	«Разработка технологических решений при проектировании зданий и сооружений»	6
БП-06	«Разработка специальных разделов проектной документации»	7
БП-07	«Разработка проектов организации строительства»	8
БП-08	«Проектные решения по охране окружающей среды»	9
БП-09	«Проектные решения по обеспечению пожарной безопасности»	10
БП-10	«Обследование строительных конструкций и грунтов основания зданий и сооружений»	12
БП-11	«Организация проектных работ. Выполнение функций генерального проектировщика»	13
Э-01	«Проведение энергетических обследований с целью повышения энергетической эффективности и энергосбережения»	
Курсы по инженерным изысканиям		
И-01	«Инженерно-геодезические изыскания в строительстве»	1
И-02	«Инженерно-геологические изыскания в строительстве»	2,5
И-03	«Инженерно-гидрометеорологические изыскания в строительстве»	3
И-04	«Инженерно-экологические изыскания в строительстве»	4
И-05	«Организация работ по инженерным изысканиям»	7

*(согласно приказам Минрегионразвития РФ N 624 от 30 декабря 2009 г.)

**По окончании курса слушателю выдается удостоверение о краткосрочном повышении
квалификации установленного образца (72 ак. часа)**

Для регистрации на курс необходимо выслать заявку на участие, и копию диплома об образовании по телефону/факсу: 8(812) 552-94-60, 535-79-92, , e-mail: stroikursi@mail.ru.

[Http://www.engstroy.spbstu.ru](http://www.engstroy.spbstu.ru) – полнотекстовая версия журнала в сети Интернет.
Бесплатный доступ, обновление с каждым новым выпуском

Инженерно-строительный журнал

НАУЧНОЕ ИЗДАНИЕ

ISSN 2071-4726

Свидетельство о государственной регистрации: ПИ №ФС77-38070,
выдано Роскомнадзором

Специализированный научный
журнал. Выходит с 09.2008.

Включен в Перечень ведущих
периодических изданий ВАК РФ

Периодичность: 8 раз в год

Учредитель и издатель:

Санкт-Петербургский
политехнический университет
Петра Великого

Адрес редакции:

195251, СПб, ул. Политехническая,
д. 29, Гидрокорпус-2, ауд. 227А

Главный редактор:

Вера Михайловна Якубсон

Научный редактор:

Николай Иванович Ватин

Выпускающий редактор:

Екатерина Александровна Линник

Технический редактор:

Ксения Дмитриевна Борщева

Редакционная коллегия:

д.т.н., проф. В.В. Бабков;
д.т.н., проф. М.И. Бальзанников;
к.т.н., проф. А.И. Боровков;
д.т.н., проф. Н.И. Ватин;
PhD, professor M. Вельжкович;
д.т.н., проф. А.Д. Гиргидов;
д.т.н., проф. Э.К. Завадскас;
д.ф.-м.н., проф. М.Н. Кирсанов;
D.Sc., professor M. Кнежевич;
д.т.н., проф. В.В. Лалин;
д.т.н., проф. Б.Е. Мельников;
д.т.н., проф. Ф. Неправишта;
д.т.н., проф. Р.Б. Орлович;
Dr. Sc. Ing., professor
Л. Пакрастиньш;
Dr.-Ing. Habil., professor
Х. Пастернак;
д.т.н., проф. А.В. Перельмутер;
к.т.н. А.Н. Пономарев;
д.ф.-м.н., проф. М.Х. Стрелец;
д.т.н., проф. О.В. Тараканов.

Содержание

КОНСТРУКЦИИ

- | | |
|---|----|
| Гусев Е., Сердюк Д.О., Артебякина Г.И.,
Афанасьева Е.А., Горемыкин В.В. Работа несущих
элементов большепролетного стального покрытия
велодрома (англ.) | 3 |
| Белащ Т.А., Рыбаков П.Л. Здания с подвесными
конструкциями в сейсмических районах (англ.) | 17 |

РАСЧЕТЫ

- | | |
|--|----|
| Прядко Ю.Н., Мущанов В.Ф., Бартоло Х., Ватин Н.И.,
Руднева И.Н. Усовершенствование численных методов
расчета надежности узлов висячих покрытий (англ.) | 27 |
| Кожаева К.В. Расчет оптимизированных способов
засыпки речного подводного трубопровода с
использованием APMWinMachine 9.7 (англ.) | 42 |

МАТЕРИАЛЫ

- | | |
|--|----|
| Бызов В.Е., Мелехов В.И. Увеличение ресурсов
конструкционных пиломатериалов для строительных
конструкций (англ.) | 67 |
|--|----|

© ФГАОУ ВО СПбПУ, 2016

На обложке: иллюстрации авторов к статьям номера

Установочный тираж 1000 экз.

Подписано в печать 01.12.16. Формат 60x84/8, усл. печ. л. 9,5. Заказ № 3333.

Отпечатано в типографии СПбПУ. СПб, ул. Политехническая, д. 29

Контакты:

Тел. +7(812)535-52-47 E-mail: mce@ice.spbstu.ru

Web: <http://www.engstroy.spbstu.ru>

[Http://www.engstroy.spbstu.ru](http://www.engstroy.spbstu.ru) – full-text open-access version in Internet. It is updated immediately with each new issue.

Magazine of Civil Engineering

SCHOLAR JOURNAL

ISSN 2071-4726

Peer-reviewed scientific journal

Start date: 2008/09

8 issues per year

Publisher:

Peter the Great St. Petersburg Polytechnic University

Indexing:

Scopus, Russian Science Citation Index (WoS), Compendex, DOAJ, EBSCO, Google Academia, Index Copernicus, ProQuest, Ulrich's Serials Analysis System

Corresponding address:

227a Hydro Building, 29 Polytechnicheskaya st., Saint-Petersburg, 195251, Russia

Editor-in-chief:

Vera M. Yakubson

Science editor:

Nikolay I. Vatin

Executive editor:

Ekaterina A. Linnik

Technical editor:

Ksenia D. Borshcheva

Editorial board:

V.V. Babkov, D.Sc., professor
 M.I. Balzannikov, D.Sc., professor
 A.I. Borovkov, PhD, professor
 M. Veljkovic, PhD, professor
 E.K. Zavadskas, D.Sc., professor
 M.N. Kirsanov, D.Sc., professor
 M. Knezevic, D.Sc., professor
 V.V. Lalın, D.Sc., professor
 B.E. Melnikov, D.Sc., professor
 F. Nepravishta, D.Sc., assoc. professor
 R.B. Orlovich, D.Sc., professor
 L. Pakrastish, Dr.Sc.Ing., professor
 H. Pasternak, Dr.-Ing.habil., professor
 A.V. Perelmuter, D.Sc., professor
 A.N. Ponomarev, PhD, professor
 M.Kh. Strelets, D.Sc., professor
 O.V. Tarakanov, D.Sc., professor

Contents

STRUCTURES

- | | |
|---|----|
| Gusevs J., Serduks D., Arrebjakina G.I., Afanasjeva E.A., Goremkina V. Behaviour of load-carrying members of velodromes' long-span steel roof | 3 |
| Belash T.A., Rybakov P.L. Buildings with suspended structures in seismic areas | 17 |

CALCULATIONS

- | | |
|---|----|
| Priadko I.N., Mushchanov V.P., Bartolo E., Vatin N.I., Rudniewa I.N. Improved numerical methods in reliability analysis of suspension roof joints | 27 |
| Kozhaeva K.V. Calculation of optimized methods of the river underwater pipeline backfill with the use of APMWinMachine 9.7 | 42 |

MATERIALS

- | | |
|--|----|
| Byzov V.E., Melekhov V.I. Structural sawn timber: resource enhancement | 67 |
|--|----|

© Peter the Great St. Petersburg Polytechnic University. All rights reserved.

On the cover: authors' illustrations

+7(812) 535-52-47

E-mail: mce@ice.spbstu.ru

Web: [Http://www.engstroy.spbstu.ru/eng/index.html](http://www.engstroy.spbstu.ru/eng/index.html)

doi: 10.5862/MCE.65.1

Behaviour of load-carrying members of velodromes' long-span steel roof

Работа несущих элементов большепролетного стального покрытия велодрома

J. Gusevs,
D. Serduks,
Riga Technical University, Riga, Latvia
G.I. Artebjakina,
E.A. Afanasjeva,
*Peter the Great St. Petersburg Polytechnic
University, St. Petersburg, Russia*
V. Goremkins,
Riga Technical University, Riga, Latvia

Студент Е. Гусев,
д-р техн. наук, профессор Д.О. Сердюк,
*Рижский технический университет, Рига,
Латвия*
студент Г.И. Артебякина,
студент Е.А. Афанасьева,
*Санкт-Петербургский политехнический
университет Петра Великого, Санкт-
Петербург, Россия*
д-р техн. наук, ведущий научный сотрудник
В.В. Горемыкин
*Рижский технический университет, Рига,
Латвия*

Key words: arch; wind load; static scheme

Ключевые слова: арка; ветровая нагрузка;
статическая схема

Abstract. Long-span roofs have been of an increased interest within the last sixty years. An arch-type steel roof of velodrome with the maximum span, height, and length equal to 109.50, 23.07, and 126.00 m respectively, is considered as the object of the current investigation. The choice of the preferable structural solution and behaviour analysis of load-carrying members of the long-span arch-type steel roof of the velodrome is considered as the aim of the current study. The distribution of internal forces and stresses in the trihedral lattice steel arch with a triangular web such as displacements under the action of design loads were investigated for fixed, double-hinged, and three-hinged static schemes. It was stated that the preferable structural scheme is the fixed arch.

Аннотация. Большепролетные крыши вызывают повышенный интерес в течение последних шестидесяти лет. Арковидная стальная крыша велодрома с максимальным пролетом, высотой и длиной, равными 109.5, 23.07 и 126 м соответственно, была выбрана как объект исследования. Выбор предпочтительного конструктивного решения и анализ поведения несущих элементов большепролетной арки велодрома является целью исследования. Распределение внутренних усилий и напряжений в элементах стальной арки с трехгранный решеткой, а также перемещения, под воздействием расчетной нагрузки были исследованы для защемленной, двухшарнирной и трехшарнирной статических схем. Было показано, что предпочтительной статической схемой для большепролетной арки является защемленная арка.

Introduction

Long-span roofs have been of an increased interest among civil engineers and architects within the last sixty years [1]. Structures with one span cause a special interest due to the possibility to use the rational internal space for several types of residential and industrial buildings [2]. Sporting halls, indoor swimming pools, velodromes, ice halls, exhibition and concert halls, market halls as well as roofs of railway stadiums, bus stations, and airports are examples of such residential buildings [3]. Buildings in the aircraft industry and plants for producing structures with overall dimensions such as storages of bulked materials are examples of such industrial buildings [4]. The length of the buildings spans changes within the limits from 30 to 70 m [5]. The buildings with especially long spans within the limits from 70 to 300 m are used quite rarely [6, 7]. The interior of the velodrome where spans of the roof's structures change within the limits from 50 to 80 m is shown in Figure 1.

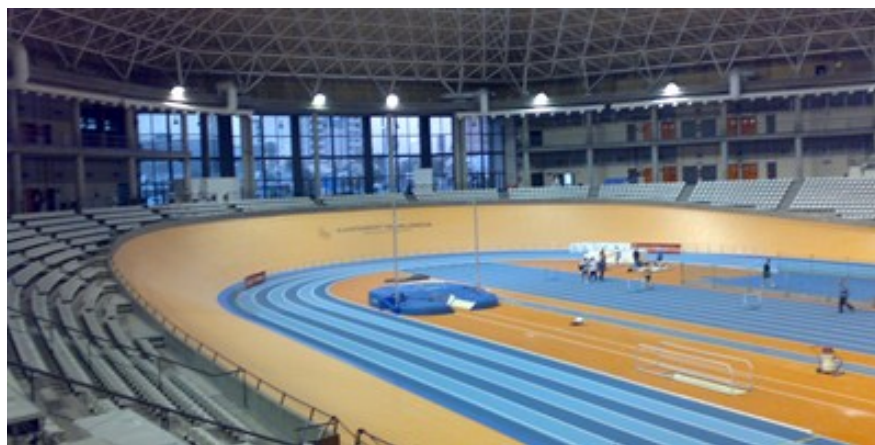
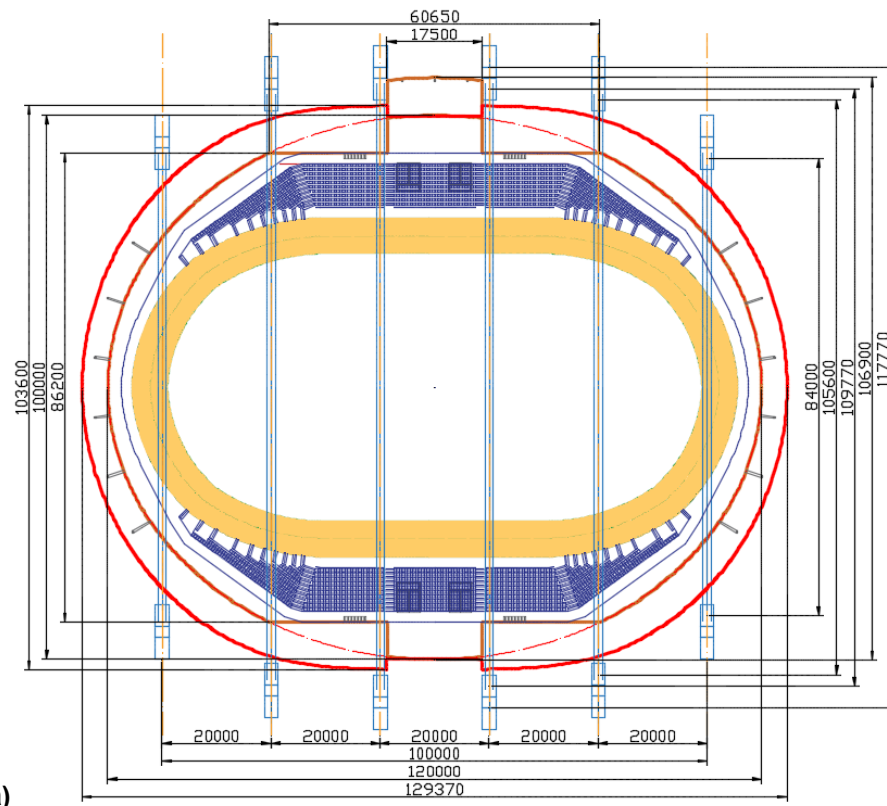


Figure 1. Interior of the velodrome [1]

An arch-type steel roof of the velodrome with the maximum span, height, and length equal to 109.50, 23.07, and 126.00 m respectively, is considered as the object of the current investigation. Steel is considered as a structural material based on the existing experience of implementing similar structures [8]. The choice of the preferable structural solution and behaviour analysis of load-carrying members of the long-span arch-type steel roof of the velodrome is considered as the aim of the current study. The distribution of internal forces and stresses in the main load-carrying structural members such as displacements under the impact of design loads must be investigated in the course of the current study.

Description of the object under investigation

The trihedral lattice steel arch with a triangular web is considered as a main load-carrying structure of the steel roof of the velodrome as the most appropriate for the purposes of this building [8]. The top chord of the trihedral lattice steel arch was formed with two round pipes, but the bottom one was formed with only one. Elements of the arches' lattice are also round pipes. The roofing is based on the main trihedral lattice purlins which has the spans equal to 20 m and is placed with the bay equal to 6 m and additional purlins, which are based on the main ones. Additional purlins have double-tee cross-sections. The purlins also play the role of bracings. The plan of the considered arch-type steel roof and its cross-section are given in Figure 2.



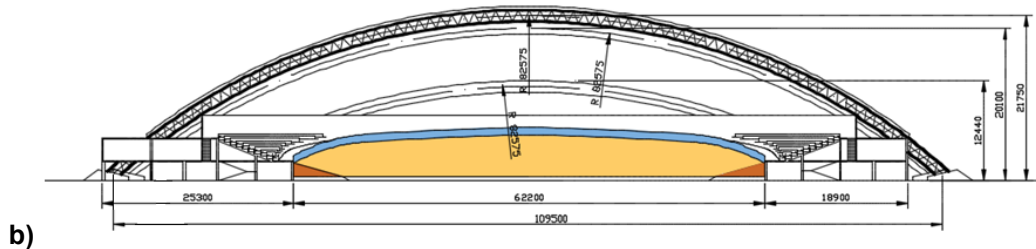


**Figure 2. Plan a) and cross-section
b) of the arch-type steel roof of the velodrome [9]**

The hall of the velodrome is covered with the roof, which is based on six trihedral lattice steel arches with a triangular web. The arches differ in spans and can be divided into three pairs with different spans. The central pair has the maximum span equal to 109.50 m. Two other pairs have spans equal to 105.50 and 84 m. This difference in spans is necessary to provide the elliptical shape of the roof in plan (see Figure 3).

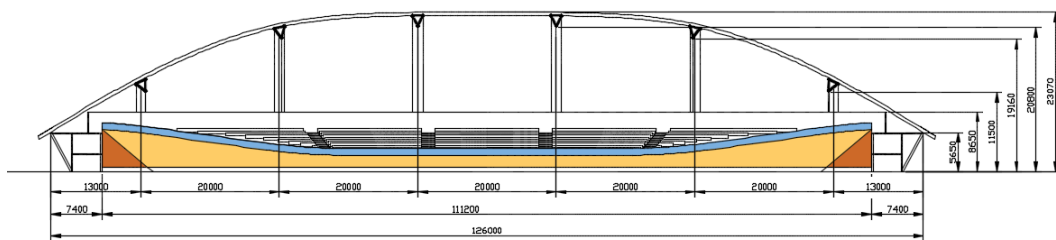


**Figure 3. Section of the arch-type steel roof of the velodrome
in a longitudinal direction [9]**

Cross-sections of the arch in the central pair are placed in a vertical position. Cross-sections of two other pairs are placed with inclination, which is necessary to provide the spherical shape of the roof. The behaviour of the central pair will only be considered in the current investigation because this pair has the maximum span, maximum height, and the heaviest load respectively.

Approach to problem solution

The behaviour of the trihedral lattice steel arch with a triangular web was investigated for a static case of loading [10]. The structure is considered under the impact of permanent (dead weight) and variable loads (snow and wind), which were determined by the recommendation of EN 1991. The choice of the preferable structural solution and behaviour analysis for the trihedral lattice steel arch with a triangular web is carried out for three static schemes [11]: fixed arch, double-hinged arch, and three-hinged arch (see Figure 4).

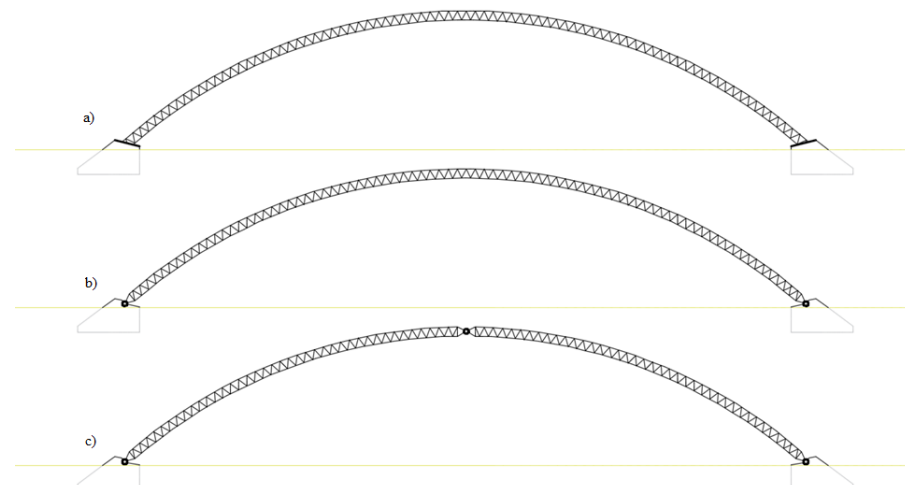


**Figure 4. Static schemes of the trihedral lattice steel arch with a triangular web:
a) fixed arch; b) double-hinged arch; c) three-hinged arch [8]**

Three numerical models were created with the software Autodesk Robot Structural Analysis Professional 2015 to investigate the three mentioned variants of the trihedral lattice steel arch with a triangular web [12]. The current investigation is carried out in the following stages:

- Development of a numerical model of the trihedral lattice steel arch;
- Modelling of load actions(symmetric and asymmetric);
- Global analysis of the trihedral lattice steel arch using the developed numerical model;
- Determination of the elements' cross-sections and correction of the developed model if necessary [13];
- Behaviour analysis with the developed numerical model [14].

Internal forces, strains, and stresses, acting in the elements of chords and lattices, such as displacements of the arch's supports and nodes under the impact of the design static loads should be determined in the course of the current investigation [15]. The comparison of the mentioned behaviour enables choosing the best static scheme of the considered steel arch.

Numerical result

Three variants of the trihedral lattice steel arch with a triangular web with the span, height, and radius of the neutral axis equal to 109.5, 20.75, and 82.58 m respectively, are considered within the current study [8]. The width of the top chord of the arch is equal to 1.50 m. The depth of the trihedral cross-section and the lengths of the side grains are equal to 1.50 and 1.68 m respectively. The distances between the nodes of the top and bottom chords are equal to 1.515 and 1.485 m respectively. The radii of the top and bottom chords are equal to 83.33 and 81.83 m respectively (see Figure 5).

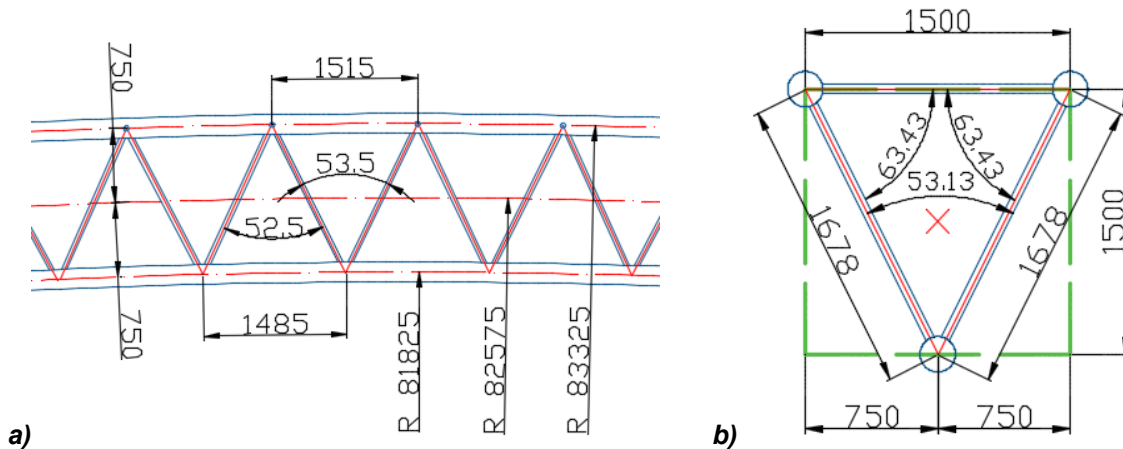


Figure 5. Geometrical scheme of the trihedral lattice steel arch with a triangular web [9]:}
a) dimensions of the arch in the longitudinal direction;
b) dimensions of the arch's cross-section

The length of the arch axis is equal to 119.7 m. Steel of grade S355 is considered as a structural material of the arch [16]. The six steel arches with three different spans are placed with the bay equal to 20 m. The 3D model of the arch-type steel roof is shown in Figure 6.

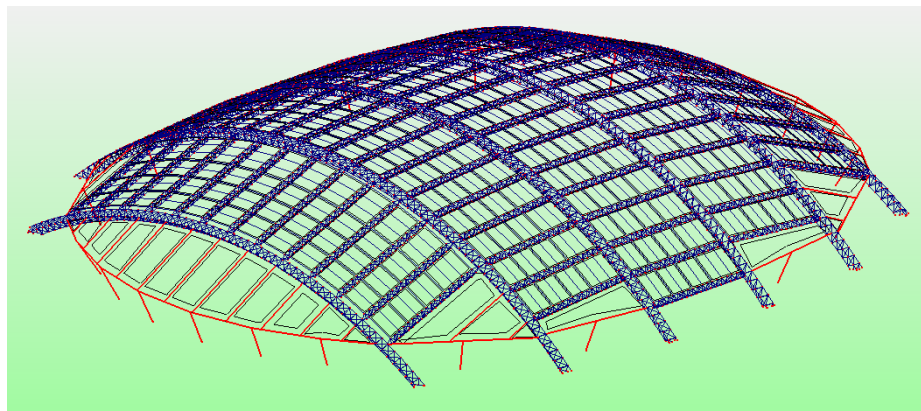


Figure 6. 3D model of the arch-type steel roof [9]

Additional purlins are placed with the bay equal to 2 m. A simple beam is considered as a static scheme of the additional purlins. Cladding panels work in both directions and are based on the main and additional purlins [17].

The structure was analysed at the static action of permanent, snow, and wind loads [18]. Snow and wind loads were determined for the city of Riga. Two variants of the snow load action were considered: undrifted and drifted ones. The design value of the surface snow load was determined by equation 1 [19]:

$$s_d = \mu_3 \cdot C_e \cdot C_t \cdot s_k \cdot \gamma_f \cdot 1,34, \quad (1)$$

where s_k is a characteristic value of the snow surface load; C_e is an exposure coefficient; C_t is a thermal coefficient; γ_f is safety factors; μ_3 shows factors, which allow for the roof's shape influence on the snow load; 1.34 are factors, which take into account the influence of the cladding panels' works on the snow load.

Equation 1 is written for the case of the drifted snow load. Factors μ_3 should be replaced with μ_1 in the case of the undrifted snow load. The characteristic value of the snow surface load was equal to 1.25 kPa. The safety factors were equal to 1.50. The thermal and exposure coefficients both were equal to 1.0. Three variants of the drifted snow load were considered (see Figure 7).

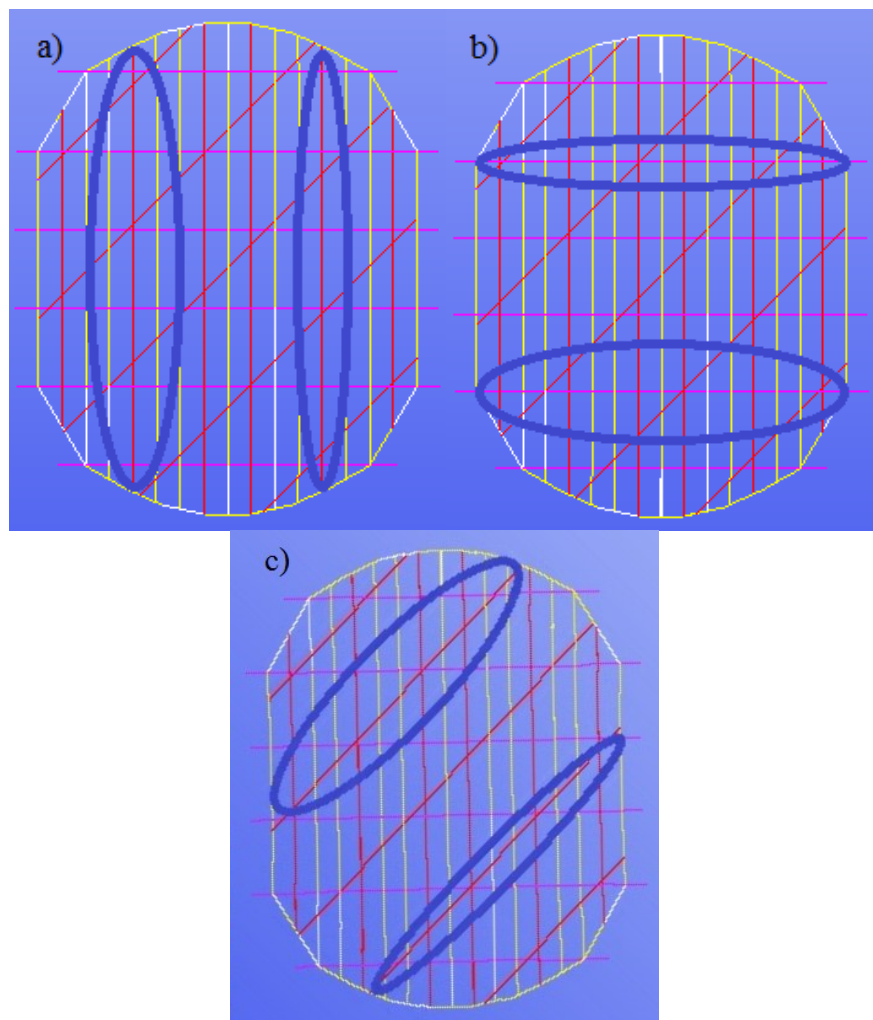


Figure 7. Variants of the drifted snow load: a) wind blows in the longitudinal direction; b) wind blows in the transversal direction; c) wind blows in the diagonal direction [9]

All the variants of snow load were formed under the impact of the wind which blows in the transversal, longitudinal, and diagonal directions respectively [20].

The wind load upon the roof was determined with the software Autodesk Robot Structural Analysis Professional 2015 for the cases when the wind blows in transversal, longitudinal, and diagonal directions which form angles 0°, 45°, and 90° with the longitudinal axis of the structure (see Figure 8) [21].

Гусев Е., Сердюк Д.О., Артебякина Г.И., Афанасьева Е.А., Горемыкин В.В. Работа несущих элементов большепролетного стального покрытия велодрома // Инженерно-строительный журнал. 2016. № 5(65). С. 3–16.

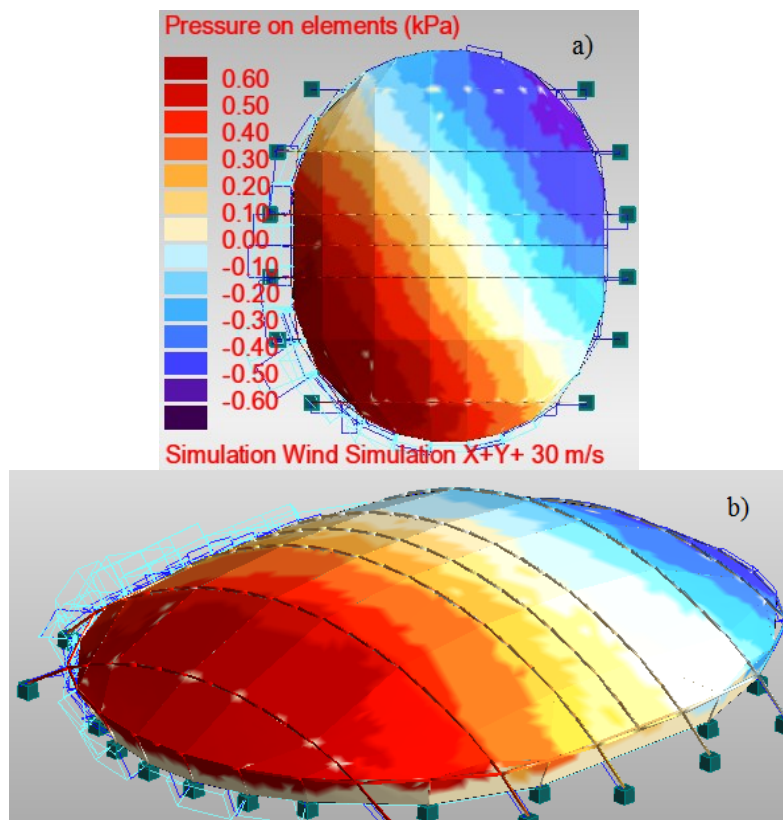


Figure 8. Values of the wind load: a) wind blows in the longitudinal direction; b) wind blows in the transversal direction [9]

The wind load was determined for the basic wind velocity equal to 20 m/s. The corresponding value of the basic wind velocity pressure was equal to 0.24 kPa [22].

The characteristic value of the roofing panels was taken 0.35 kPa [8].

The values of the maximum stresses in the main load-bearing members of the trihedral lattice steel arch were obtained with the software Autodesk Robot Structural Analysis Professional 2015 for the fixed arch, double-hinged arch and three-hinged arch [23]. The values of normal stresses in the bottom chord of the trihedral lattice steel arch are given in Figures 9, 10, and 11 for arches with spans equal to 84, 105.5, and 109.5 m respectively. The values were obtained for the load combination including permanent and accidental snow loads.

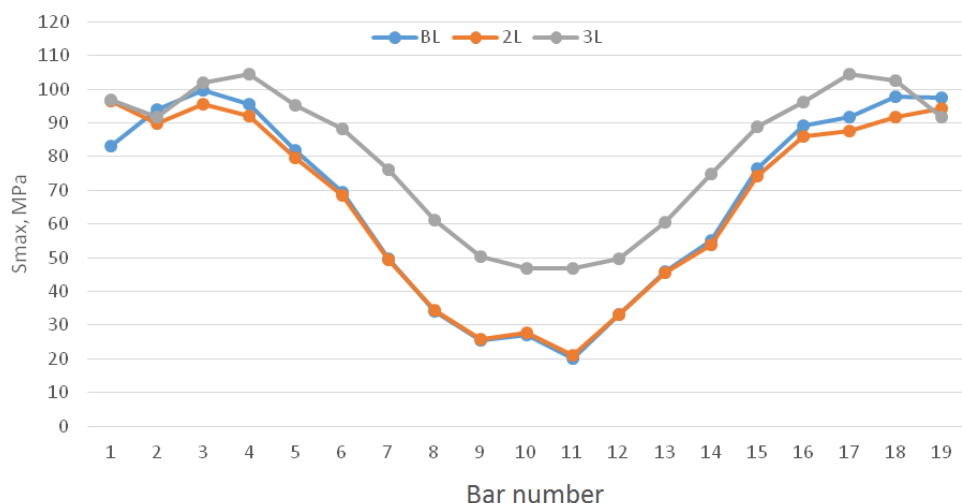


Figure 9. Values of normal stresses in the bottom chord of the trihedral lattice steel arch for the load combination including permanent and accidental snow loads for the arch with the span equal to 84 m; B1 – fixed arch, L2 – double-hinged arch, L3 – three-hinged arch

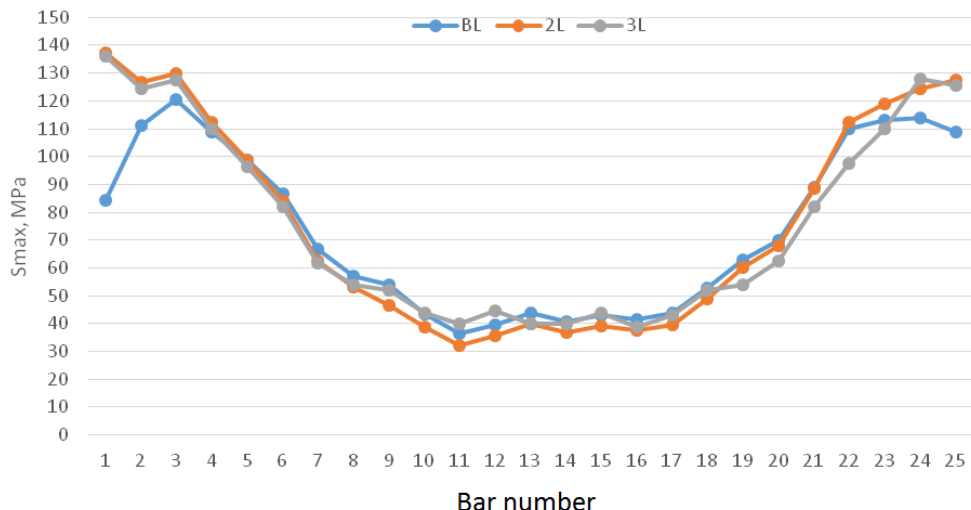


Figure 10. Values of normal stresses in the bottom chord of the trihedral lattice steel arch for the load combination including permanent and accidental snow loads for the arch with the span equal to 105.5 m

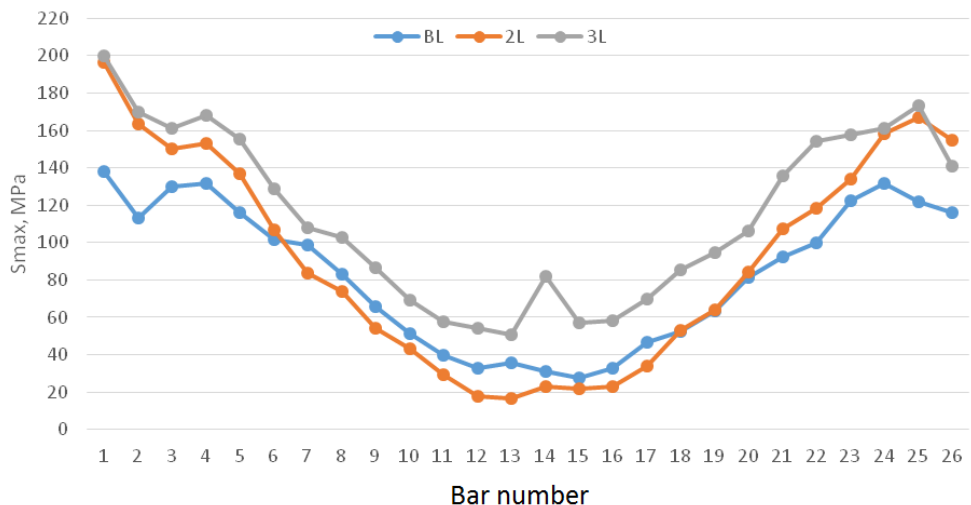


Figure 11. Values of normal stresses in the bottom chord of the trihedral lattice steel arch for the load combination including permanent and accidental snow loads for the arch with the span equal to 109.5 m.

The numeration of the elements is given in Figure 12.

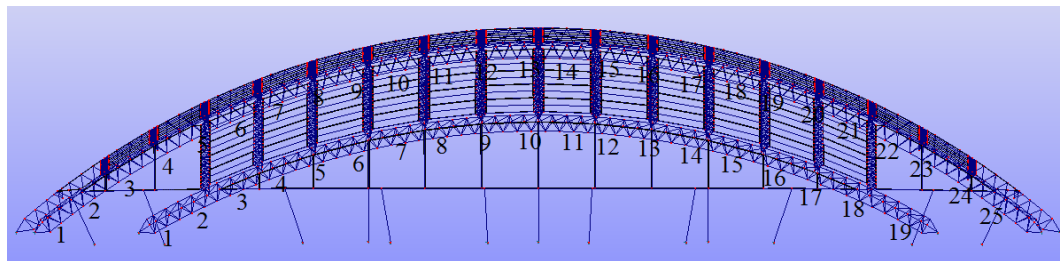


Figure 12. Numeration of elements of the trihedral lattice steel arch [6]

Values of normal stresses in the members of the bottom chord of the trihedral lattice steel arch, with the span equal to 84 m, change within the limits from 20 to 100 MPa, from 20 to 95 MPa, and from 47 to 105 MPa for the fixed, double-hinged and three-hinged arches respectively. The values of normal stresses for the arches with the spans equal to 105.5 and 109.5 m change within the limits from 32 to 138 MPa, and from 19 to 200 MPa respectively. The values of normal stresses in the bottom chord of the trihedral lattice steel arch are given in Figures 13, 14, and 15 for the load combination including the permanent drifted snow load and wind loads.

Гусев Е., Сердюк Д.О., Артебякина Г.И., Афанасьева Е.А., Горемыкин В.В. Работа несущих элементов большепролетного стального покрытия велодрома // Инженерно-строительный журнал. 2016. № 5(65). С. 3–16.

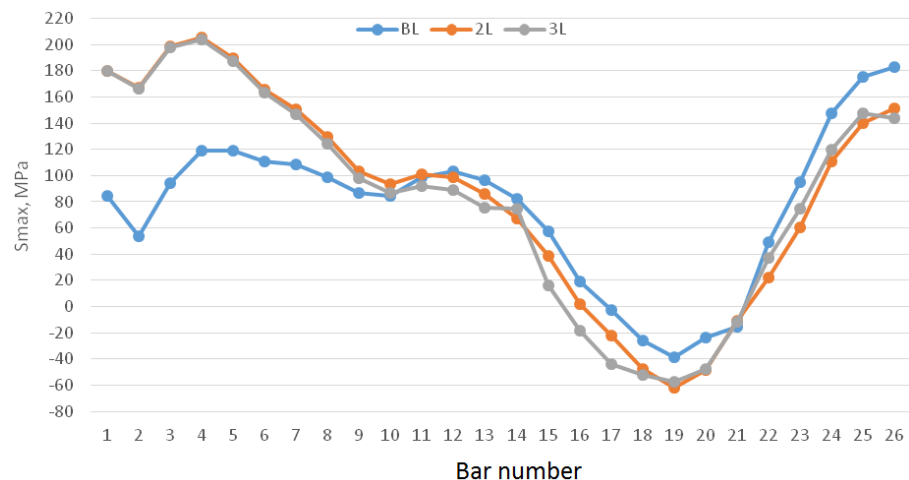


Figure 13. Values of the normal stresses in the bottom chord of the trihedral lattice steel arch for the load combination including the permanent drifted snow load and wind loads for the arch with the span equal to 84 m

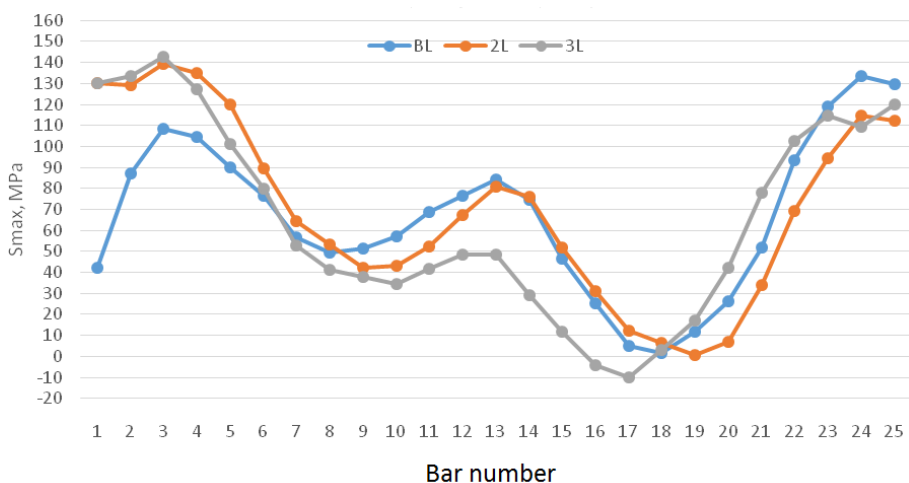


Figure 14. Values of the normal stresses in the bottom chord of the trihedral lattice steel arch for the load combination including the permanent drifted snow load and wind loads for the arch with the span equal to 105.5 m

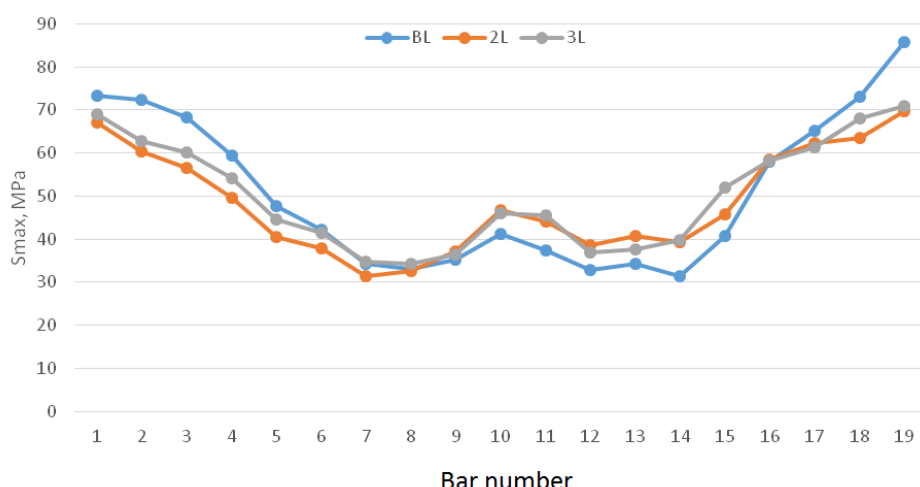


Figure 15. Values of the normal stresses in the bottom chord of the trihedral lattice steel arch for the load combination including the permanent drifted snow load and wind loads for the arch with the span equal to 109.5 m

Values of the normal stresses in the members of the bottom chord of the trihedral lattice steel arch, with the span equal to 84 m, change within the limits from 74 to 85 MPa, from 32 to 72 MPa, and from 35 to 72 MPa for the fixed, double-hinged, and three-hinged arches respectively. The maximum values of normal stresses for the arches with the spans equal to 105.5 and 109.5 m are equal to 142 and 204 MPa respectively. The values of the normal stresses in the bottom chord of the trihedral lattice steel arch are given in Figure 10 for the load combination including the permanent drifted snow load and wind loads. The wind load is acting in the transversal direction.

The distribution of normal stresses between the top and bottom chords of the trihedral lattice steel arch is given in Figures 16, 17, and 18 for the arch with the span equal to 84 m.

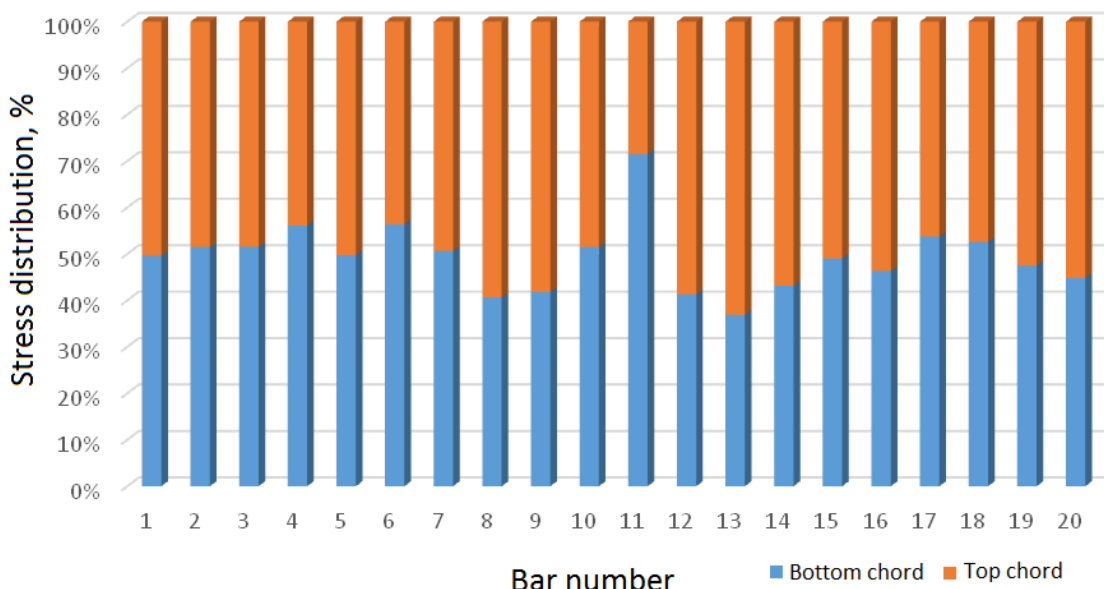


Figure 16. Distribution of normal stresses between the top and bottom chord of the trihedral lattice steel arch with the span equal to 84 m for the load combination including permanent and accidental snow loads for the fixed arch

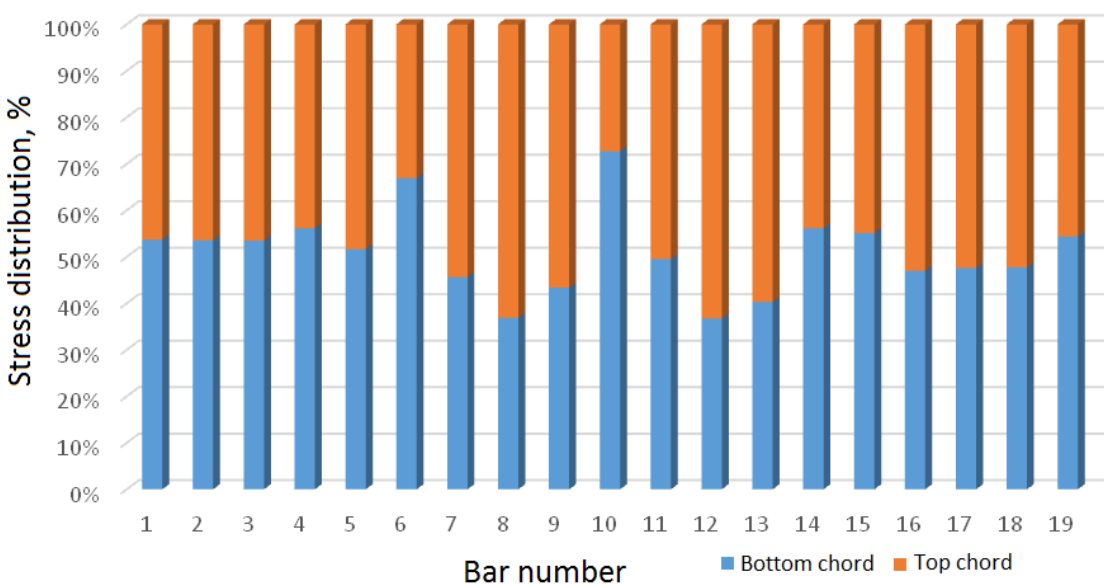


Figure 17. Distribution of normal stresses between the top and bottom chord of the trihedral lattice steel arch with the span equal to 84 m for the load combination including permanent and accidental snow loads for the double-hinged arch

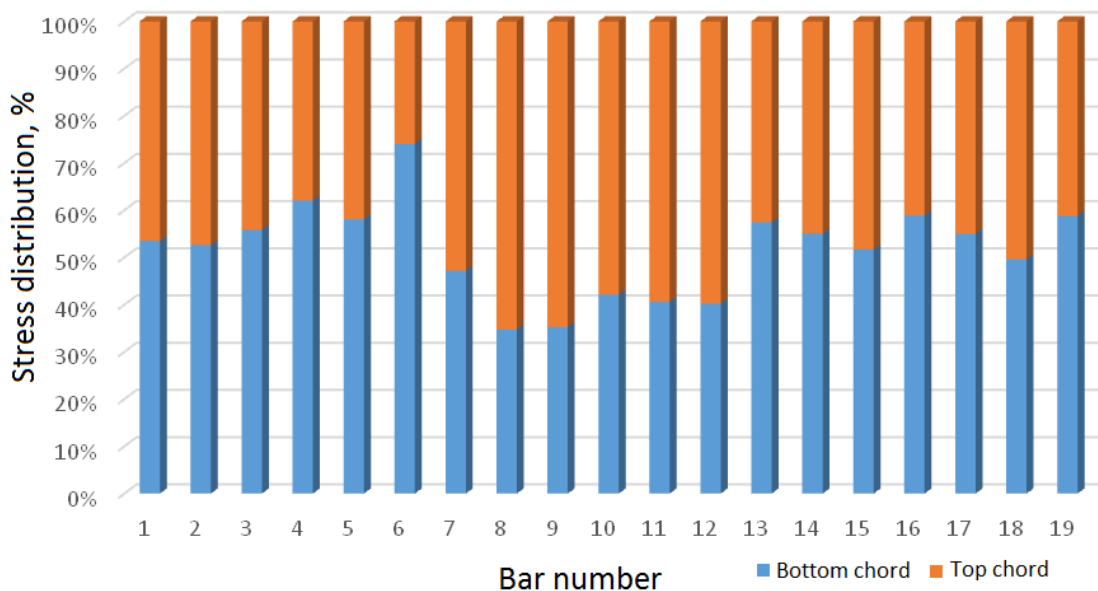


Figure 18. Distribution of normal stresses between the top and bottom chord of the trihedral lattice steel arch with the span equal to 84 m for the load combination including permanent and accidental snow loads for the three-hinged arch

The distribution of normal stresses between the top and bottom chords of the trihedral lattice steel arch with the spans equal to 105.5 and 109.5 m is close to the distribution shown in Figures 16, 17, and 18.

Values of the maximum vertical displacements of the considered steel arches were determined for five load combinations and shown in Figures 19, 20, and 21. The maximum vertical displacements were determined in halves and quarters of the arch spans. The nodes designations, where the maximum vertical displacements were determined, are given in Figure 22.

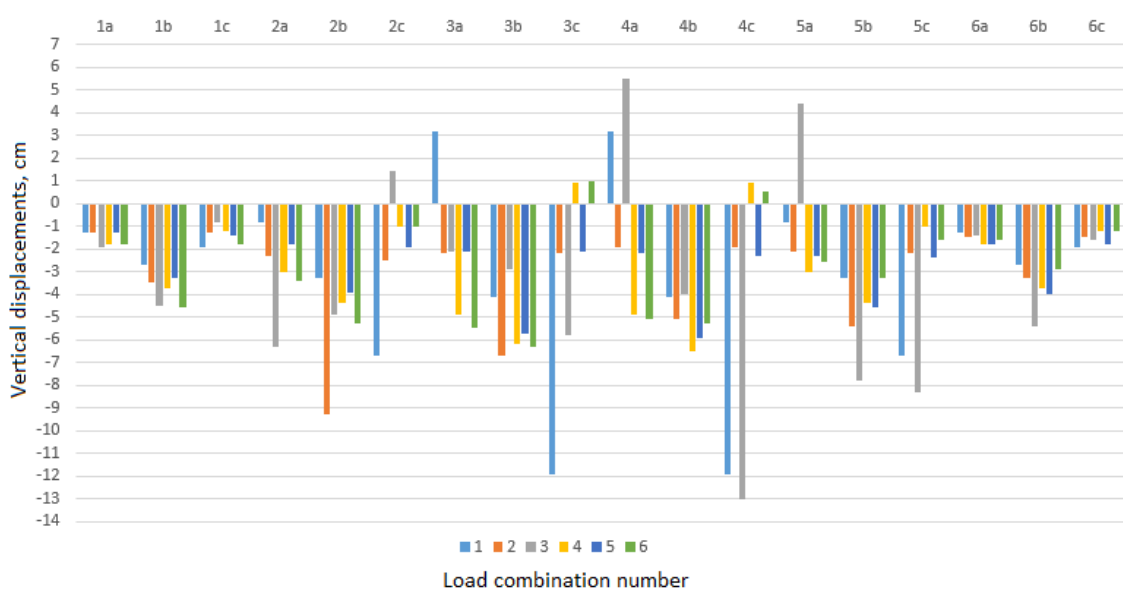


Figure 19. The maximum vertical displacements of the steel arch with the span equal to 84 m for the load combinations including permanent, snow, and wind loads for the fixed arch

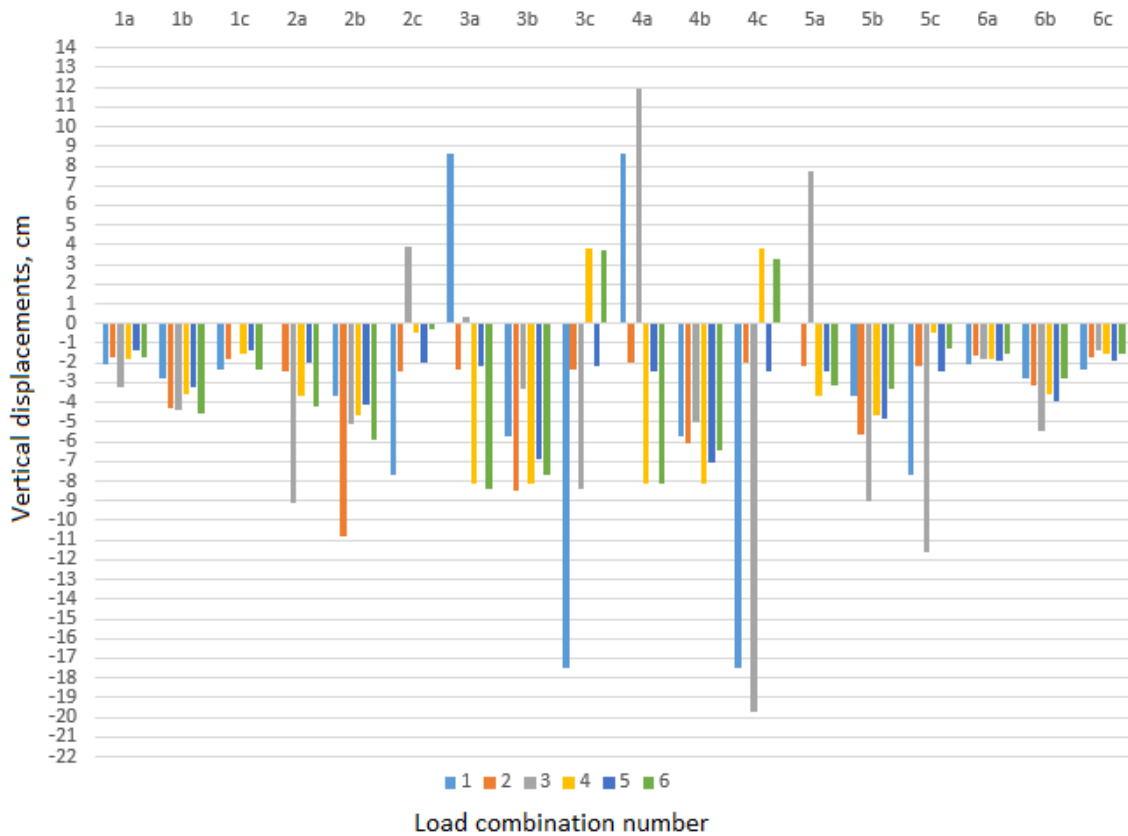


Figure 20. The maximum vertical displacements of the steel arch with the span equal to 84 m for the load combinations including permanent, snow, and wind loads for the double-hinged arch

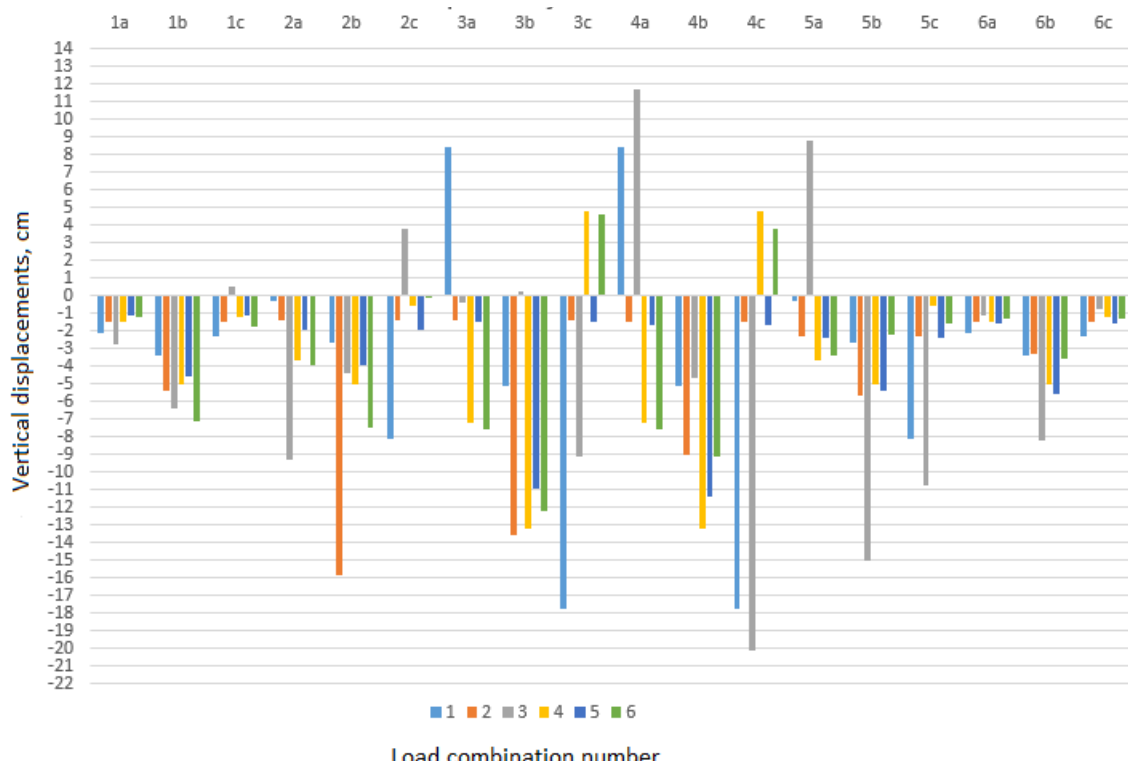


Figure 21. The maximum vertical displacements of the steel arch with the span equal to 84 m for the load combinations including permanent, snow, and wind loads for the three-hinged arch

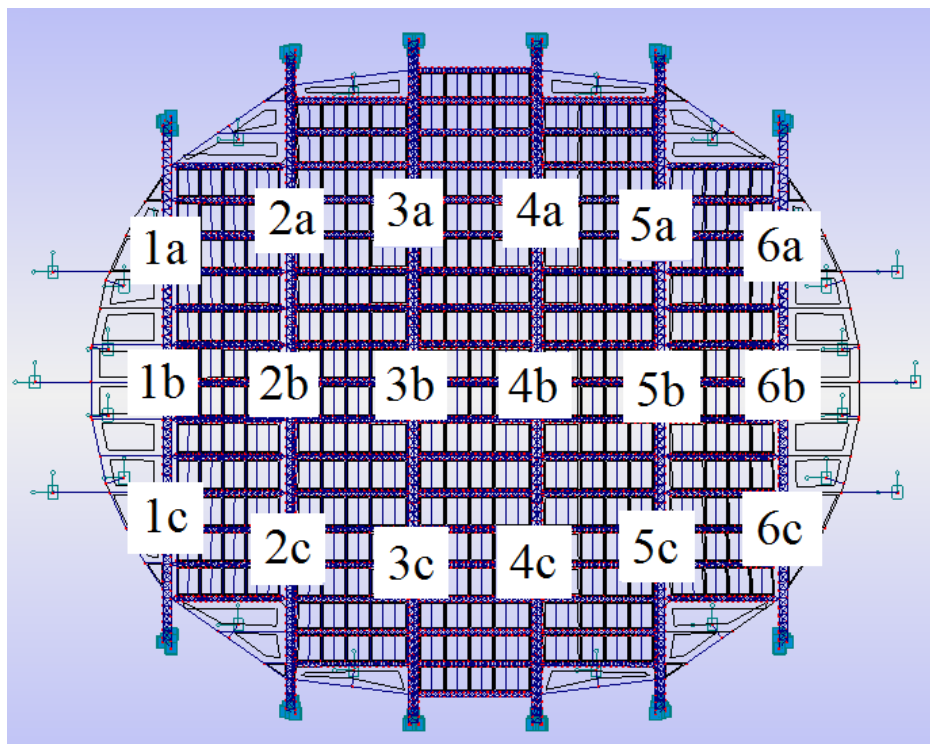


Figure 22. Nodes designations, where the maximum vertical displacements were determined [6]

Five combinations of the loads were formed on the basis of permanent load, drifted and undrifting snow load, and wind, which blows in the transversal, longitudinal, and diagonal directions. The first load combination includes the dead weight of the structure, drifted snow in the longitudinal direction, and wind in the diagonal direction. The second load combination includes the dead weight, undrifting snow load in the longitudinal direction, and wind in the transversal direction. The third load combination includes the dead weight of the structure, drifted snow in the longitudinal direction, and wind in the transversal direction. The fourth load combination includes the dead weight, wind in the diagonal direction, and undrifting snow in the transversal direction. The fifth load combination includes the dead weight, wind in the longitudinal direction, and undrifting snow in the longitudinal direction. The maximum vertical displacements were determined for the fixed arch, double-hinged arch, and three-hinged arch.

The obtained values of the maximum vertical displacements of the steel arches change within the limits of 12 cm up to 20 cm down. The maximum values of the vertical displacements were obtained for the three-hinged arch. The maximum values of the vertical displacements for the double-hinged arch are comparable with the values obtained for the three-hinged arch.

The results of the conducted static analysis allows us to make a conclusion that the preferable structural scheme is the fixed arch.

Conclusions

The structural solution for the arch-type steel roof of the velodrome was chosen. The trihedral lattice steel arch with a triangular web and the maximum span equal to 109.5 m is considered as the main load-carrying structure of the steel roof of the velodrome and as the most appropriate for the purposes of this building. The distribution of internal forces and stresses in the trihedral lattice steel arch with a triangular web such as displacements under the impact of the design loads were investigated for the fixed, double-hinged, and three-hinged static schemes. It was stated that the preferable structural scheme is the fixed arch.

Acknowledgement

The research leading to these results has been funded by Latvia state research programme under the grant agreement "Innovative Materials and Smart Technologies for Environmental Safety, IMATEH". Project Nr.3, PVS ID1854, Task Nr.3.

References

1. Chen W.F., Lui E.M. *Handbook of structural engineering*. New York: CRC Press, 2005. 625 p.
2. Arnold R., Banister C., Weir A., Dabasia D., Goodliffe D. Delivering London 2012: The velodrome. *Proceedings of the Institution of Civil Engineers: Civil Engineering*. 2011. № 164. Pp. 51–58.
3. Ermolov V. *Inzhenernie konstrukcii* [Engineering Structures]. Moscow: High School, 1991. 408 p. (rus)
4. Barabash M., Laznjuk M., Martinova M., Presnjakov N. *Sovremennye tehnologii rascheta i proektirovaniya metallicheskikh i derevyanных konstrukcij* [Modern calculation and design techniques of steel and timber structures]. Moscow: Publisher of Association of building universities, 2008. 328 p. (rus)
5. Wu D., Yang Q., Tamura Y. Estimation of internal forces in cladding support components due to wind-induced overall behaviors of long-span roof structure. *Journal of Wind Engineering and Industrial Aerodynamics*. 2015. No. 142. Pp. 15–25.
6. Sanarskiy V.I. *Tehnologija vozvedenija bolseproletnykh konstrukcij* [Technology of large span structures assembling]: Ucebnnoe posobije. Saratov: Saratovskij gosudarstvennyj tehnicheskij universitet, 2009. 167 p. (rus)
7. Harries A., Brunelli G., Rizos I. London 2012 Velodrome - integrating advanced simulation into the design process. *Journal of Building Performance Simulation*. 2013. No. 6. Pp. 401–419.
8. Macdonald Angus J. *Structure and Architecture*. 2 nd edition. Oxford: Architectural press, 2001. 150 p.
9. Gusev E. *Behaviours Analysis of Load-carrying Members of Long-span Steel Roof*. Riga: RTU, 2015. 109 p.
10. Goremikins V., Rocens K., Serduks D., Pakrastins L., Vatin N. Cable truss topology optimization for prestressed long-span structure. *Advances in Civil Engineering and Building Materials*. 2014. No. 4. Pp. 363–368.
11. Schierle G.G. *Architectural Structures*. Los Angeles: University of Southern California, 2006. 227 p.
12. Tang Z., Xie X., Wang T., Wang J. Study on FE models in elasto-plastic seismic performance evaluation of steel arch bridge. *Journal of Constructional Steel Research*. 2015. No. 113. Pp. 209–220.
13. Kikot A.A., Grigorjev V.V. Vliyanije shiriny poyasa i parametrov stenki na effektivnostj stalnogo tonkostennogo kholodnognutogo profilya Sigma-obraznogo secheniya pri rabote na izgib [Influence of Flange Width and Wall Parameters on Effectiveness of Cold-Formed Steel Sigma-profile in Bending Behaviour. *Magazine of Civil Engineering*. 2013. No. 1. Pp. 97–102. (rus)]
14. Blazevica-Juhnevica O., Serduks D., Ozolins R., Goremikins V., Pakrastins L. Choice of rational parameters of combined structure. *Procedia Engineering*. 2015. No. 117. Pp. 85–93.
15. Vatin N.I., Havula J., Martikainen L., Sinelnikov A.S., Orlova A.V., Salamakhin S.V. Thin-walled cross-sections and their joints: tests and FEM-modelling. *Advanced Materials Research*. 2014. Vols. 945–949. Pp. 1211–1215.
16. Mohamad Al Ali, Isaev S.A., Vatin N.I. Development of Modified Formulae for Detection of Welding Stresses in the Welded Steel Cross-section. *Materials physics and Mechanics*. 2016. No. 26. Pp. 9–15.
17. Hirkovskis A., Serduks D., Goremikins V., Pakrastins L., Vatin N.I. Behaviour analysis of load-bearing aluminium members. *Magazine of Civil Engineering*. 2015. No. 5. Pp. 86–96.
18. EN 1991 Eurocode 1: Actions on structures: part 1-1: Densities, self-weight and imposed loads. Brussels: European Committee for Standardisation. 2002. 47 p.
19. EN 1991-1-3 Eurocode 1: Actions on structures: part 1-3: Snow loads. Brussels: European Committee for Standardisation. 2003. 59 p.
20. Ding Z., Yukio Tamura Y. Contributions of wind-induced overall and local behaviors for internal forces in cladding

Гусев Е., Сердюк Д.О., Артебякина Г.И., Афанасьева Е.А., Горемыкин В.В. Работа несущих элементов большепролетного стального покрытия велодрома // Инженерно-строительный журнал. 2016. № 5(65). С. 3–16.

Литература

1. Chen W.F., Lui E.M. *Handbook of structural engineering*. New York: CRC Press, 2005. 625 p.
2. Arnold R., Banister C., Weir A., Dabasia D., Goodliffe D. Delivering London 2012: The velodrome // Proceedings of the Institution of Civil Engineers: Civil Engineering. 2011. № 164. Pp. 51–58.
3. Ермолов В. Инженерные конструкции. Москва: Высшая школа, 1991. 408 с.
4. Барабаш М., Лазнюк М., Мартынова, М., Пресняков, Н. Современные технологии расчета и проектирования металлических и деревянных конструкций. Москва: Издательство Ассоциации строительных вузов, 2008. 328 с.
5. Wu D., Yang Q., Tamura Y. Estimation of internal forces in cladding support components due to wind-induced overall behaviors of long-span roof structure // Journal of Wind Engineering and Industrial Aerodynamics. 2015. № 142. Pp. 15–25.
6. Санарский В.И. Технология возведения большепролетных конструкций. Саратов: Саратовский государственный технический университет, 2009. 167 с.
7. Harries A., Brunelli G., Rizos I. London 2012 Velodrome - integrating advanced simulation into the design process // Journal of Building Performance Simulation. 2013. № 6. Pp. 401–419.
8. Macdonald Angus J. *Structure and Architecture*. 2 nd edition. Oxford: Architectural press, 2001. 150 p.
9. Gusev E. Behaviours Analysis of Load-carrying Members of Long-span Steel Roof. Riga: RTU, 2015. 109 p.
10. Goremikins V., Rocens K., Serduks D., Pakrastins L., Vatin N. Cable truss topology optimization for prestressed long-span structure // Advances in Civil Engineering and Building Materials. 2014. № 4. Pp. 363–368.
11. Schierle G.G. *Architectural Structures*. Los Angeles: University of Southern California, 2006. 227 p.
12. Tang Z., Xie X., Wang T., Wang J. Study on FE models in elasto-plastic seismic performance evaluation of steel arch bridge // Journal of Constructional Steel Research. 2015. № 113. Pp. 209–220.
13. Кикоть А.А., Григорьев В.В. Влияние ширины пояса и параметров стенки на эффективность стального тонкостенного холодногнутого профиля Сигма-образного сечения при работе на изгиб // Инженерно-строительный журнал. 2013. № 1. С. 97–102.
14. Blazevica-Juhnevica O., Serduks D., Ozolins R., Goremikins V., Pakrastins L. Choice of rational parameters of combined structure // Procedia Engineering. 2015. № 117. Pp. 85–93.
15. Vatin N.I., Havula J., Martikainen L., Sinelnikov A.S., Orlova A.V., Salamakhin S.V. Thin-walled cross-sections and their joints: tests and FEM-modelling // Advanced Materials Research. 2014. Vols. 945–949. Pp. 1211–1215.
16. Mohamad Al Ali, Isaev S.A., Vatin N.I. Development of Modified Formulae for Detection of Welding Stresses in the Welded Steel Cross-section. *Materials physics and Mechanics*. 2016. No. 26. Pp. 9–15.
17. Hirkovskis A., Serduks D., Goremikins V., Pakrastins L., Vatin N.I. Анализ работы несущих элементов из алюминиевых сплавов // Инженерно-строительный журнал. 2015. № 5. С. 86–96.
18. EN 1991 Eurocode 1: Actions on structures: part 1-1: Densities, self-weight and imposed loads. Brussels: European Committee for Standardisation. 2002. 47 p.
19. EN 1991-1-3 Eurocode 1: Actions on structures: part 1-3: Snow loads. Brussels: European Committee for Standardisation. 2003. 59 p.
20. Ding Z., Yukio Tamura Y. Contributions of wind-induced overall and local behaviors for internal forces in cladding

- Snow loads.* Brussels: European Committee for Standardisation. 2003. 59 p.
20. Ding Z., Yukio Tamura Y. Contributions of wind-induced overall and local behaviors for internal forces in cladding support components of large-span roof structure. *Journal of Wind Engineering and Industrial Aerodynamics.* 2013. № 115. Pp. 162–172.
 21. Steenbergen R. The use of Eurocode EN 1991-1-4 for building dynamics under wind load. *Journal of Wind Engineering and Industrial Aerodynamics.* 2014. № 129. Pp. 107–108.
 22. EN 1991-1-4 Eurocode 1: Actions on structures: part 1-4: Wind actions. Brussels: European Committee for Standardisation. 2005. 149 p.
 23. Guo Y., Chen H, Pi Y. Bradford M. In-plane strength of steel arches with a sinusoidal corrugated web under a full-span uniform vertical load: Experimental and numerical investigations. *Engineering Structures.* 2015. № 110, Pp. 105–115.
- support components of large-span roof structure // *Journal of Wind Engineering and Industrial Aerodynamics.* 2013. № 115. Pp. 162–172.
21. Steenbergen R. The use of Eurocode EN 1991-1-4 for building dynamics under wind load // *Journal of Wind Engineering and Industrial Aerodynamics.* 2014. № 129. Pp. 107–108.
22. EN 1991-1-4 Eurocode 1: Actions on structures: part 1-4: Wind actions. Brussels: European Committee for Standardisation. 2005. 149 p.
23. Guo Y., Chen H, Pi Y. Bradford M. In-plane strength of steel arches with a sinusoidal corrugated web under a full-span uniform vertical load: Experimental and numerical investigations // *Engineering Structures.* 2015. № 110, Pp. 105–115.

Jevgenijs Gusevs,
+37112345678; jevgenijs.gusevs@rtu.lv

Dmitrijs Serduks
+37126353082; Dmitrijs.Serduks@rtu.lv

Gulnaz Artebjakina,
kino.i.nemcy@mail.ru

Elizabeth Afanasjeva,
lizik.1993@bk.ru

Vadims Goremkins,
+37129231772; goremkins@gmail.com

Евгений Гусев,
+37112345678;
эл. почта: jevgenijs.gusevs@rtu.lv

Дмитрий Олегович Сердюк
+37126353082;
эл. почта: Dmitrijs.Serduks@rtu.lv

Гульназ Ильшатовна Артебякина,
эл. почта: kino.i.nemcy@mail.ru

Елизавета Андреевна Афанасьева,
эл. почта: lizik.1993@bk.ru

Вадим Валерьевич Горемыкин,
+37129231772;
эл. почта: goremkins@gmail.com

© Gusevs J., Serduks D., Artebjakina G.I., Afanasjeva E.A., Goremkins V., 2016

doi: 10.5862/MCE.65.2

Buildings with suspended structures in seismic areas

Здания с подвесными конструкциями в сейсмических районах

**T.A. Belash,
P.L. Rybakov,**
Petersburg State Transport University,
St. Petersburg, Russia

**д-р техн. наук, профессор Т.А. Белащ,
магистр П.Л. Рыбаков,**
Петербургский государственный
университет путей сообщения
Императора Александра I, Санкт-
Петербург, Россия

Key words: seismic; suspended structures;
oscillations period; finite element method

Ключевые слова: сейсмостойкость;
подвесные конструкции; период колебания;
метод конечных элементов

Abstract. Using suspended structures in construction is one of the methods to improve the earthquake buildings resistance. This subject became very popular in the 60–70s of the 20th century. However, at that time there were no available methods to provide full studies devoted to the buildings of this type. Soon, however, the opportunity appeared due to the development of computer engineering. This caused further analysis and disclosure of the full potential of suspension systems. This article discusses five different structural layouts including using suspended structures. SOFiSTiK computer system was used to calculate them. The time of oscillations was the main criterion to evaluate the schemes. It is well-known that earthquake exposure on the building decreases if the time of oscillations increases. It was found that the time of oscillations of the buildings with suspended structures is greater by several times in comparison with the buildings with traditional structural system. Taken into consideration the given fact, we can suggest that the efficiency of suspension systems in seismic conditions is provided.

Аннотация. Использование подвесных конструкций в строительстве, является одним из способов повышения сейсмостойкости зданий. Данная тема получила наибольшую популярность в 60–70х годах 20 века. Однако в то время не существовало доступных методов для полноценного исследования зданий такого типа. В результате развития вычислительной техники, такая возможность появилась. Это послужило причиной дальнейшего анализа и раскрытия всего потенциала подвесных систем. В статье рассмотрено пять различных конструктивных схем зданий, в том числе с использованием подвесных конструкций. Для их расчёта использовался программно вычислительный комплекс SOFiSTiK. Основным критерием оценки схем стал период собственных форм колебания. Как известно, при увеличении периода, уменьшается сейсмическая нагрузка, действующая на здание. Было выявлено, что период колебания у зданий с подвесными конструкциями в несколько раз больше, чем у зданий с традиционной конструктивной системой. Этот факт позволяет говорить о том, что эффективность подвесных систем в условиях сейсмики обеспечивается.

Introduction

Increased seismic stability of buildings can be achieved in various ways. There are many approaches designed to handle this challenging task in Russian and global practice. One of them is the search for the most efficient and reliable structural systems among which buildings with suspended structures form a separate group. Suspended systems of buildings are characterized by a variety of geometric shapes that depends on installation methods, cost, the duration of erection, and space and layout requirements. The solutions put forward by Russian experts to increase seismic stability through the use of suspended structures have been previously reflected in the works by I.L. Korchinsky, N.N. Skladnev, G.Sh. Chanukvadze, P.I. Ostromensky, I.I. Grigorieva [1–6].

Most of the research in this area was conducted in the 60–70s of the 20th century. During the same period some suspended-type buildings were erected both in earthquake-prone and in safe areas of the globe – in Antwerp, Mexico City, Vancouver, London, Munich, Madrid, Minneapolis (USA), Kota Kinabalu (Malaysia) [7–14]. In 1979, American expert Wolfgang Schuller was the first who codified the

classification of suspended systems [15]. The rigid shaft principle is applied in the design of most suspended buildings.

Although experts from Russia and the former USSR were also conducting some research and searching for solutions of buildings with suspended structures, none of them was built. One of such solutions was a suspended building proposed and patented by I.L. Korchinsky in 1971. In this model, loads are transferred from floors to the foundation entirely through trusses located at the top of the shaft. Seismic stability increased due to the fact that the structure design was fitted out with extra dampers placed at the points where suspensions were attached to trusses and at the points where trusses were supported by the shaft (Fig. 1) [1].

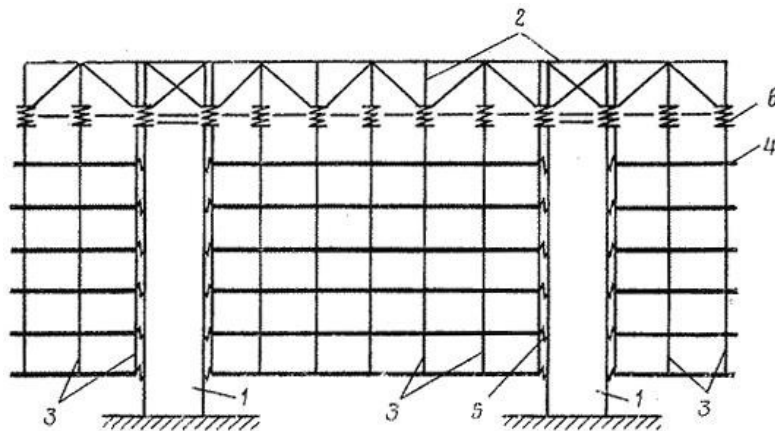


Figure 1. Suspended building: 1 – reinforced concrete shaft; 2 – double-cantilever trusses; 3 – suspensions; 4 – suspended floors; 5 – dampers in the form of elastic links; 6 – extra dampers

In 1976, G.Sh. Chanukvadze developed another model of an earthquake-proof building with suspended structures. The complicated damper system was considered to be the main drawback of the building option proposed by I.L. Korchinsky.

In the proposed solution, suspensions were made prestressed and junctions of floors and the central core – rigid and swivel with floor-by-floor alternation (Fig. 2). Thus, loads were transferred to the foundation partly through the shaft truss and partly through cantilevered supports on the shaft itself. According to the author, this design was to reduce arising forces affecting the building and caused by wind and seismic effects [3].

Afterwards, the model was further refined by its authors in order to avoid possible resonance in the event of heavy earthquakes. For this purpose, suspensions anchored in the foundation were equipped with shutoff links (Fig. 3) [4].

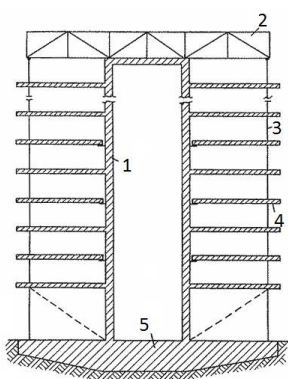


Figure 2. Suspended building: 1 – core; 2 – truss; 3 – suspensions; 4 – floors; 5 – foundation

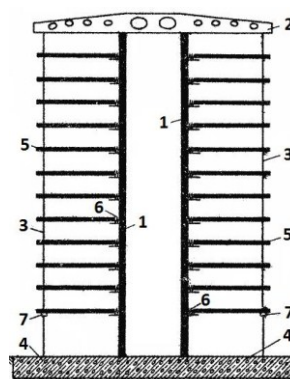


Figure 3. Suspended building: 1 – core; 2 – truss; 3 – suspensions; 4 – foundation; 5 – floors; 6 – pivots; 7 – shutoff links

N.N. Skladnev, an expert of the Central Research Institute of Construction Structures named after Kucherenko [2], made a great contribution to the study of the operation of suspended systems in seismic conditions.

Belash T.A., Rybakov P.L. Buildings with suspended structures in seismic areas. *Magazine of Civil Engineering*. 2016. No. 5. Pp. 17–26. doi: 10.5862/MCE.65.2

Currently, the development and construction of buildings with suspended structures are almost abandoned. The reason for this may be the fact that the solutions proposed previously have proved to be difficult to implement on the engineering side. In addition, calculation methods that existed before the 90s could not fully reflect the nature of effects of the seismic impact. Consequently, the study of these systems was suspended.

However, along with increasingly sophisticated computer technologies and increased capacities of electronic computers, methods to calculate mathematical models are being elaborated as well. Computing complexes are continuously emerging and they are being updated. They are capable to perform the most complicated tasks in the field of dynamic linear and nonlinear oscillations.

SOFiSTiK is one of such complexes. There is a wide range of design and load simulation capabilities among the features of SOFiSTiK. Another advantage of this complex is a possibility to work with macros that allow you to make adjustments to any computation module by using programming language CADINP [16].

State-of-the-art capabilities of this computation complex enable us to proceed with research into the system of buildings with suspended structures that is somewhat abandoned, but not very explored.

Research objective was carrying out the comparative analysis of dynamic parameters (the period and the frequency of natural oscillations) buildings with suspended constructions.

Methods

One of the most common building configurations in the form of a cantilevered cap on a single shaft in the shape of a cylinder as per the classification by Wolfgang Schuller was taken to pursue the research [15]. The chosen shape corresponds to several basic theses of the efficient configuration of buildings in seismic areas [17]. Then, five options of computational schemes were selected. Each of them was distinguished by different structural solutions affecting dynamic characteristics of a building. The work took into consideration the experience of Russian experts in the field of automated computation [18, 19]. The standard module "Natural modes and frequencies" of SCC SOFiSTiK was used to determine the frequency.

As is well-known, in current standards the value of seismic load for the i -th mode of natural oscillations of buildings or facilities – S_{0ik}^j – is conventionally calculated by the following formula:

$$S_{0ik}^j = gm_k^j A K_A \beta_i K_\psi \eta_{ik}^j$$

where m_k^j – the mass of the building or the moment of inertia of the corresponding mass of the building; g – acceleration due to gravity; A – the factor which values should be taken on the basis of the estimated seismicity; K_A – the factor which value should be taken depending on combinations of the estimated seismic intensity; β_i – the dynamic factor corresponding to the i -th mode of natural oscillations of buildings or facilities; K_ψ – the damping factor; η_{ik}^j – the factor depending on the mode of building or facility deformation under its natural oscillations by the i -th mode.

The value of the dynamic factor β_i should be taken as per the graph (Fig. 4) depending on the estimated period of natural oscillations T_i of a building or facility by the i -th mode.

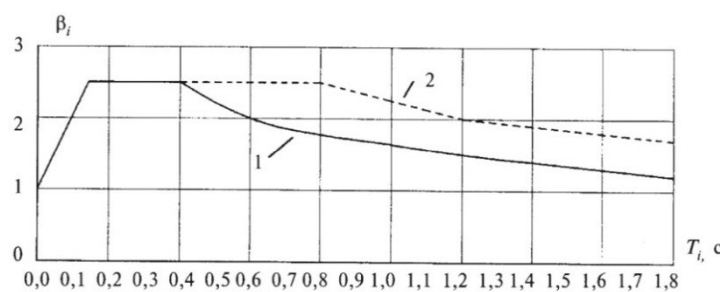


Figure 4. Dependence of the dynamic factor on the period of natural oscillations:
1 – curve for soils of Category I and II; 2 – curve for soils of Category III

The graph shown above clearly illustrates that the dynamic factor decreases along with an increase in the natural oscillation period that ultimately reduces the seismic load. This fact is a stimulus for low-frequency adjustment of a building, which can be implemented in particular due to the introduction

of suspended structures. Therefore, at the first stage of the research, the period of natural oscillations was the key parameter that determined efficiency of the considered schemes.

Results and Discussion

The first scheme of the building has a conventional shaft system without the use of special means to ensure seismic protection. In this scheme, the load is transferred from floors to the foundation through the rigid reinforced concrete shaft and metal H-columns placed along the perimeter. In the first scheme as in the rest, the foundation is taken as a solid slab. Figure 5 shows the computational scheme of the building and its model from the software complex SOFiSTiK.

The standard module "own forms and frequencies" was used to determine the frequency of own forms of oscillations. The calculation was made by the ASE module with a choice of the following parameters: the number of forms of oscillations – 6, the computation was carried by Lantsosh's method, the attenuation factor according to Rayleigh was accepted by-5%. Columns, plates, beams – slabby, rod and beam terminal elements were used for the bearing structural elements.

The model of the building has 13 floors, the height of the floor is accepted by 4 m, the diameter of a trunk is equal to 8 m, the external diameter is equal to 20 m. The walls of a kernel and overlapping are made of monolithic reinforced concrete 0.3 m thick. Sixteen metal columns which are replaced further with guys are located on perimeter of the building. The base is executed in the form of a monolithic reinforced concrete plate 2 m thick, with a diameter of 20 m. The console grillage at building top holding guys is executed in the form of a reinforced concrete plate 0.6 m thick. He is supported by inclined metal beams on trunk tops.

For reinforced concrete designs B 25 concrete and A 400 fittings is accepted. Columns are made of steel C 245 with a profile 20K2. This model was used for comparison with other settlement schemes.

The computation of this scheme made it possible to determine its oscillation period equal to 1.08 seconds.

The second scheme is similar to the first one, but it still differs from it since it has a seismic isolation system represented by rubber-metal supports (RMS) installed in the foundation. The principle of this system operation consists in increasing the period of natural oscillations of structures thereby the seismic load on the building decreases.

To consider the operation of the seismic isolation system, another foundation slab was included into the model at the distance of 1m from the first. Point links were arranged between the slabs simulating RMS operation, which enable us to secure the element not pivotally but movably along its axes with the required rigidity. Lateral rigidity of rubber-metal supports is much less than longitudinal thereby they allow the structures mounted on them to oscillate horizontally while remaining at the design elevation. This RMS property was taken into account when setting the parameters of Point links. The oscillation period of a building of this scheme amounted to 2.49 seconds.

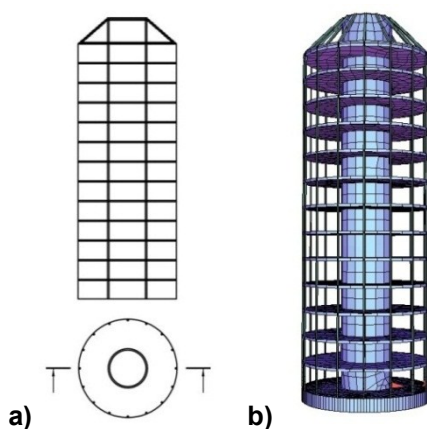


Figure 5. First computational scheme:
a) structural layout; b) computational model of SOFiSTiK program

Figure 6 shows the features of the scheme and computational model.

The third scheme was drawn up considering the operation of the system of suspended structures. When modeling all schemes of this type, the specificity of cable-stayed structures described in various Belash T.A., Rybakov P.L. Buildings with suspended structures in seismic areas. *Magazine of Civil Engineering*. 2016. No. 5. Pp. 17–26. doi: 10.5862/MCE.65.2

works was taken into consideration [20–32]. For the comparative analysis of all five schemes to be objective, the building configuration was retained and the columns were replaced with cable stays. In this scheme, the load was transferred from floors to the foundation according to the type of suspended building by Chanukvadze G.Sh. [3] – partly through cable stays and grillage at the shaft top, partly through cantilevered supports on the shaft itself. Grillage means a space structure holding cable stays and consisting of a reinforced concrete slab, sloping metal beams and continuation of the shaft walls.

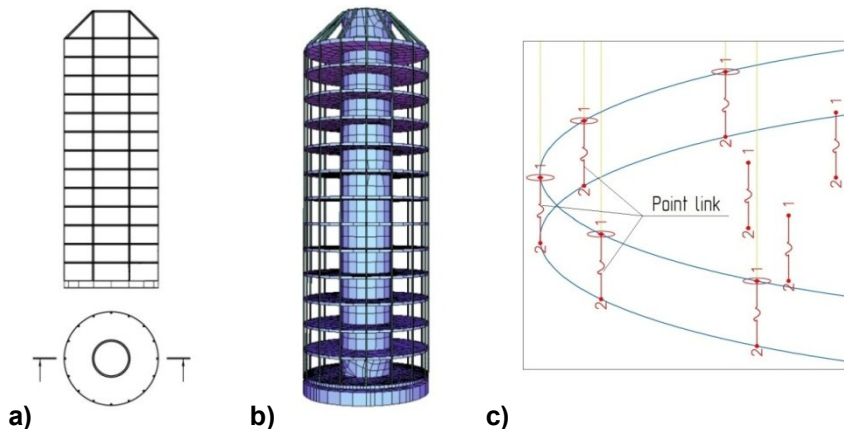


Figure 6. Second computational scheme:
a) structural layout; b) computational model of SOFiSTiK program;
c) display of Point links in SOFiPLUS preprocessor

The units where floors were supported by the shaft were made by means of an elastic link element – Point link. The operating principle of these elements remained the same as in the previous scheme. Each floor disc was supported at 16 link points having lateral rigidity much less than longitudinal which enabled the floor discs to oscillate relatively freely in the horizontal direction. Figure 7 shows the scheme of the floor support unit and its representation in SOFiPLUS. Figure 8 shows the computational scheme and model of the third option.

The scheme parameters are dependent on the lateral rigidity of supports, which can vary depending on the desired period of the model oscillation. As it has been said above, the seismic load decreases along with the decrease in the dynamic factor, consequently, the maximum period of oscillation is the most efficient [33–36].

To determine the dependencies and search for an option with the greatest period, the lateral rigidity of each support varied from 25 kN to 175 kN in increments of 25 kN. The variation range was taken considering the actual rigidity of support elements. The period ranged from 4.83 to 2.13 seconds. Since a floor disc was supported by 16 supports, the total increment of rigidity variation per floor was 400 kN ($25 \text{ kN} \times 16 = 400 \text{ kN}$).

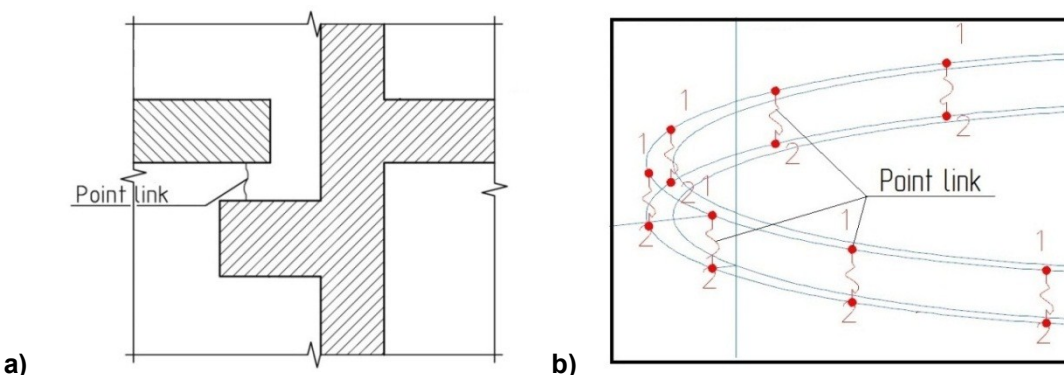


Figure 7. Floor support unit:
a) support unit scheme; b) display of the unit in SOFiPLUS

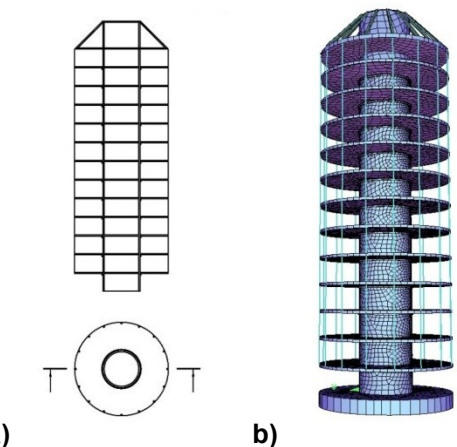


Figure 8. Third computational scheme of the building:
a) structural layout; b) computational model of SOFiSTiK program

The fourth computational scheme uses the suspended system as well. The difference between this scheme and the previous scheme consists in the fact that floor discs are suspended by cable stays not just along the outer contour, but also along the inner contour. In this scheme, the loads are transferred from floors to the foundation solely through the shaft grillage as per the example of the building according to Korchinsky I.L. [1]. Figure 9 shows the features of the structural layout and computational model.

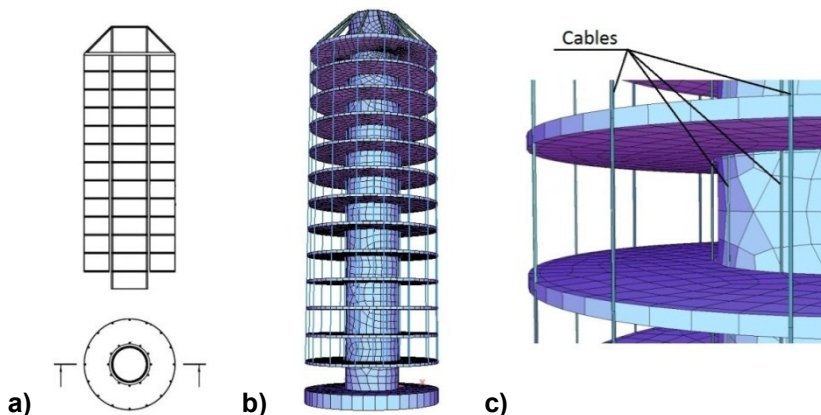


Figure 9. Fourth computational scheme of the building: a) structural layout;
b) computational model of SOFiSTiK program;
c) enlarged area of the model showing the location of cable stays in it

To analyze this scheme, the parameters affecting the oscillation period that varied during the study were determined. Firstly, the building height ranged from 4 to 18 storeys in increments of 2 storeys. In all schemes, the storey height was equal to 4 m. As a result, it was found that within the considered range of variation in the building height, the period of natural oscillations ranged from 7 to 14.7 seconds.

The second parameter of variation was the weight of the lower suspended floor, which varied from 300 t to 1400 t in increments of about 150 t. The change in this parameter allowed extending the oscillation period of a 5-storey model from 7.1 to 7.63 seconds, but it did not virtually affect the properties of a 15-storey model.

The evaluation of dynamic parameters of the fourth scheme shows that it is possible to substantially extend the period of natural oscillations and achieve the maximum reduction of seismic load on the building in a structural way. However, due to considerable yield such systems lead to swinging of suspended elements that can cause the destruction of the entire building.

If we follow the recommendations to design buildings on seismic isolating structures of foundations [37, 38], and for multi-storey buildings as well, the duration of the most efficient period of natural oscillations ranges from 3 to 4 seconds. Apparently, the oscillation period falling within this range is also the most preferable for buildings with suspended structures.

At the next stage, we considered the fifth computational scheme of a building with suspended structures. It took into account advantages and drawbacks of the previous schemes. The main drawback of the third scheme is high cost and complexity of cantilevered supports, as well as their difficult maintenance. The drawback of the fourth scheme is the uncontrolled oscillation of suspended elements, which may cause resonance in case of seismic exposure.

The fifth computational scheme combines the positive aspects of the third option – the possibility to adjust the rigidity of supports and oscillation amplitude. The fourth option – the relative simplicity of design and maintenance alongside with reliability.

The fifth scheme is similar to the third one, but in this case, floor discs are attached to the shaft by means of cable suspensions. Figure 10 shows the features of the structural layout and model.

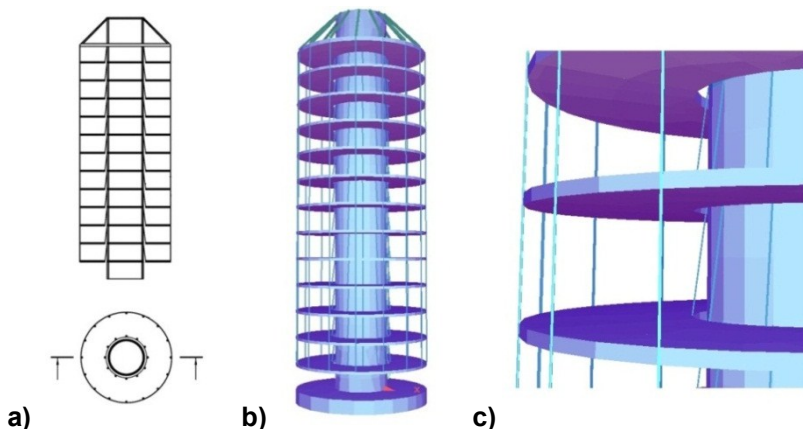


Figure 10. Fifth computational scheme of the building: a) structural layout; b) computational model of SOFiSTiK program; c) enlarged area of the model showing the location of cable stays in it

The principle of the operation of cable suspensions is based on the properties of a mathematical pendulum. When floors oscillate because of seismic exposure, the angle of the deviation of suspensions is increasing and, consequently, the force tending to place the floor back is also increasing.

While studying this computational scheme, the length of suspensions, the angle of their deviation from the vertical and the height of the building varied. The length ranged from 0.9 m to 4.4 m in increments of 0.5 m. The deviation angle changed from 0° to 6° with an interval of 1.5°. The height of the building varied from 4 to 18 storeys in increments of 2 storeys.

After all the computations, it was found that the maximum period of oscillation – 4.71 seconds – belongs to a building having the maximum length and minimum angle of deviation of suspensions, as well as the maximum height.

It is worth noting that at the minimum angle of the deviation of cable stays there is the need to install cantilevers thereby the storey area may be reduced. To avoid this, the maximum displacement of suspended elements should be less than the distance between the suspended and non-suspended part of the building.

Conclusions

Based on the results of the research conducted the following conclusions were drawn:

- Buildings with suspended structures can be considered as earthquake-proof systems and their use may result in a significant reduction of seismic loads.
- Decrease in seismic loading in buildings with suspended designs is connected with the reduction of the coefficient of dynamism due to increase in the period of own fluctuations.
- The results of the comparative analysis of various versions of settlement schemes established that the fifth settlement scheme with use of guy suspensions, the second scheme with the use of rubber-metal support and the third scheme are the most effective for multi-storey buildings with suspended designs.

4. The fourth scheme has the greatest period of own fluctuations, but in case of this scheme the building can receive a serious swing during an earthquake that as a result will lead to its collapse. This scheme is unserviceable without the introduction of oscillation damping elements.

5. The first scheme with traditional barreled constructive system has the form of fluctuations similar to the fluctuations of the console compressed core. The maximum period of own fluctuations in this scheme did not exceed 1.08 sec.

6. The findings form the basis for further research considering actual characteristics of seismic effects [39].

References

- Korchinsky I.L., Grill A.A., Chernyavsky I.Z., Popov I.V., Kaplan V.E., Fridburg V.I. *Podvesnoe zdanie* [Suspended building]. SU USSR 477227. 1975 (rus)
- Skladnev N. N. *Vysotnye zdaniya s zhystkim stvolom i podveshennymi na predvaritel'no napryazhennyh vantah ehtazhami, prednaznachennye dlya sejsmicheskikh rajonov* [The high-rise buildings with a rigid trunk and floors suspended on previously strained guys intended for seismic countries]. Moscow. 1994. 18 p. (rus)
- Chanukvadze G.Sh., Mardzhanishvili M.A., Mikabadze Yu.G. *Podvesnoe sejsmostojkoe zdanie* [Suspended aseismic building]. SU USSR 613065. 1978. (rus)
- Chanukvadze G.Sh., Mardzhanishvili M.A., Mikabadze Yu.G. *Mnogoetazhnoe sejsmostojkoe zdanie s podveshennymi ehtazhami* [The multystoried earthquake-resistant building with the suspended floors]. SU USSR 791871.1980. (rus)
- Ostromensky P.I., Nikiforov I.S., Bolotov A.S. *Sejsmostojkoe zdanie podvesnogo tipa* [Seismic building of suspended type]. Patent RU 2186183. 2002. (rus)
- Grigorieva I.I. *Issledovanie kolebanij podveshennogo perekrytiya pri sejsmicheskem vozdejstvii* [The study of oscillations of the suspended ceiling in the seismic impact]. *Scientific and Technical VNIIIS abstract collection: a series of 14 Earthquake building*. Moscow: VNIIIS State Construction Committee of the USSR. 1979. Vol.8. Pp. 18–21. (rus)
- De bp-building in Antwerpen* [Electronic resource]. URL: http://www.debalansvanbraem.be/braem_over_bouwen/de_bp_building_in_antwerpen (reference date: 04.06.2016).
- Hanging a building in air* [Electronic resource]. URL: <http://www.innovation-creativity.com/hanging-a-building-in-air.html> (reference date: 06.04.2016).
- Westcoast transmission building* [Electronic resource]. URL: <https://structurae.net/structures/westcoast-transmission-company-tower> (reference date: 06.04.2016).
- Allen E., Zalewski W. *Shaping Structures*. John Wiley & Sons. New York, 1998. 416 p.
- 40 let «4 cilindram» — glavnemu ofisu BMW v Myunhene [40 years "4 cylinders" - BMW head office in Munich] [Electronic resource]. URL: <https://www.press.bmwgroup.com/russia/article/detail/T0143990> RU (reference date: 06.04.2016). (rus)
- Torres de Colon y un enchufe Art Deco* [Electronic resource]. URL: <http://www.miradormadrid.com/torres-colon-enchufe-art-deco> (reference date: 06.04.2016).
- The building of the Federal Reserve Bank of Minneapolis (USA)*. [Electronic resource]. URL: <http://synthart.livejournal.com/157725.html> (reference date: 06.04.2016).
- Belash T.A., Rybakov P.L. *Zdaniya s podvesnymi konstrukciami v sejsmicheskikh rajonah* [Buildings with suspended structures in seismic regions]. *Collection of materials of scientific-methodical conference* (Problems and achievements in the field of construction engineering). SPb: PGUPS, 2015. Pp. 31–37. (rus)
- Sculler W. *Konstrukcii vysotnyh zdanij* [Structures of high-rise buildings]. Translation from English Kilimnik L.Sh., an edition of Kazina G.A. Moscow: Stroyizdat, 1979.

Belash T.A., Rybakov P.L. Buildings with suspended structures in seismic areas. *Magazine of Civil Engineering*. 2016. No. 5. Pp. 17–26. doi: 10.5862/MCE.65.2

Литература

- Корчинский И.Л., Гриль А.А., Чернявский И.З., Попов И.В., Каплан В.Е., Фридбург В.И.. Подвесное здание. А.с. СССР № 477227. 1975.
- Складнев Н.Н. Высотные здания с жёстким стволом и подвешенными на предварительно напряжённых вантах этажами, предназначенные для сейсмических районов: афтотр. дис. ... канд. техн. наук. М., 1994. 18 с.
- Чануквадзе Г.Ш., Марджанишвили М.А., Микаладзе Ю.Г. Подвесное сейсмостойкое здание. А.с. СССР № 613065. 1978.
- Чануквадзе Г.Ш., Марджанишвили М.А., Микаладзе Ю.Г. Многоэтажное сейсмостойкое здание с подвешенными этажами. А.с. СССР № 791871. 1980.
- Остроменский П.И., Никифоров И.С., Болотов А.С. Сейсмостойкое здание подвесного типа. Патент РФ № 2186183. 2002.
- Григорьева И.И. Исследование колебаний подвешенного перекрытия при сейсмическом воздействии // Научно-технический реферативный сборник. М.: ЦШИС, 1979. Т. 8. 18–21 с.
- De bp-building in Antwerpen [Электронный ресурс]. URL: http://www.debalansvanbraem.be/braem_over_bouwen/de_bp_building_in_antwerpen# (дата обращения: 06.04.2016).
- Hanging a building in air [Электронный ресурс]. URL: <http://www.innovation-creativity.com/hanging-a-building-in-air.html#> (дата обращения: 06.04.2016).
- Westcoast transmission building [Электронный ресурс]. URL: <http://docomomo.ca/bc-2000/type/commercial/westcoast/index.html> (дата обращения: 06.04.2016).
- Allen E., Zalewski W. *Shaping Structures*. New York: John Wiley & Sons, 1998. 416 p.
- 40 лет «4 цилиндрам» — главному офису BMW в Мюнхене [Электронный ресурс]. URL: <http://bmw-balauto.ru/news/1/221/> (дата обращения: 06.04.2016).
- Torres de Colón [Электронный ресурс]. URL: http://en.wikipedia.org/wiki/Torres_de_Colon (дата обращения: 06.04.2016).
- Tun Mustapha Tower [Электронный ресурс]. URL: http://en.wikipedia.org/wiki/Tun_Mustapha_Tower (дата обращения: 06.04.2016).
- Белаш Т.А., Рыбаков П.Л. Здания с подвесными конструкциями в сейсмических районах // Сборник материалов научно-методической конференции (Проблемы и достижения в области строительного инженеринга). СПб: ФГБОУ ВПО ПГУПС, 2015. С.31–37.
- Шуллер В. Конструкции высотных зданий / Пер. с англ. Л.Ш. Килимник, ред. Г.А. Казина. М: Стройиздат, 1979. 248 с.
- Лобанов В.И. Расчет конструкций с гарантней качеством // САПР и графика. 2014. № 11. С. 14–15.
- Арнольд К., Рейтерман Р. Архитектурное проектирование сейсмостойких зданий / Пер. с англ. Л.Л. Пудовкиной; ред. С.В. Поляков, Ю.С. Волков. М.: Стройиздат, 1987. 195 с.

- 248 p. (rus)
16. Lobanov V.I. *Raschet konstrukcij s garantiej kachestva* [Calculation of structures with guarantee of quality]. CAD and graphics. 2014. No. 11. Pp. 14–15. (rus)
 17. Arnold C., Reitherman R. *Building Configuration and Seismic Design*. John Wiley & Sons. New York, 1982.
 18. Lalin V.V., Rozin L.A., Kushova D.A. Variacionnaya postanovka ploskoj zadachi geometricheski nelinejnogo deformirovaniya i ustoichivosti uprugih sterzhnej [Variation statement of a flat problem of geometrically nonlinear deformation and stability of elastic cores]. Magazine of Civil Engineering. 2013. No. 1(36). Pp. 87–96. (rus)
 19. Veryovkin D.G., Mosina N.V., Chubakov M.J. Opyt primeneniya programmnogo kompleksa SCAD Office dlya analiza sistemy sejsmозashchity zdaniya Respublikanskogo nacional'nogo teatra dramy v Gorno-Altaiske [Experience with software SCAD Office complex for the analysis of seismic building system of the Republican National Drama Theater in Gorno-Altaisk]. CADmaster. 2005. No. 4(29). 8 p. (rus)
 20. Belyy G.I. Metody rascheta strehnevyyh ehlementov konstrukcij iz tonkostennyyh holodnognutyyh profilej [Some methods of calculating rod elements of constructions from thin-walled cold-bent profiles]. Vestnik grazhdanskikh inzhenerov. 2014. No. 4(45). Pp. 32–37. (rus)
 21. Belyy G.I. K raschetu na ustoichivost' sterzhnevyyh ehlementov konstrukcij iz tonkostennyyh holodnognutyyh profilej [To the calculation of rod element stability of structures made of thin-walled cold-formed profiles]. Vestnik grazhdanskikh inzhenerov. 2016. No. 3(56). Pp. 46–51. (rus)
 22. Süleyman Adanur, Murat Günaydin, Ahmet Can Altunişik, Barış Sevim. Construction stage analysis of Humber Suspension Bridge. Applied Mathematical Modelling. 2012 Vol. 36. No. 11. Pp. 5492–5505.
 23. Brian J. Sullivan. The finite element method and earthquake engineering: The 2006 Benjamin Franklin Medal in civil engineering presented to Ray W. Clough. Journal of the Franklin Institute. 2010. Vol. 347. No. 4. Pp. 672–680.
 24. Li Hongnan, Song Benyou. Seismic response reduction for tall buildings by suspended mass pendulums. Earthquake Engineering & Engineering Vibration. 1995. No. 4(15). Pp. 55–61. (ch)
 25. B. Samali, K.C.S. Kwok. Use of viscoelastic dampers in reducing wind- and earthquake-induced motion of building structures. Engineering Structures. 1995. Vol. 17. No. 9. Pp. 639–654.
 26. X. Zhaoa, J.M. Ding, H.H. Suna. Structural design of Shanghai Tower for wind loads. Procedia Engineering. 2011. Vol. 14. Pp. 1759–1767.
 27. 4 – Friction-vibration interactions. Handbook of Friction-Vibration Interactions. 2014. Pp. 153–305.
 28. Apaydin N.M., Bas S., Harmandar E. Response of the Fatih Sultan Mehmet Suspension Bridge under spatially varying multi-point earthquake excitations // Soil Dynamics and Earthquake Engineering. 2016. Vol. 84. Pp. 44–54.
 29. Apaydin N.M. Earthquake performance assessment and retrofit investigations of two suspension bridges in Istanbul. Soil Dynamics and Earthquake Engineerin. 2010. Vol. 30. No. 8. Pp. 702–710.
 30. Mahmoud H., Chulahwat A. Response of building systems with suspended floor slabs under dynamic excitations. Engineering Structures. 2015. Vol. 104. Pp. 155–173.
 31. Belash T.A., Uzdin A.M. Issledovaniya v oblasti sejsmostoikogo stroitel'stva v Peterburgskom gosudarstvennom universitete putej soobshcheniya [Researches in the field of aseismic construction at the St.Petersburg State Transport University]. Earthquake Engineering. Safety of Structures. 2015. No. 6. Pp. 15–20.
 32. Kalugina-Pablos K.N. Podvesnye konstrukcii ("Gorod v gorode. Parenie") [Suspended designs ("The city in the city. Soaring")]. Science, education and experimental design: Book of Abstracts. Moscow, 2014. Pp. 402–403.
 33. Çelebi M., Ulusoy H.S., Nakata N. Responses of a tall building in Los Angeles, California, as inferred from local and distant earthquakes // Earthquake Spectra. 2016. Vol. 32. № 3. Pp. 1821–1843.
 34. Moehle J. Seismic design of reinforced concrete buildings. New York: McGraw-Hill Education, 2014. 760 p.
 35. Becker T.C., Yamamoto S., Hamaguchi H., Masahiko Higashino M., Nakashima M. Application of isolation to high-rise buildings: a Japanese design case study through a U.S. design code lens // Earthquake Spectra. 2015. Vol. 31. № 3. Pp. 1451–1470.
 36. Giammona A.P., Ryan K.L., Dao N.D.. Evaluation of assumptions used in engineering practice to model здания с подвесными конструкциями в сейсмических районах // Инженерно-строительный журнал. 2016. № 5(65). С. 17–26.

- building in Los Angeles, California, as inferred from local and distant Earthquakes. *Earthquake Spectra*. 2016. Vol. 32. No. 3. Pp. 1821–1843.
34. Moehle J. *Seismic design of reinforced concrete buildings*. McGraw-Hill Education. New York, 2014. 760 p.
 35. Becker T.C., Yamamoto S., Hamaguchi H., Masahiko Higashino M., Nakashima M. Application of isolation to high-rise buildings: a Japanese design case study through a U.S. Design Code Lens. *Earthquake Spectra*. 2015. Vol. 31. No. 3. Pp. 1451–1470.
 36. Giammona A.P., Ryan K.L., Dao N.D.. Evaluation of assumptions used in engineering practice to model buildings isolated with triple pendulum isolators in SAP2000. *Earthquake Spectra*. 2015. Vol. 31. No. 2. Pp. 637–660.
 37. Uzdin A.M., Elizarov S.V., Belash T. A.. *Sejsmostojkie konstrukcii transportnyh zdanij i sooruzhenij: uchebnoe posobie dlya studentov vuzov zheleznodorozhnogo transporta* [Earthquake resistant design of transport buildings and structures: the education guidance for students of railway transport]. Moscow: Training center for education on the railways, 2012. 500 p (rus)
 38. Arutunyan A.R. *Sejsmostojkie konstrukcii transportnyh zdanij i sooruzhenij: uchebnoe posobie dlya studentov vuzov zheleznodorozhnogo transporta* [Modern methods of buildings seismic isolation] *Magazine of Civil Engineering*. 2010. No. 3(13). Pp. 56–60. (rus)
 39. Belash T.A., Rybakov P.L. Ob effektivnosti ispol'zovaniya konstruktivnyh sistem s podvesnymi konstrukciyami [The effective use of structural systems of buildings with suspended structures]. *Earthquake Engineering. Safety of Structures*. 2016. No. 4. Pp. 33–36.

Tatiana Belash,
+7(921)9910115; belashta@mail.ru

Pavel Rybakov,
+7(981)7012491; mojiuctap@gmail.co

Татьяна Александровна Белаш,
+7(921)9910115; эл. почта: belashta@mail.ru

Павел Леонидович Рыбаков,
+7(981)7012491; эл. почта:
mojiuctap@gmail.com

© Belash T.A., Rybakov P.L., 2016

doi: 10.5862/MCE.65.3

Improved numerical methods in reliability analysis of suspension roof joints

Усовершенствование численных методов расчета надежности узлов висячих покрытий

I.N. Priadko,*Kiev National University of Construction and Architecture, Kiev, Ukraine***V.P. Mushchanov,***Donbas National Academy of Civil Engineering and Architecture, Makivka, Ukraine***H. Bartolo,***Polytechnic Institute of Leiria, Leiria, Portugal***N.I. Vatin,***Peter the Great St. Petersburg Polytechnic University, St. Petersburg, Russia***I.N. Rudneva,***Kyiv National University of Construction and Architecture, Kyiv, Ukraine***Канд. техн. наук, доцент Ю.Н. Прядко,***Киевский Национальный Университет Строительства и Архитектуры, Киев, Украина***д-р техн. наук, проректор по научной работе, заведующий кафедрой****В.Ф. Мущанов,***Донбасская национальная академия строительства и архитектуры, Макеевка, Украина***PhD, профессор кафедры Гражданского строительства Х. Бартоло,***Политехнический институт в г. Лейрия, Лейрия, Португалия***д-р техн. наук, директор Инженерно-строительного института Н.И. Ватин,**
*Санкт-Петербургский политехнический университет Петра Великого, Санкт-Петербург, Россия***канд. техн. наук, доцент И.Н. Руднева,***Киевский национальный университет строительства и архитектуры, Киев, Украина*

Key words: roof; suspension devices; suspension system; suspensions; civil engineering; constructions; buildings; roof joints; reliability indices; stress-strain analysis

Ключевые слова: покрытие; висячие конструкции; висячие системы; висячий; гражданское строительство; сооружения; здания; узлы крыши; показатели надежности; анализ напряженно-деформированного состояния

Abstract. Modern structures require more complex designs. There is an increased need for accurate approaches to assessing uncertainties in loads, geometry, material properties, and operational environments. However, information is scarce on the reliability of suspension roofs together with their joints. There is an urgent need for estimating stress-strain state and reliability of welded joints, so recommendations can be given based on the obtained data. In this paper, reliability of large-span suspension roofs was investigated and a fundamental approach is proposed for reliability determination of these joints at the design phase of suspension rod roofs. In this work, several joints were investigated: supporting joints between rigid threads and external/internal contours, intermediate joints of top /lower chords of supporting threads, as well as joints between vertical/horizontal links and supporting thread of a roof. To measure reliability of joints, logic and probabilistic methods were used conjointly with other methods based on mathematical statistics. The proposed approach can be applied to design of suspension roof systems and help to develop better designs for better safety, quality control and efficiency of these structures, providing economic and social benefits.

Прядко Ю.Н., Мущанов В.Ф., Бартоло Х., Ватин Н.И., Руднева И.Н. Усовершенствование численных методов расчета надежности узлов висячих покрытий // Инженерно-строительный журнал. 2016. № 5(65). С. 27–41.

Аннотация. Проектирование современных конструкций требует комплексного подхода, обусловленного учетом большого количества факторов при расчете, а также оценки неточностей нагрузок, геометрии сечений, физических свойств материалов и условий эксплуатации. Отсутствие необходимых для оценки надежности покрытий в целом исследований надежности их узлов обуславливает актуальность задачи оценки напряженно-деформированного состояния и надежности сварных узлов покрытий и выработке рекомендаций относительно таких конструкций на основе полученных данных. В связи с этим в статье проанализированы проблемы надежности большепролетных висячих покрытий и описаны принципиальные подходы к учету надежности узлов в расчетах надежности висячих стержневых покрытий. В качестве расчетных принятые опорные узлы крепления изгибно-жесткой нити к внешнему и внутреннему контуру, промежуточные узлы верхнего и нижнего поясов несущей нити, узлы крепления вертикальных и горизонтальных связей к несущим нитям покрытия. В анализе приняты логико-вероятностные методы оценки надежности узлов и методы, основанные на математической статистике. Описанные подходы могут применяться при проектировании новых висячих покрытий, способствуя получению более сложных конструктивных форм с повышенной надежностью несущих элементов, а также на стадии эксплуатации, обеспечивая надежность существующих конструкций.

Introduction

Structural reliability is a fundamental part of building structures, which combines design problems, work planning, production, erection and operation of buildings and structures. Reliability of steel structures in buildings and statically determined and non-determined systems have been investigated by several researchers, such as G. Augusti, A. Baratt, V. Bolotin etc. The major problems and some examples are described by S.F. Pichugin [1] and G. Shpete [2].

In civil engineering, reliability measurement of complex systems is usually concerned with examination and analysis of two principal kinds of joints:

a) series connection, failure-free work probability of which at independent components is determined as:

$$P_m = \prod_{i=1}^m P_i, \quad (1)$$

where P_i is probability of failure-free work of i -component;

b) parallel connection

$$P_m = 1 - \prod_{i=1}^m (1 - P_i) \quad (2)$$

Series connection in probabilistic sense can be used to describe statically determined systems, e.g. trusses, though practical assessment of reliability of real structures cannot be reduced to application of a simple equation (1) due to the correlation between resistance indices of components.

Activities of statically non-determined systems are definitely associated with parallel connections, but reliability assessment cannot be defined by (1), because of the redistribution of forces in a system after the failure of its individual components, which are dependent. Thus, reliability assessment of statically non-determined structures requires a thorough and careful analysis of the stress-stained state and failure under load, and also consideration of distinct features of component failures and the system as a whole.

Reliability analysis of a statically non-determined system is usually made by the following methods and techniques: a method of states, probabilistic method of limiting equilibrium, Monte-Carlo method, Markovian model of reliability analysis [1]. Analytical and computational methods used in the technical reliability theory for computation of complex systems, which can be applied for reliability analysis of statically indeterminate systems, are shown in Figure 1.

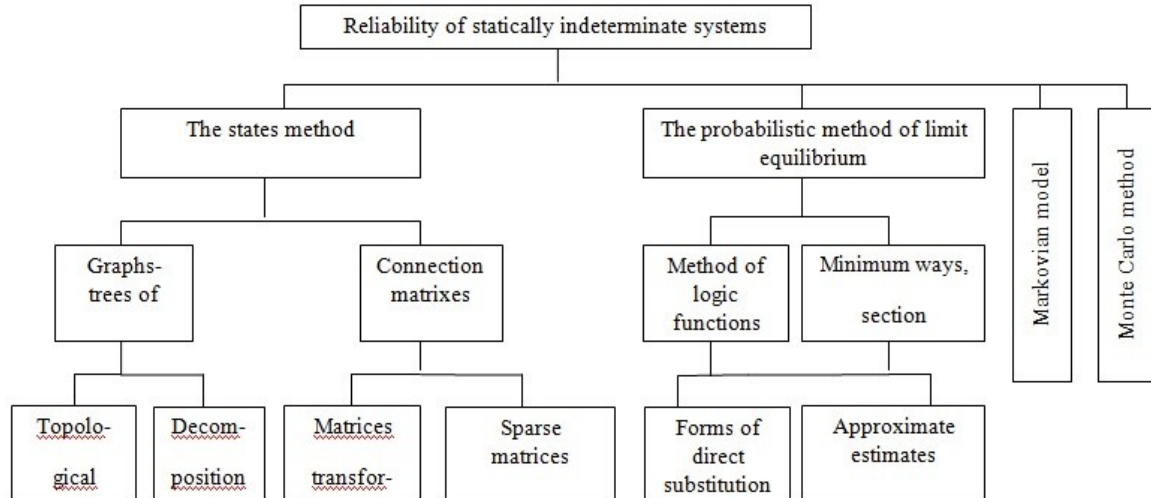


Figure 1. Methods for assessing reliability of statically indeterminate systems

Reliability of steel structures of buildings and constructions representing the statically determined or undefinable systems of elements was reviewed by several research studies by F. Otto, G. Behnisch etc. Certain problems and examples were considered by several researchers, as described by Z. Kala [3]. T. Guo et al. [4], K. Kwon and D.M. Frangopol [5] and Z. Wu et al. [6] achieved good results in determination of the reliability parameters of unique structures.

Relevant scientific experience in the field of structural reliability assessment has been provided by Y. Luo et al. [7] and N. Xiao et al. [8], while Z. Qiu et al. [9] in the field of probabilistic interval reliability of structural systems.

The problem of reliability is especially concerned with unique large-span structures. Suspension shells are among the ones having an increased level of responsibility and their failure can lead to serious economic and social consequences. In the design phase, some problems can occur that are not described in existing regulatory documents. The novelty of technical conceptions demands that a structural engineer should have profound specific knowledge and experience in designing such kind of structures. Requirements of reliability, technological and economic efficiency must be met, as well as the environmental and social factors should be considered.

Nowadays, one of the most dynamic type of large-span structures in architectural and structural view are suspension roofs (Fig.2 and Fig. 3).

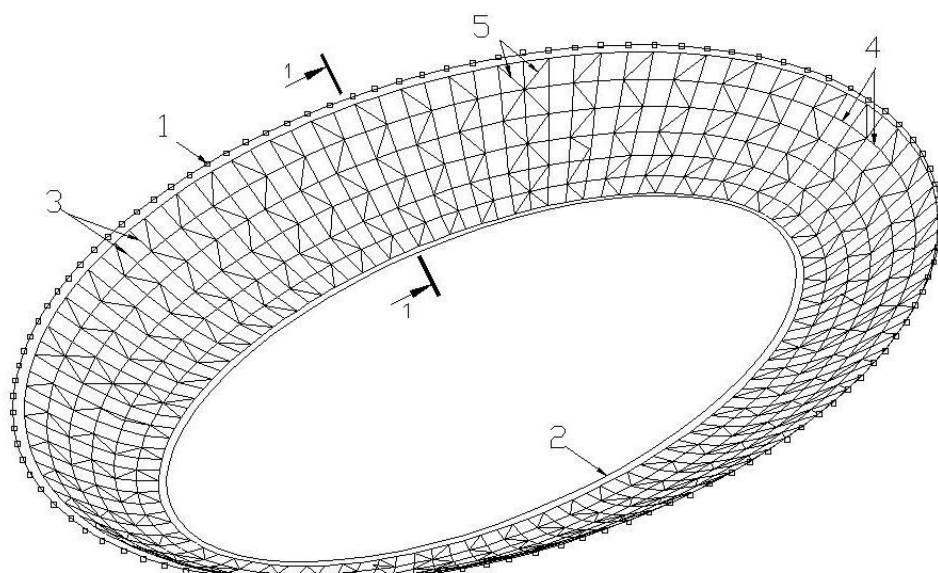


Figure 2. Structural schematic drawing of spatial and rod roof:
1, 2 – external and internal contours, 3, 4, 5 – radial, annular and diagonal components

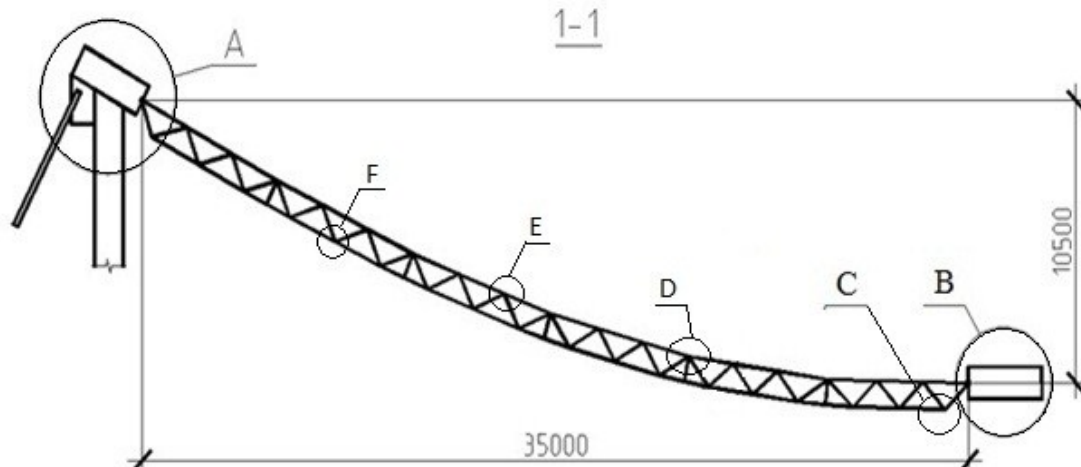


Figure 3. Structural schematic drawing of spatial and rod roof. Open-cut mine 1–1

Large-span roofs have a higher level of responsibility as their failure can lead to serious economic and social consequences. In this context, the design of these unique structures should be based on an integrated approach of rational selection of design solutions. These solutions are related to functionality, architectural design, manufacturing and installation techniques, and operating conditions. The requirements for reliability, manufacturability and cost-effectiveness, given environmental and social factors, should be fully implemented.

The history of shell design goes back to the 1890. Shell design has progressed since the 1930s, and important contributions to the design theory of large-span spatial shells were made by several authors, such as A. Kotli, L. Donell etc. Today, this issue has been pursued by E. Gorokhov, V. Mushchanov, I. Priadko [10] and I.N. Rudneva [11].

Over the last 15 years in particular, the advent of powerful computers and the development of sophisticated nonlinear CAE software (ADINA [12], ABAQUS [13] among others) have enabled engineers to utilize suspension roofs in complicated large scale structures, some of them classified as unique examples of civil engineering excellence [14].

Probabilistic assessment of reliability is one of the most important tasks to be taken into account in structures with high responsibility. The main property that determines the reliability of these structures is their ability to save the pre-defined operational quality during its lifetime. The quantitative characteristic of this property is the probability of failure-free operation.

Several authors from the CIS countries have been working on the reliability assessment of large-span suspension devices and cable-stayed structures, such as V. Muschanov [10], A.A. Sventikov [15], D.Yu. Drobot [16]. Big contribution in stress-strain analysis was made by D. Dol et al. [17], V.V. Eremin [18], D.B. Kiselev et al. [19]. The issues of failure-free operations of the large-span roofs were described by M.I. Farfel [20] and I.V. Smelyanskiy et al. [21].

Among the foreign researchers who made relevant investigations in the area of large span structures V. Goremkins et al. [22], O. Blazevica-Juhnevica et al. [23] should be pointed out.

Joints play a significant role in the composition of structures. Their application in numerical simulation permits to investigate the impact of structural forces on the joints operation and gather the necessary base of statistic stressed-strained state of such kind of joints. At the same time, modern approaches in computer engineering give a chance to assess reliability of joints in a suspension system, bearing in mind the parameters of stressed-strained state and the correlation between the function of structural supporting capacity and elements of joints.

N. Chowdhury [24] and M. Skorupa [25] investigated the stressed-strained status of steel structural joints. However, some questions remain about the stress-strain state (SSS) of suspension roof joints.

Nowadays, there are few investigations on the reliability of roofs and their joints as a whole, though there is an urgent need to assess the stressed-strained state and reliability of roof welded joints, in our view, as well as to create guidelines for these structures.

Priadko I.N., Mushchanov V.P., Bartolo E., Vatin N.I., Rudneva I.N. Improved numerical methods in reliability analysis of suspension roof joints. *Magazine of Civil Engineering*. 2016. No. 5. Pp. 27–41. doi: 10.5862/MCE.65.3

Provision of required levels of reliability at design work for large-span roofs is a topical issue, in particular regarding suspension and rod shells, which strongly determine the efficiency of large-span roof structure. This issue has been investigated by E. Gorokhov, V. Mushchanov and I. Pryadko [26], together with the design method of rigid threads with through section, based on the determination of numerical indices of reliability. The framework of this method is shown in Figure 4. The reference values of this method are presented in Table 1.

The proposed method provides a sequence of solutions for some problems, as follows: how to determine rational geometric parameters of a structure; how to obtain appropriate rigidity characteristics of major supporting elements; how to determine a track of elements' destruction for a typical roof diagram, followed by evaluation of stressed and strained state of a structure; and how to determine the numerical safety indices of a structure (lower and upper safety limits).

Table 1. The reference values of the method described in Figure 4.

h	– height of the threads section;
a_{ub}, a_{lb}	– distance from the center of gravity of the composite section to the center of the cross section of the upper and lower thread chords respectively;
α, k, k', k''	– correction coefficients;
$\bar{D}_1, \bar{D}_4, \bar{W}, \bar{U}$	– dimensionless spatial and stiffness parameters;
$\tilde{A}, \tilde{S}, \tilde{M}, \tilde{N}, \tilde{\sigma}_y$	– random values of supporting contour section, snow load, forces and stresses in the elements respectively;
v_N, v_M, v_A	– random values of the area section of supporting contour, of the snow load, of the forces and stresses in the elements respectively;
$P_{syst}, P_{span}, P_{ext.con}, P_{int.con}$	– probabilities of failure of roof system, load-supporting threads, external and internal contours respectively.

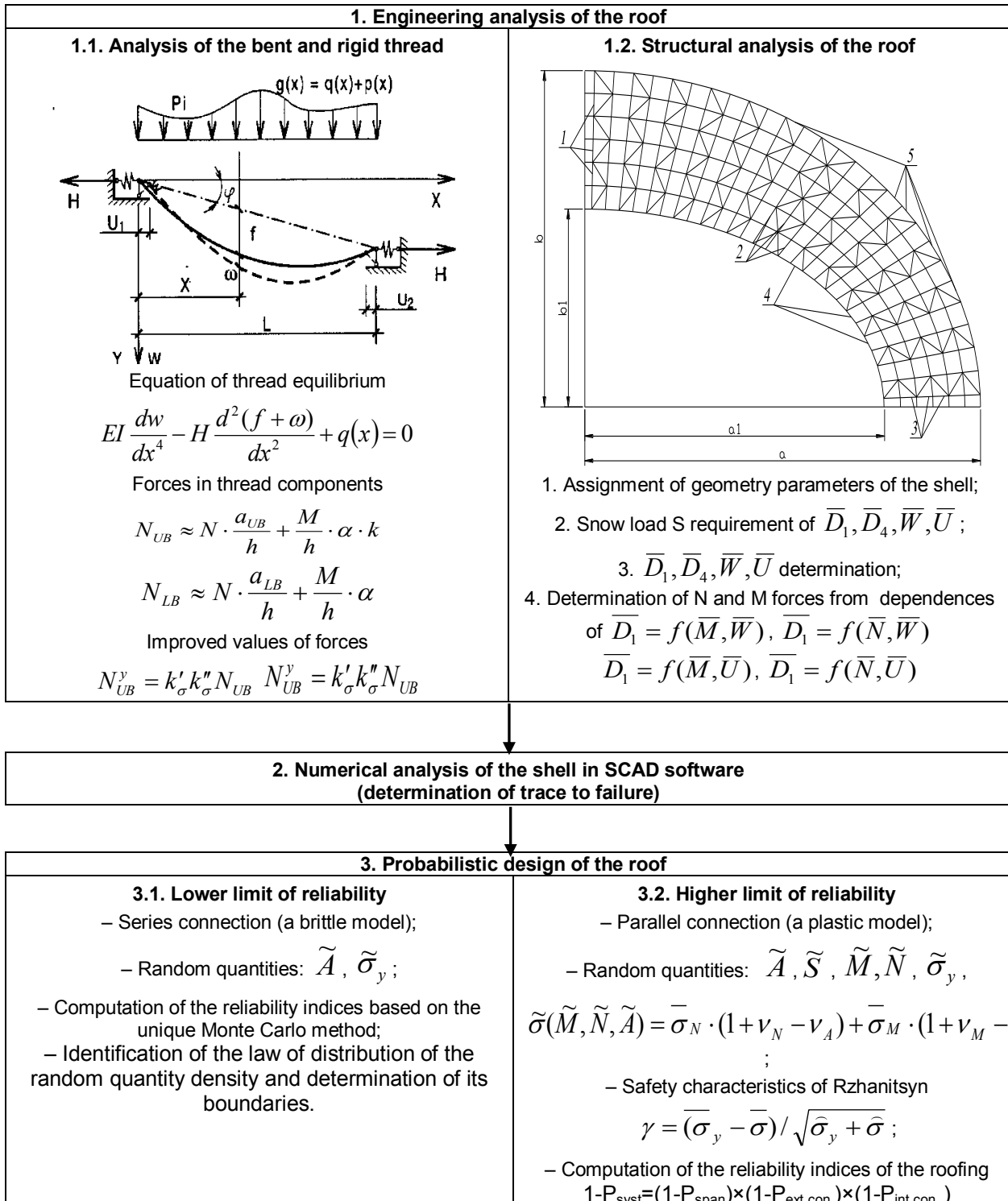


Figure 4. Method for determination of numerical indices of reliability for a suspension roof

The above-described method also has shortcomings. It does not take into account shell joints for determination of roof reliability, which opens new areas for research. To overcome this limitation, the first step was already made with the introduction of this new approach. Some issues have already been considered [27], where the fundamental concerns were to determine the reliability of suspension roofs joint by numerical methods, though only with the aid of common approaches for typical joints of suspension roofs. In this work, the abovementioned method was used for joints of suspensions, and subsequently modelled in modern CAD software.

The main objective at this stage is to get better understanding of the fundamental approaches to determine the reliability of suspension roof joints by numerical methods, using modern CAD system simulation.

Methods

To apply the method (Fig. 4), a new roof was designed using standard football stadium roof dimensions. To perform the structural analysis the following dimensions were used: $a = 186 \text{ m}$; $b = 136 \text{ m}$; $a_1 = 123 \text{ m}$; $b_1 = 85 \text{ m}$ (Fig.2). The main load-supporting elements of the roof are external contour, supported by stadium columns or walls; internal unsupported contour supported by thrust; rigid threads with a truss form (Fig. 5). The roof contours are designed by welded box-section from steel sheet. All the other elements of the supporting structure are made by box-shaped profile. Two types of design load are considered: a constant load (structure weight) and a temporary load (snow), which is 160 kg/m^2 for Donetsk (Ukraine) [28], as the test was done at Donetsk. After completing all the necessary computations, the design scheme was created in AutoCad 2014 for the macro-analysis. As shown in Figure 2, the external contour is fixed along its length, though the internal contour is not fixed and is only supported by the thrust. The obtained scheme was successfully transported to Abaqus/CAE 6.13-1 to perform the macroanalysis and determine the forces and deformations in the rods. At the same time, the 3d models of the joints of the roof (microanalysis) was created using SolidWorks 2014, and also transported to Abaqus/CAE (Fig. 5).

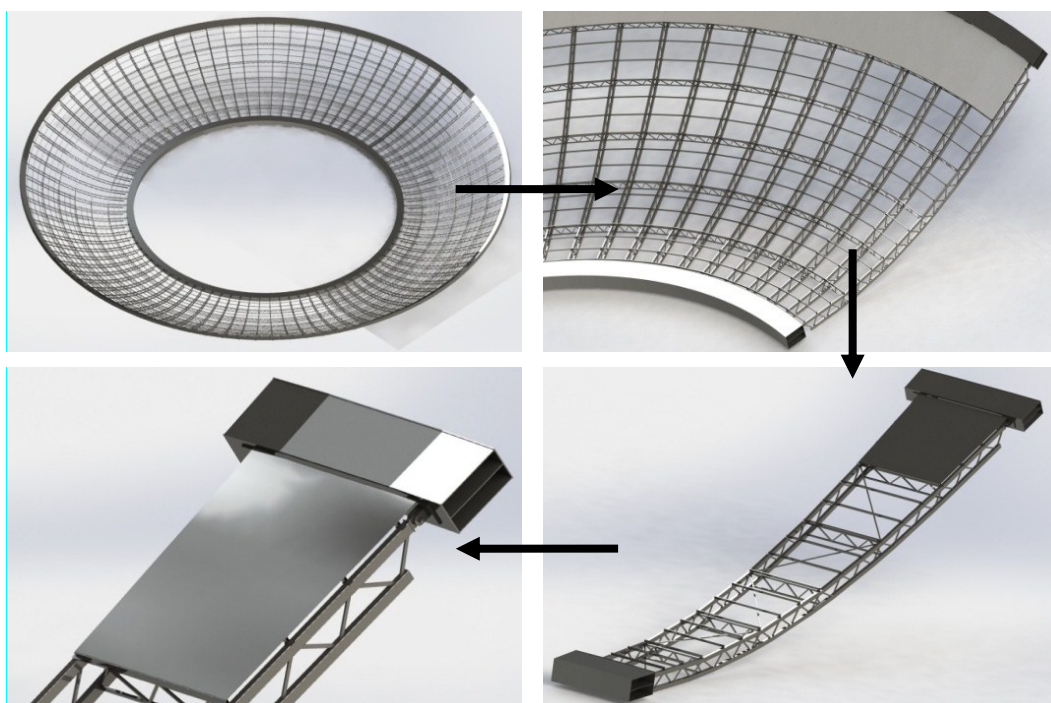


**Figure 5. Suspension roof of the stadium with a cut on the elliptic plan
(transition from the rod scheme to 3D model)**

Additionally, critical external loads and the internal forces were applied in the clipping element zones of model joints, to obtain the critical stresses in the elements and the irreversible deformation, as it is necessary to obtain the deformability of the model and identify the most vulnerable areas. Furthermore, the displacements with all fastenings were applied to the 3d models in order to determine the stress and strain state (Fig. 2, 6). All joint element connections were welded. The exception is the joint connection between the pin and the truss, respectively "A" and "B". In this case, the contact interaction was slipping without friction. Models were divided by grids with a mesh size of 30 mm to perform microanalysis. The simulation results are shown in Figures 7, 9, 10, and 11.

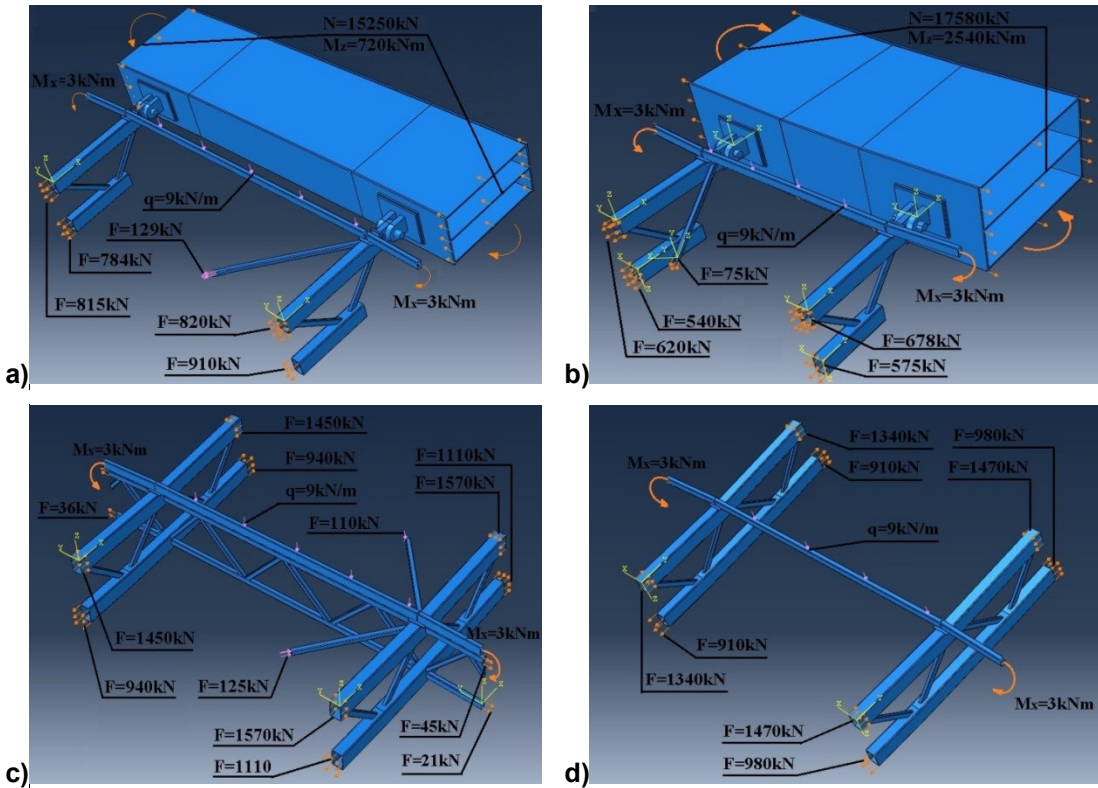


Figure 6. 3D models of the roof joints:
a) Joints A and C; b) Joints B and C; c) Joints D and F; d) Joints E and F

Let us consider the fundamental approaches to reliability of the major joints of the roof to determine its structural form. There are supporting joints of rigid thread to external contour A (Fig. 7) and internal contour B (Fig. 9), connecting joints of the supporting brace with the lower chord of the truss C (Fig. 7), intermediate joints of upper and lower chords of supporting threads D, E and F (Fig. 10 and 11). Not every joint collapse will lead to the collapse of the entire roof, and Table 1 shows the types of connections of the joints in the roof (sequential or parallel connections).

According to the accepted logic and probabilistic simulation rules [1], the requirements for trouble-free element operation are indicated by X, and failure cases by X'. The joint operation described by the function of the included logical variables – the function of Boolean algebra (FBA) $y(X_1, X_2, \dots, X_n)$ is named as the case of the system capacity (a joint).

The shortest way for successful functioning (SWSF), describing the probability of trouble-free operation of a minimum set of elements, is necessary for trouble-free operation of the system, expressed in the form of conjunction (logical multiplication) of elements (3):

$$P_i = \Lambda_{i \in (K_{pl})} X_i, \quad (3)$$

where K_{pl} – is a set of elements included in the given equation.

The condition of the system capacity (a joint) is described in the form of disjunction (logical adding) of all d shortest ways of successful functioning (SWSF) in the system (4), as follows:

$$y(X_1, X_2, \dots, X_n) = V_{i=1}^d P_i = V_{i=1}^d [\Lambda_{i \in (K_{pl})} X_i] \quad (4)$$

Results and discussion

Lets start with the supporting joint of the suspension roof to the outer supporting contour "A" (Fig. 7).

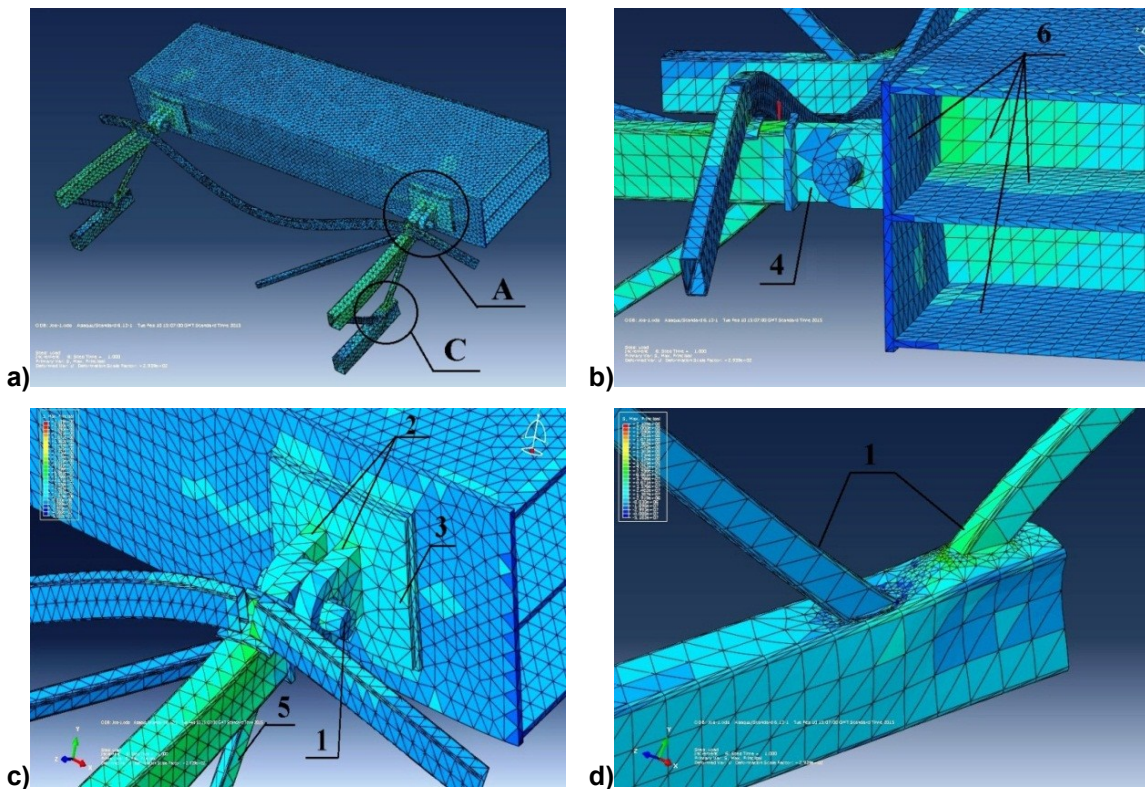


Figure 7. Deformed 3d model in the supporting zone of the external contour:
a) General view; b) Joint A (View 1); c) Joint A (View 2); d) Joint C

Regarding the actual operation of this joint, its failure can occur in consequence of several factors, as follows:

- 1 – a pin crushing;
- 2 – break of the fasteners between the thread and the contour;
- 3 – break of the mounting plate between the contour and the truss;
- 4 – break of the fasteners between the upper chord element and the pin;
- 5 – collapse of the supporting brace;
- 6 – loss of stability of the support contours elements.

These failures are represented in the form of elements in a common structural scheme (Fig.8). In this case, there is no sound base to represent twin welds in the form of parallel connections, as each element enables to carry out a function of strength capacity. In the investigated joint, one of the two welds cannot take a double load, and a twin weld is actually a single weld superimposed by two plots affecting the connection.

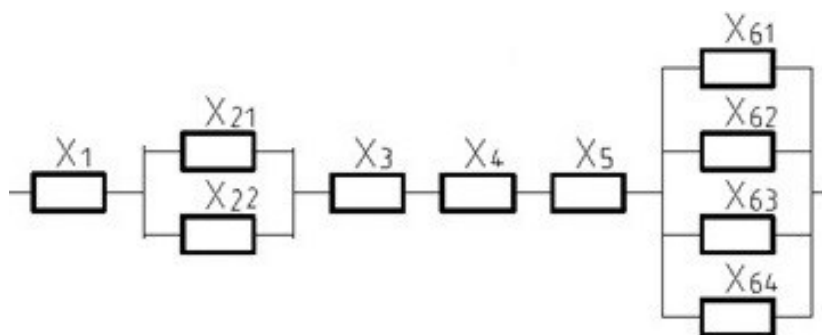


Figure 8. Reliability of joint A. Structural schematic drawing

In the connection 2, if the pin has a stop at the edges, the redistribution of the stresses will be possible after one of the fastening elements fails. However, this will dramatically increase the impact on the remaining elements, which can be affected by a parallel connection of the dependent elements. A similar situation can be observed in connection 6: whenever one of the contour elements loses the stability, the load will be distributed to other elements.

The system operation capacity affecting the operation of the joint (Fig.7) is described in equation 5, as follows:

$$y(X_1, X_2, \dots, X_{11}) = X_1 \cdot (X_{21} \vee X_{22}) \cdot X_3 \cdot X_4 \cdot X_5 \cdot (X_{61} \vee X_{62} \vee X_{63} \vee X_{64}) \quad (5)$$

For the conversion from a logical to probability function, the analysis of the correlated bonds between the elements can be carried out. Given that approximately all the forces in the joint are proportional to the roof load (main roof and snow load), the case of non-destruction of all the elements: can be described by equation 6, as follows:

$$Y_i = X_i = R_i - S_i = \sigma_{Ti} - \sigma_{qi} \geq 0, \quad (6)$$

where parameters σ_{qi} are functionally connected, and the second parameter σ_{Ti} is the same for details 1, 6 and welds 2 to 5. Thus, the corresponding requirements of the trouble-free operation X_1 to X_6 have tight correlation connections with $r \approx 1$. As a result, converting FBA (5) to a probabilistic form, the outlined groups of elements can be presented by the weakest units with P_{imin} .

Probability steel properties of details 1 to 6 and welds 2 to 5 should be taken independently, due to the reliability factor of the joint. Consequently, the correlations between the elements X_i and X_j accordingly to [1] can be determined by equation 7:

$$r_{ij} = \frac{\hat{\sigma}_q^2}{\sqrt{\hat{\sigma}_T^2 + \hat{\sigma}_q^2}} \quad (7)$$

A common expression for the standard ratio $\hat{\sigma}_T^2 / \hat{\sigma}_q^2$, with regard to the variability and standardized deviations of designed values γ_T and γ_q , respectively is used for snow and fixed load [28]. Taking into account the abovementioned concepts about correlation connections, we get correlation coefficients $r_{ij} \leq 0.5$ between the conditions of joint elements' failure with independent strength of steel. Bearing in mind such a comparatively weak correlation, the failure of elements can be considered independent.

Converting from FBA (5) to the probability equation of trouble-free operation (1) of the supporting joint A (Fig. 7), we obtain equation 8, as follows:

$$P_A = P_1 \cdot (1 - Q_{21} \cdot Q_{22}) \cdot \min(P_3, P_4, P_5) \cdot (1 - Q_{61} \cdot Q_{62} \cdot Q_{63} \cdot Q_{64}) \quad (8)$$

A similar analysis of the other above-mentioned joints of the roof is illustrated in Figures 9, 10 and 11.

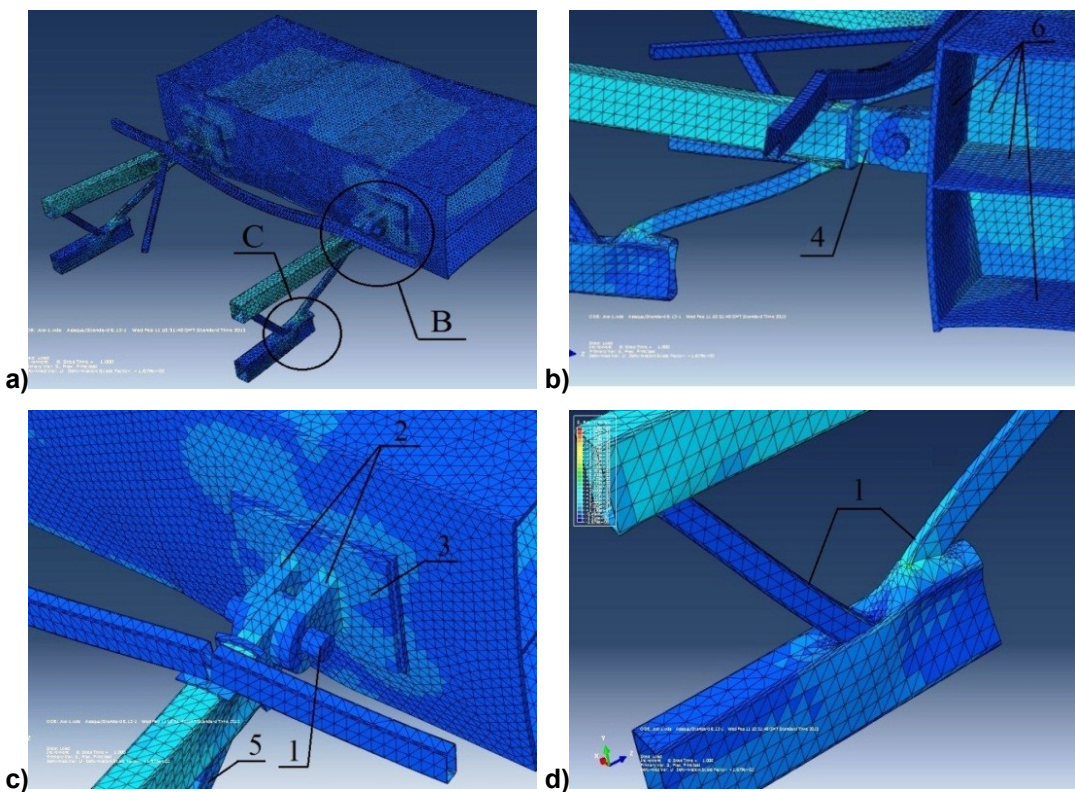


Figure 9. Part of deformed 3D model of unsupported internal contour:
a) General view; b) Joint B (View 1); c) Joint B (View 2); d) Joint C

Figure 10 shows the simulation results of 3d models of joints D and F.

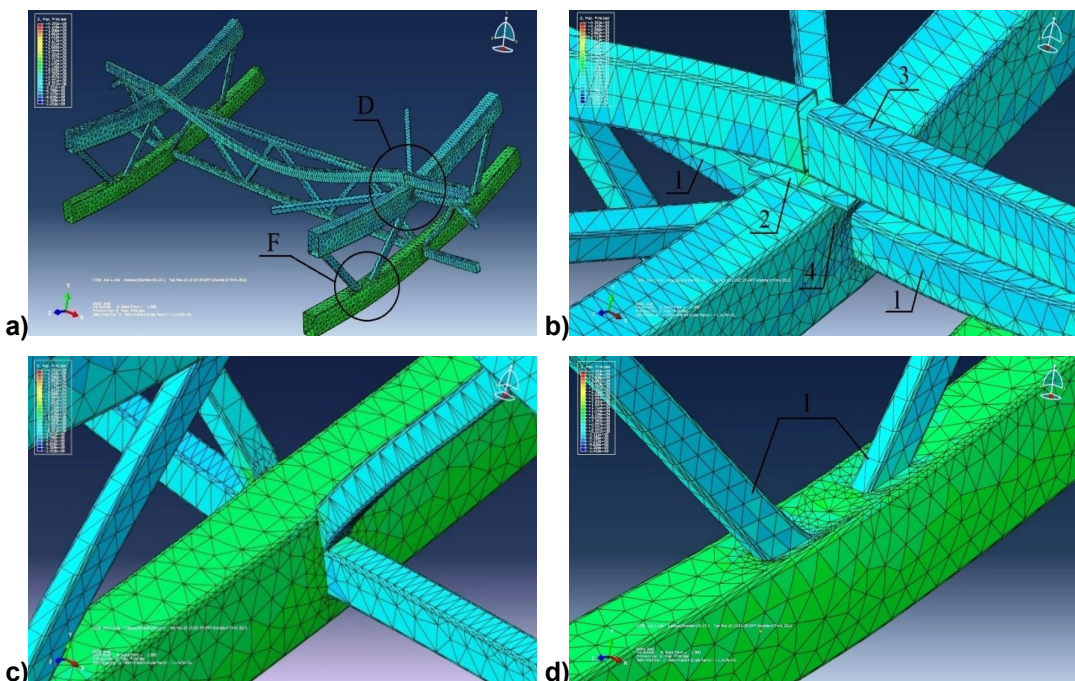


Fig.10. Deformed 3D model in the zone of fastening vertical links to the trusses:
a) General view; b) Joint D (View 1); c) Joint D (View 2); d) Joint F.

Figure 11 shows the simulation results of 3D model of joint E

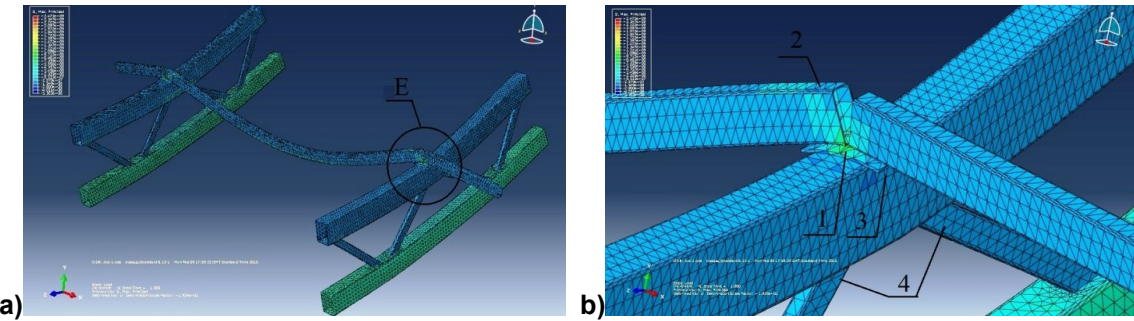


Fig.11. Deformed 3d model in the zone of fastening beam to the upper chord:
a) General view; b) Joint E

Starting from the operation of the abovementioned joints, Table 1 describes possible failures of the elements in the joints, as well as the types of their connections at reliability design stage.

Table 2. Failures of joint elements

Notation of joint	Type of failures of joint elements	Type of connection of joint elements	Type of connection of joint in the roof
A (Fig. 7)	See above	(Fig. 8)	Sequential
B (Fig. 9)	1 – a pin crushing; 2 – break of the fasteners between the thread and the contour; 3 – break of the mounting plate between the contour and truss; 4 – break of the fasteners between the upper chord element and the pin; 5 – collapse of the supporting brace; 6 – loss of stability of the support contours elements.	Sequential Parallel Sequential Sequential Sequential Parallel	Sequential
C (Fig. 7)	1 – collapse of the welds between the supporting brace and the lower truss chords	Sequential	Parallel
D (Fig. 10)	1 – collapse of the welds between the elements of vertical linkages and truss chords; 2 – collapse of the intermediate plate between the beam and truss chord due to local buckling or failure of welds; 3 – beams collapse due to failure of welds. 4 – local buckling of the upper chord at the place of fastening to beams. 5 – collapse of the intermediate trusses braces due to the failure of welds or local buckling.	Parallel Sequential Sequential Sequential Parallel	Parallel
E (Fig. 11)	1 – collapse of the intermediate plate between the beam and truss chord due to local buckling or failure of welds; 2 – beams collapse due to failure of welds. 3 – local buckling of the upper chord at the place of fastening to beams. 4 – collapse of the intermediate trusses braces due to the failure of welds or local buckling.	Sequential Sequential Sequential Parallel	Parallel
F (Fig. 10)	1 – collapse of the intermediate plate between the beam and truss chord due to local buckling or failure of welds;	Parallel	Parallel

On the basis of above-mentioned information, the formulae of probability of trouble-free operation of joints have been obtained:

$$P_B = P_1 \cdot (1 - Q_{21} \cdot Q_{22}) \cdot \min(P_3, P_4, P_5) \cdot (1 - Q_{61} \cdot Q_{62} \cdot Q_{63} \cdot Q_{64}), \quad (9)$$

$$P_C = P_1, \quad (10)$$

$$P_D = \min((1 - Q_{11} \cdot Q_{12}), (1 - Q_{51} \cdot Q_{52})) \cdot \min(P_2, P_3) \cdot P_4, \quad (11)$$

$$P_E = (1 - Q_{41} \cdot Q_{42}) \cdot \min(P_1, P_2) \cdot P_3, \quad (12)$$

$$P_F = 1 - Q_{11} \cdot Q_{12}, \quad (13)$$

where P_B, P_C, P_D, P_E, P_F – correspond to probability of trouble-free operation of joints B, C, D, E, F.

With regard to the accepted types of joint connections (Table 1), the probability of the trouble-free operation of the joint system may be described in the following way:

$$P_{sys} = P_A \cdot P_B \cdot (1 - Q_{C1} \cdot \dots \cdot Q_{Cn}) \cdot (1 - Q_{D1} \cdot \dots \cdot Q_{Dm}) \cdot (1 - Q_{E1} \cdot \dots \cdot Q_{Ek}) \cdot (1 - Q_{F1} \cdot \dots \cdot Q_{Fh}) \quad (14)$$

where n, m, k, h – are the number of designed joints C, D, E, F respectively.

Values of n, m, k, h are determined when the roof span part is destructed.

At this stage, the fundamental approaches to define the reliability of the joints in suspension roof were determined by numerical methods.

Further investigation is needed, based on the method of Mushchanov-Pryadko [10], to develop a new method to design suspension roofs, founded on reliability numerical indices of designed structures taking into account joints' operation. This method can be applied in 2 stages:

- a) Analysis of the systems' reliability at the macro level, considering the geometric characteristics of the sections of the main structural elements;
- b) Analysis of the reliability of the system at the micro level, when a reliability analysis of the most strained structural elements is performed, based on the analysis of the behavior of joints.

Conclusions

The reliability of large-span suspension roofs was investigated and a fundamental approach is proposed to determine reliability of their joints at the design phase. Some major principles are laid down in these conclusions:

1. Structural design of the reliability of joints in suspension roofs shows that these joints are mainly described by sequential schemes including parallel connections of dependent elements, corresponding to multi-elementary connections selected at the design scheme.
2. There is a correlation between joint elements in the structure, due to the same steel strength properties which allow reducing the number of elements and increase the final reliability of the joints.
3. The reliability of the joints of suspension roofs depends on the number of its supporting elements, as an increase in the the number of elements leads to reduction in its reliability, while low-element joints have greater reliability. Other important factor is the homogeneity of strengths of elements: reliability of joints is lower whenever the reliability of elements is independent. This situation is true if the elements are produced with different types of steel, by various producers, if different types of welding are used, etc.
4. Due to their multi-elementary nature, joints can be less reliable than elements themselves (rods of columns, span parts of suspension threads, etc), so they should be considered when reliability of structures is assessed.
5. The proposed approach may be used for suspension and convex rod shells with similar design joint solutions.
6. After performing the reliability analysis of joints, there is a need to increase the supporting capacity of the structure in zones with fixed critical stresses by increasing the weld sizes, installing additional bolts, additional elements or using high strength steels, etc.
7. The proposed approach can be applied to the design of suspension roof systems providing economic and social benefits. Design companies and customers will benefit from this approach by using a reliability-based model that allows efficient management of complex systems and maintenance of sufficient reliability and functionality levels of such systems.

References

- Pichugin S.F. *Nadezhnost stalnyih konstruktsiy proizvodstvennyih zdaniy* [Reliability of the steel structures of industrial buildings]. Moscow: ASV, 2011. 452 p. (rus)
- Shpete G. *Nadezhnost nesuschih stroitelnyih konstruktsiy* [Reliability of the bearing structures]. Moscow: Stroyizdat, 1994. 288 p. (rus)
- Kala Z., Kala J. Sensitivity analysis of stability problems of steel structures using shell finite elements and nonlinear computation methods. *WSEAS Transactions on Applied and Theoretical Mechanics*. 2009. No. 4(3). Pp. 105–114.
- Guo T., Sause R., Frangopol D. M. Time-dependent reliability of box-girder bridge considering creep, shrinkage, and corrosion. *Journal of Bridge Engineering*. 2011. No. 16(1). Pp. 29–43.
- Kwon K., Frangopol D. M. Bridge fatigue reliability assessment using probability density functions of equivalent stress range based on field monitoring data. *International Journal of Fatigue*. 2010. No. 32(8). Pp. 1221–1232.
- Wu Z., Wang S., Ge X. Application of latin hypercube sampling technique to slope reliability analysis. *Rock and Soil Mechanics*. 2010. No. 31(4). Pp. 1047–1054.
- Luo Y., Kang Z., Li A. Structural reliability assessments based on probability and convex set mixed model. *Computers & Structures*. 2009. No. 87(21–22). Pp. 1408–1415.
- Xiao N., Huang H., Wang Z. Reliability sensitivity analysis for structural systems in interval probability form. *Structural and Multidisciplinary Optimization*. 2011. No. 44(5). Pp. 691–705.
- Qiu Z., Yang D., Elishakoff I. Probabilistic interval reliability of structural systems. *International Journal of Solids and Structures*. 2008. No. 45(10). Pp. 2850–2860.
- Gorokhov E., Mushchanov V., Priadko I. Ensuring the required level of reliability during the design stage of – latticed shells with a large opening. *Journal of Civil Engineering and Management*. 2015. No. 21(3). Pp. 282–289.
- Mushchanov, V.F., Rudneva I.N., Priadko Yu.N. Napryazhenno-deformirovannoe sostoyanie visyachey sistemy, obrazovannoy sistemoy izgibno-zhestkih nitey, pri uchete podatlivosti opor [Stress and strain state of the suspension roof structure performed by the rigid threads in accordance with the pliability of the supports]. *Metallicheskie konstruktsii*. 2012. No. 18(1). Pp. 5–16. (rus)
- ADINA – Theory and Modelling Guide*. Volume 1: Adina Solids & Structures. ADINA R & D, Inc., Watertown, 71 Elton Avenue, MA 02472 USA, 2015.
- Programmer's manual for ANSYS, release 11.0. ANSYS Inc., 2007.
- Littlefield D., Jones W. Great Modern Structures. 100 Years of Engineering Genius. London: Carlton Books Ltd, 2012.
- Sventikov A.A. Otsenka progressiruyuscheego razrusheniya prostranstvennyih visyachih sterzhnevyyih pokryitiy. [Estimation of the active collapse of the spatial suspension bar-roofs]. *Stroitel'naya mehanika i raschet sooruzheniy*. 2010. No. 5. Pp. 34–38. (rus)
- Drobot D.Yu. Otsenka zhivuchesti krytogo konkobezhnogo tsentra v Krylatskom. [Durability estimation of the covered skating complex in Krylatsky district]. *Vestnik MGСU*. 2009. No. 2. Pp. 116–119. (rus)
- Dol D.V., Kim Yu.V., Shumeyko G.S. Metodika rascheta visyachey membranyi pokryitiya sooruzheniya s uchetom uprugo-plasticheskikh deformatsiy s primeneniem lineynyih splaynov [Computation method of the suspension roof shell considering the elastic-plastic deformations applying the linear splines]. *Sovremennye nauchnye issledovaniya i innovatsii*. 2014. No. 2(34). 12 p. (rus)
- Eremin V.V. Analiz napryazhenno-deformirovannogo sostoyaniya visyachey kombinirovannoy sistemy na Priadko I.N., Mushchanov V.P., Bartolo E., Vatin N.I., analysis of suspension roof joints. *Magazine* doi: 10.5862/MCE.65.3

Литература

- Пичугин С. Ф. Надежность стальных конструкций производственных зданий. М.: АСВ, 2011. 452 с.
- Шпете Г. Надежность несущих строительных конструкций. М.: Стройиздат, 1994. 288 с.
- Kala Z., Kala J. Sensitivity analysis of stability problems of steel structures using shell finite elements and nonlinear computation methods // *WSEAS Transactions on Applied and Theoretical Mechanics*. 2009. № 4(3). Pp. 105–114.
- Guo T., Sause R., Frangopol D. M. Time-dependent reliability of box-girder bridge considering creep, shrinkage, and corrosion // *Journal of Bridge Engineering*. 2011. № 16(1). Pp. 29–43.
- Kwon K., Frangopol D. M. Bridge fatigue reliability assessment using probability density functions of equivalent stress range based on field monitoring data // *International Journal of Fatigue*. 2010. № 32(8). Pp. 1221–1232.
- Wu Z., Wang S., Ge X. Application of latin hypercube sampling technique to slope reliability analysis // *Rock and Soil Mechanics*. 2010. № 31(4). Pp. 1047–1054.
- Luo Y., Kang Z., Li A. Structural reliability assessments based on probability and convex set mixed model. *Computers & Structures*. 2009. № 87(21–22). Pp. 1408–1415.
- Xiao N., Huang H., Wang Z. Reliability sensitivity analysis for structural systems in interval probability form // *Structural and Multidisciplinary Optimization*. 2011. № 44(5). Pp. 691–705.
- Qiu Z., Yang D., Elishakoff I. Probabilistic interval reliability of structural systems // *International Journal of Solids and Structures*. 2008. № 45(10). Pp. 2850–2860.
- Gorokhov E.V., Mushchanov V.F., Priadko I.N. Ensuring the required level of reliability during the design stage of – latticed shells with a large opening // *Journal of Civil Engineering and Management*. 2015. № 21(3). Pp. 282–289.
- Мушканов В.Ф., Руднева И.Н., Прядко Ю.Н. Напряженно-деформированное состояние висячей системы, образованной системой изгибно-жестких нитей, при учете податливости опор // *Металлические конструкции*. 2012. № 18(1). С. 5–16.
- ADINA – Theory and Modelling Guide*. Volume 1: Adina Solids & Structures. ADINA R & D, Inc., Watertown, 71 Elton Avenue, MA 02472 USA, 2015.
- Programmer's manual for ANSYS, release 11.0. ANSYS Inc., 2007.
- Littlefield D., Jones W. Great Modern Structures. 100 Years of Engineering Genius. London: Carlton Books Ltd, 2012.
- Свентиков А.А. Оценка прогрессирующего разрушения пространственных висячих стержневых покрытий // *Строительная механика и расчет сооружений*. 2010. № 5. С. 34–38.
- Дробот Д.Ю. Оценка живучести крытого конькобежного центра в Крылатском // *Вестник МГСУ*. 2009. № 2. С. 116–119.
- Доль Д.В., Ким Ю.В., Шумейко Г.С. Методика расчета висячей мембранный покрытия сооружения с учетом упруго-пластических деформаций с применением линейных сплайнов // *Современные научные исследования и инновации*. 2014. № 2(34). 12 с.
- Еремин В.В. Анализ напряженно-деформированного состояния висячей комбинированной системы на основе ПВК ЛИРА // *Строительство и архитектура*. 2013. № 2(17). С. 86–93.
- Киселев Д.Б., Крылов А.С., Трушин С.И. Особенности работы большепролетного покрытия футбольного стадиона в Казани // *Промышленное и гражданское строительство*. 2013. № 10. С. 29–32.
- Фарфель М.И. Обеспечение безаварийной Rudneva I.N. Improved numerical methods in reliability of Civil Engineering. 2016. No. 5. Pp. 27–41.

- osnove PVK LIRA [Stress and strain state estimation of the combined suspension roof applying LIRA software]. *Stroitel'stvo i arhitektura*. 2013. No. 2(17). Pp. 86–93. (rus)
19. Kiselev D.B., Kryilov A.S., Trushin S.I. Osobennosti raboty bolsheproletnogo pokrytiya futbolnogo stadiona v Kazani [Features of the structures behavior of the large-span stadium roof in Kazan]. *Promyshlennoe i grazhdanskoe stroitelstvo [Industrial and civil engineering]*. 2013. No. 10. Pp. 29–32. (rus)
 20. Farfel M.I. Obespechenie bezavariynoy ekspluatatsii unikalnogo bolsheproletnogo pokrytiya bolshoy sportivnoy arenii olimpiyskogo stadiona "Luzhniki" [Ensuring of the failure-free operation of the large-span Olympic stadium roof "Luzhniki"]. *Stroitel'naya mehanika i raschet sooruzhenii*. 2012. No. 6. Pp. 56–61. (rus)
 21. Smelyanskiy I.V., Kopylychenko R.A. Uchet nedeformiruemosti kontura pri raschete kombinirovannyih visyachih system [Computation of the combined roof structures in accordance with non deformation of the counter]. *Vestnik Tverskogo Gosudarstvennogo Tehnicheskogo Universiteta*. 2007. No. 11. Pp. 79–83. (rus)
 22. Goremikins V., Rocens K., Serduks D., Pakrastins L., Vatin N. Cable truss topology optimization for prestressed long-span structure. *Advanced in Civil Engineering and Building Materials*. 2015. No. 4. Pp. 363–367.
 23. Blazevica-Juhnevica O., Serduks D., Ozolins R., Goremikins V., Pakrastins L. Choice of rational parameters of combined structure. *Procedia Engineering*. 2015. № 117. Pp. 85–93.
 24. Chowdhury N., Chiu W.K., Wang J. Static and fatigue testing thin riveted, bonded and hybrid carbon fiber double lap joints used in aircraft structures. *Composite Structures*. 2015. No. 121. Pp. 315–323.
 25. Skorupa M., Korbel A., Skorupa A., Machniewicz T. Observations and analyses of secondary bending for riveted lap joints. *International Journal of Fatigue*. 2015. No. 72. Pp. 1–10.
 26. Gorokhov E., Mushchanov V., Pryadko I. Reliability provision of rod shells of steady roofs over stadium stands at stage of design work. *Procedia Engineering*. 2013. No. 57. Pp. 353–363.
 27. Muschanov, V.F., Pryadko Yu.N. Fundamental approaches towards joints operation at reliability designs of suspension roofs. *Metallicheskie konstruktsii*. 2014. No. 20(1). Pp. 35–47. (rus)
 28. DBN V.1.2-2:2006. Sistema obespecheniya nadezhnosti i bezopasnosti stroitelnyih ob'ektov. Nagruzki i vozdeystviya [System of the reliability and safety ensuring of the building structures. Loads and impacts]. Normyi proektirovaniya [Building codes]. K.: Minbud Ukrayini, 2006. 61 p. (rus)

Iurii Priadko,
+38(095)4208982; *yura_pryadko@mail.ru*
Volodymyr Mushchanov,
+38(050)3680804; *mvf@donnasa.edu.ua*
Helena Bartolo,
+351933623765; *helena.bartolo@ipleiria.pt*
Nikolai Vatin,
+79219643762; *vatin@mail.ru*
Iryna Rudnieva,
+3(8050)6203231; *irene_p@mail.ru*

эксплуатации уникального большепролетного покрытия большой спортивной арены олимпийского стадиона «Лужники» // Строительная механика и расчет сооружений. 2012. № 6. С. 56–61.

21. Смелянский И.В., Копыльченко Р.А. Учет недеформируемости контура при расчете комбинированных висячих систем // Вестник Тверского Государственного Технического Университета. 2007. № 11. С. 79–83.
22. Goremikins V., Rocens K., Serduks D., Pakrastins L., Vatin N. Cable truss topology optimization for prestressed long-span structure // Advanced in Civil Engineering and Building Materials. 2015. №. 4. Pp. 363–367.
23. Blazevica-Juhnevica O., Serduks D., Ozolins R., Goremikins V., Pakrastins L. Choice of rational parameters of combined structure. *Procedia Engineering*. 2015. № 117. Pp. 85–93.
24. Chowdhury N., Chiu W.K., Wang J. Static and fatigue testing thin riveted, bonded and hybrid carbon fiber double lap joints used in aircraft structures // Composite Structures. 2015. № 121. Pp. 315–323.
25. Skorupa M., Korbel A., Skorupa A., Machniewicz T. Observations and analyses of secondary bending for riveted lap joints // International Journal of Fatigue. 2015. № 72. Pp. 1–10.
26. Gorokhov E., Mushchanov V., Pryadko I. Reliability provision of rod shells of steady roofs over stadium stands at stage of design work. *Procedia Engineering*. 2013. № 57. Pp. 353–363.
27. Мущанов, В.Ф., Прядко Ю.Н. Fundamental approaches towards joints operation at reliability designs of suspension roofs // Металлические конструкции. 2014. № 20(1). С. 35–47.
28. ДБН В.1.2-2:2006. Система обеспечения надежности и безопасности строительных объектов. Нагрузки и воздействия. Нормы проектирования. К.: Минбуд України, 2006. 61 с.

Юрий Николаевич Прядко,
+38(095)4208982;
эл. почта: *yura_pryadko@mail.ru*
Владимир Филиппович Мущанов,
+38(050)3680804;
эл. почта: *mvf@donnasa.edu.ua*
Хелена Бартоло,
+351933623765;
эл. почта: *helena.bartolo@ipleiria.pt*
Николай Иванович Ватин,
+79219643762; эл. почта: *vatin@mail.ru*
Ирина Николаевна Руднева,
+3(8050)6203231; эл. почта: *irene_p@mail.ru*

© Priadko I.N., Mushchanov V.P., Bartolo E., Vatin N.I., Rudnieva I.N., 2016

doi: 10.5862/MCE.65.4

Calculation of optimized methods of the river underwater pipeline backfill with the use of APMWinMachine 9.7

Расчет оптимизированных способов засыпки речного подводного трубопровода с использованием APMWinMachine 9.7

K.V. Kozhaeva,
Ufa State Petroleum Technological University,
Ufa, Russia

Ассистент К.В. Кожаева,
Уфимский государственный нефтяной
технический университет, Уфа, Россия

Key words: river underwater pipeline; the way of backfill; backfill with cofferdams; installation of temporal loads; the calculation of optimized methods

Ключевые слова: подводный трубопровод;
способ засыпки; засыпка перемычками;
установка временных пригрузов; расчет
оптимизированных способов

Abstract. Nowadays, the standard techniques of backing the ballasted pipeline laid in a bottom trench are used: sequential deposition of soil by suction dredges along the slurry pipeline, soil discharge by self-dumping barges, soil unloading from a barge by the grapple, soil pumping from barges. The disadvantage of these methods is that backfill is done in consecutive stages, and soil, falling into water increases water specific weight to the pulp specific weight. As a result, the buoyancy force increases and, when backfill is accomplished, the pipeline is raised above the design reference mark. The aim of the research is to optimize the existing methods of pipelines backfill, which will prevent or reduce the rise of the pipeline from the design position during its backfill. The optimized methods of the submerged pipelines backfill, which use temporal metal and reinforced concrete loads or backfill by cofferdams, have been calculated with the help of APMWinMachine software. The results of the model calculation by the method of finite elements show the effectiveness of the proposed methods of the submerged pipeline backfill.

Аннотация. Сегодня засыпка уложенного в подводную траншею забалластированного трубопровода производится стандартными способами: последовательное рефулирование грунта земснарядами по пульпопроводу, сброс грунта саморазгружающимися шаландами, сброс грунта из барж путем выгрузки его грейфером, перекачивание грунта из барж. Недостатком данных методов засыпки подводного трубопровода является то, что засыпка ведется последовательно, а грунт, попадая в воду, вызывает увеличение удельного веса воды до удельного веса пульпы. Вследствие этого возрастает выталкивающая сила, под действием которой трубопровод поднимается, и после завершения засыпки оказывается выше проектной отметки. Целью работы является оптимизация существующих способов засыпки подводных трубопроводов, которая предотвратит или снизит выход трубопровода из проектного положения при его засыпке. С помощью пакета инженерных программ APMWinMachine рассмотрены и рассчитаны оптимизированные способы засыпки подводных трубопроводов, которые заключаются в использовании временных металлических или железобетонных пригрузов или засыпке трубопровода перемычками. Результаты расчетов моделей методом конечных элементов показывают эффективность предложенных способов засыпки.

Introduction

In the pipe conduit construction of submerged crossing, the problem of subaqueous pipelines escapement from the design position during the construction is commonly encountered, and, particularly, during the backfill of the trench ballasted pipelines laid in the bottom. This problem is commonly encountered in subsea pipelines construction by the trench method implemented by the public corporations such as joint stock company Podvodtruboprovodstroy (submerged crossing across the river Ob on the oil pipeline Surgut-Perm, submerged crossing across the river Ishim on the gas pipeline Ostrogozhsk-Belousov, and others), public corporation "Mezhregiontruboprovodstroy" (submerged

Kozhaeva K.V. Calculation of optimized methods of the river underwater pipeline backfill with the use of APMWinMachine 9.7. Magazine of Civil Engineering. 2016. No. 5. Pp. 42–66. doi: 10.5862/MCE.65.4

crossing across the river Volga on oil pipeline Druzhba-2, gas pipeline Yamal-Europe across the Baidarata Bay) and others.

By the trench method, the standard techniques of backing of the trench ballasted pipeline laid in the bottom are used: sequential deposition of soil by suction dredges along the slurry pipeline, soil discharge by self-dumping barges, unloading of soil from barge by grapple, soil pumping over from barges [1–14].

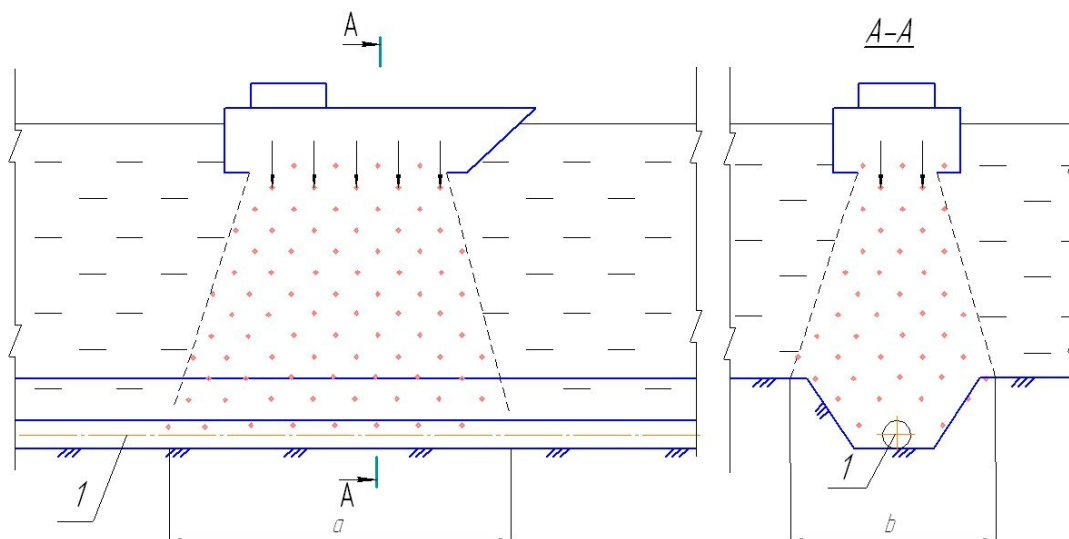
The imperfection of these methods of subaqueous pipeline backfill (especially by the method of soil discharge by self-dumping barges) is that backfill is done in consecutive stages, but soil, falling into water induces the increase of water specific weight from 1100 kg/m^3 to the pulp specific weight of 1400 kg/m^3 . As a result, the buoyancy force (under this force the pipeline elevates Archimedean force) increases and when backfill is accomplished, the pipeline is raised above the design reference mark. This is also a widely-spread problem during backfill pipeline outstretches, for instance, in marine pipelines [15–20].

Consequently, the task is to optimize the existing methods of backfill pipelines outstretches, in order to prevent or reduce the escapement of subsea pipelines from the design position during its backfill.

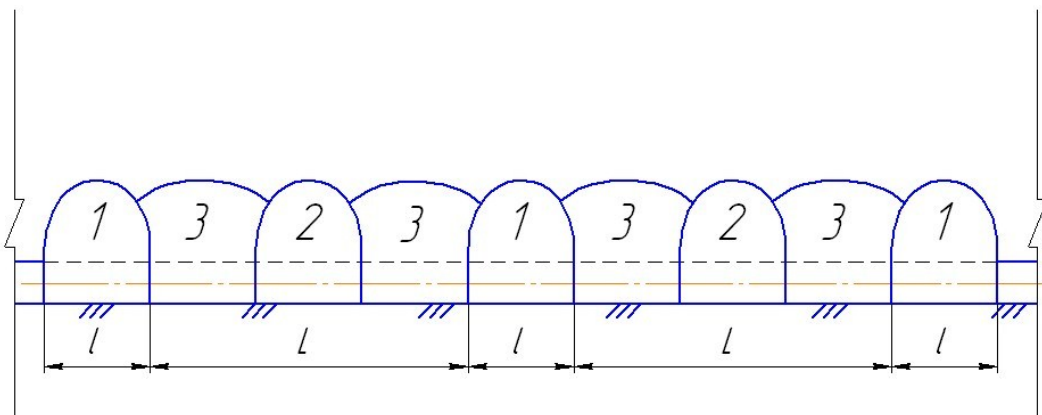
Methods

To prevent the escapement of submerged pipelines from the design position during its backfill with soil due to the increase of water special weight, and, as a result, increase of buoyancy force (Archimedean force), which influences the pipeline, the following method of backfill process rationalization of subaqueous pipe conduit is proposed [21]. The standard backfill methods of subsea pipe conduit are implemented sequentially, i.e. backfill is started from one spot and is led along the pipeline continuously. That is why water density increases because of soil balanced in water, the buoyancy force increases too, and the pipeline rises higher than the design position. There is also a flux availability which enables spreading suspended soil in the water along the developed bottom trench, hereupon the operating zone of this elevated Archimedean force increases. As a result, backfill is to be produced with extent "l" of cofferdams and "L" distance between them, and their proportions will be defined with the software APMWinMachine [22].

The backfill of subaqueous pipeline with self-dumping barges is proposed in Picture 1, during which the zone with length "a" and width "b" is developed. In this zone the specific water weight can reach 1400 kg/m^3 . The order of a submerged pipeline backfill with cofferdams by the optimized method is proposed in Picture 2.



Picture 1. The scheme of pipeline backfill with imported soil from self-dumping barges

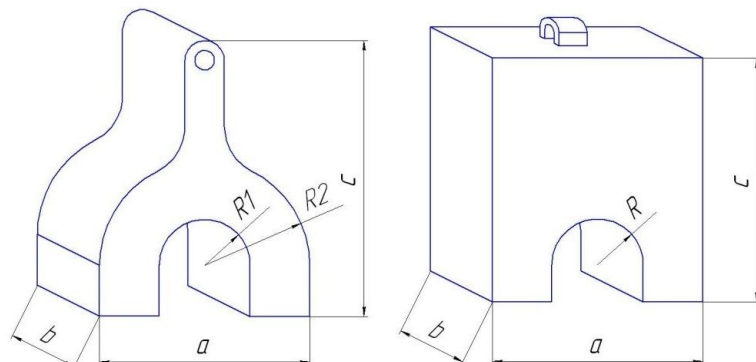


Picture 2. The order of submerged pipeline backfill with cofferdams.

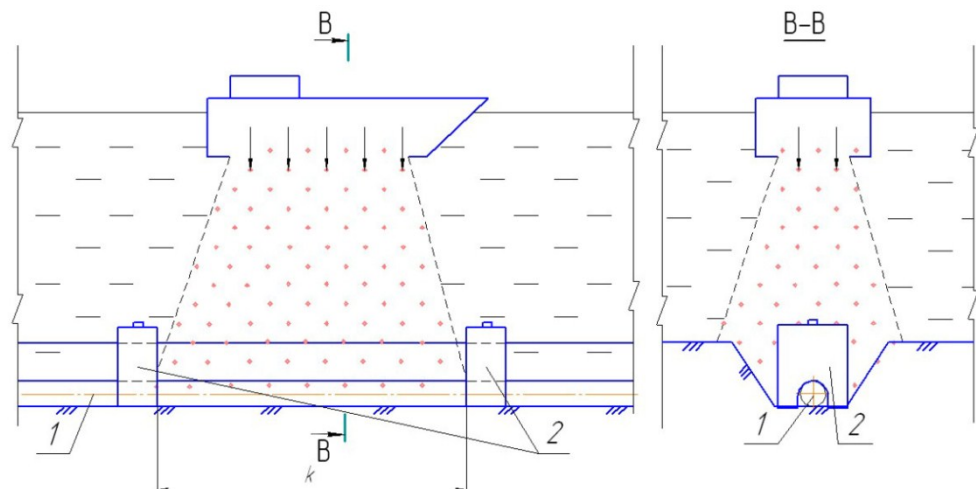
The optimized method of underwater pipeline backfill consists of the following stages. The pipeline "I" laid in a subaqueous trench is filled with cofferdams according to the order, presented in the Picture 2, with an extent "l" and distance "L" between them, the value of which is obtained by the rated way. The restraint of the cofferdam extent (approximately 10–30 meters) accommodates the absence of the floating-up capability of the pipeline in the starting period of backfill, and cofferdams themselves (number 1) do not enable the pipeline to float in the following zones (№ 2–№ 3) further on between the cofferdams (1, 2, 3 – is the sequence of the earth cofferdam backfill along the pipeline).

There is also another variant of the optimized method of a submerged pipeline backfill which is in the temporary plant of reinforced concrete and metal loads 2 on the ballasted pipeline "I" with the distance "k" between them during the execution of works as presented in Pictures 3 and 4. After the completion of works during the pipeline backfill, reinforced concrete or metal loads 2 are demounted, which means that they are of a reusable type, ipso facto, the rise in the cost of the backfill construction is negligible. The proportion of metal and concrete loads (a , b , c , R , R_1 , R_2) and also the distance "k" between them are defined by calculations in accordance with the theory of strength of materials [23] or with the assistance of different engineering programs for the determination of bending deflections and strained conditions by the method of finite elements, for example ANSYS or APMWinMachine [22].

Moreover, it is necessary to note that the given data will be different for certain conditions, which are defined by both the pipeline data (diameter, wall thickness, the behavior of pipe metal, location of the pipeline) and characteristics of the environment (type of backfill soil, alteration of specific water weight during the backfill soil), etc. During the estimation some assumptions are allowed. As far as coffering is estimated by reliability and stability of the pipeline position against the pipeline floating-up and all coffering is directed to withstand the resistance to the forces acting on the pipeline (buoyancy force, hydrodynamic action on water flow and so on), so the data referring to this influence is not considered and negative buoyancy of the pipeline compared to the effects under the standard conditions (during the backfill) goes into the pipeline stability position stock. That is why estimation is calculated for the part of buoyancy force, which occurs because of the alteration of specific water weight during the backfill soil.



Picture 3. The variants of reinforced concrete or metal loads, used in the optimized method of submerged pipeline backfill.



Picture 4. The arrangement scheme of reinforced concrete and metal loads during the optimized method of submerged pipeline backfill.

Results and Discussion

Let us calculate the parameters of the optimized backfill methods of riverside underwater transitions with an analytical approach and then, verify the accuracy of the calculation with the help of software engineering program APMWinMachine 9.7.

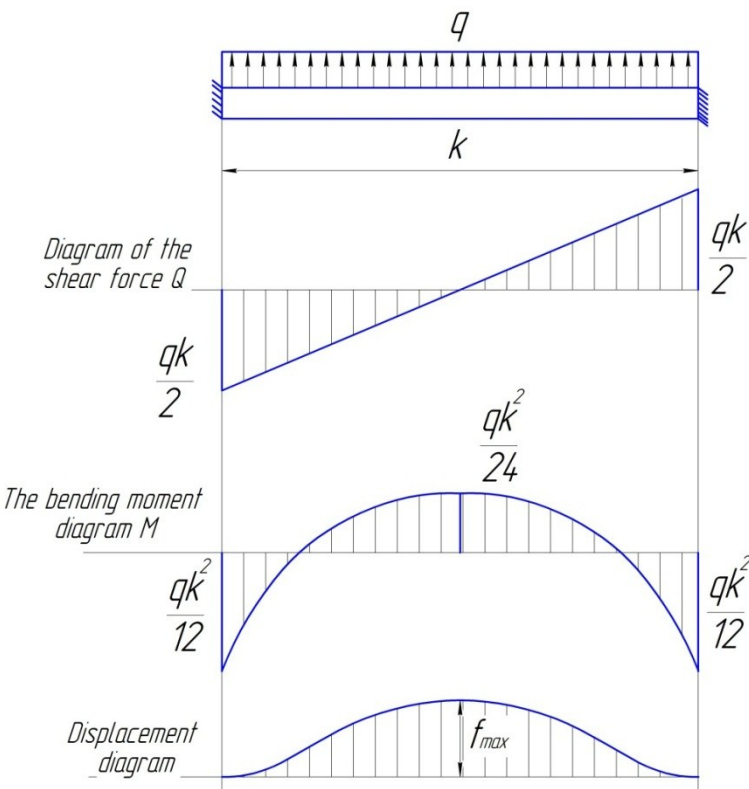
The initial data for calculation:

- the view of pumped-over product – gas;
- category of pipeline – I;
- the area of laying – Leningradsky District;
- the external diameter of the pipeline – 1020 mm;
- nominal pipeline thickness – 14 mm;
- the pressure in the pipeline – 6.3 Pa;
- fettling thickness – 30 mm;
- fettling tightness – 600 kg/m³;
- isolation thickness – 5 mm;
- backfill soil – silty;
- specific weight of soil – 18 kN/m;
- soil adherence – 2 kPa;
- single cast iron annular loads of mass – 1100 kg, 1130 pieces;
- pulp specific weight – 1400 kg/m³.

The calculation of the parameters of optimized backfill methods with the use of metal and ferric-concrete cantledges

According to [10], the acceptable deviation of pipeline axis from design position on the pipeline underwater transition is 100 mm.

The pipeline calculation is conducted according to the model of transversal-loaded beam fixed from both sides with anchorages as it is indicated in Picture 5. Shearing force diagrams Q are shown in Picture 5, as well as bending moment M and transition diagrams.



Picture 5. Design diagram and shearing force diagrams, bending moment and transition diagrams.

The distributed load "q" affects the entire area of underwater pipeline "k" and is directed upwards. The maximum bending moment emerges at the feet (ferroconcrete and metal cantledges) and is $M_{max} = M_f = \frac{qk^2}{12}$. In the "k" midspan the bending moment is equal to $M_m = \frac{qk^2}{24}$.

The maximum bending deflection is in the midspan and is defined by the formula (1):

$$f_{max} = \frac{1}{384} \cdot \frac{qk^4}{EI}, \quad (1)$$

where q – distributed load, affecting underwater pipeline as a result of its soil backfill and increase of specific water density with the soil on the quantity $\Delta\rho_w$ and estimated by formula (2), N/m:

$$q = n_p \frac{\pi D_l^2}{4} \Delta\rho_w g, \quad (2)$$

where n_p – the index of reliability of loading that equals 1,1 [11];

D_l – the external diameter of isolated lined pipeline, m;

$\Delta\rho_w$ – the alteration of water density during the pipeline backfill, submerged in the water with different soils (it is measured with the help of engineering research and by the natural experimental research), in their absence it is assumed for the most unfavorable cases as equal to $\Delta\rho_w = 300 \text{ kg/m}^3$);

g – acceleration of gravity m/s^2 ;

E – modulus of elasticity of pipe material, MPa;

I – axial moment of pipe inertia, m^4 :

$$I = \frac{\pi}{64} (D_e^4 - D_i^4), \quad (3)$$

k – opening, m.

Hereby, knowing all the necessary parameters, it is possible to estimate potential plugged bay that is the distance between temporary metal and ferroconcrete cantledges by formula (4):

Kozhaeva K.V. Calculation of optimized methods of the river underwater pipeline backfill with the use of APMWinMachine 9.7. Magazine of Civil Engineering. 2016. No. 5. Pp. 42–66. doi: 10.5862/MCE.65.4

$$k = \sqrt[4]{\frac{384 f_{max} EI}{q}}, \quad (4)$$

where f_{max} – the maximum bending deflection is in the midspan, acceptable deviation of pipeline axis from design position, $f_{max} = 100\text{мм}$.

Let us derive a formula for weighing (and in the series of dimensional measurement) cantledge:

1) each cantledge accommodates stability only in the half of the bay, that is $k/2$. The buoyancy force, affecting the pipeline section of $k/2$ length, determined by expansion of water density with the soil on the quantity $\Delta\rho_w$, is determined by formula (5):

$$F_{A,p} = q \frac{k}{2} = n_p \frac{\pi D_l^2}{4} \Delta\rho_w g \frac{k}{2}. \quad (5)$$

2) Consequently, the present buoyancy force is necessary to be pressed by usage of cantledge. The cantledge is affected by water buoyancy force with soil and it equals

$$F_{A,c} = n_p V_c \rho_{w.s}, \quad (6)$$

where V_c – the volume of cantledge is determined by formula, m^3 (7):

$$V_c = \frac{m_c}{\rho_c}, \quad (7)$$

where m_c – accumulation of cantledge, kg;

ρ_c – density of the cantledge material (steel, cast iron or ferroconcrete), kg/m^3 .

Consequently,

$$F_{A,c} = n_p \frac{m_c}{\rho_c} \rho_{w.s}. \quad (8)$$

The weight of cantledge in the air is determined by formula (9):

$$P_c = m_c g. \quad (9)$$

With the assumption that all forces affecting the cantledge must at least balance each other, we compose the equation of static balance of all the forces (10, 11):

$$P_c - F_{A,p} - F_{A,c} = 0, \quad (10)$$

$$m_c g - n_p \frac{\pi D_l^2}{4} \Delta\rho_w g \frac{k}{2} - n_p \frac{m_c}{\rho_c} \rho_{w.s} = 0. \quad (11)$$

From here the mass of cantledge is derived m_c :

$$m_c - n_p \frac{\pi D_l^2}{4} \Delta\rho_w \frac{k}{2} - n_p \frac{m_c}{\rho_c} \rho_{w.s} = 0, \quad (12)$$

$$m_c \left(1 - n_p \frac{\rho_{w.s}}{\rho_c}\right) - n_p \frac{\pi D_l^2}{4} \Delta\rho_w \frac{k}{2} = 0, \quad (13)$$

$$m_c = \frac{n_p \frac{\pi D_l^2}{4} \Delta\rho_w \frac{k}{2}}{1 - n_p \frac{\rho_{w.s}}{\rho_c}}. \quad (14)$$

Let us calculate the parameters for a specific pipeline with the initial data.

The distributed load, affecting underwater pipeline is calculated as follows:

$$q = n_p \frac{\pi D_l^2}{4} \Delta \rho_w g = 1.1 \cdot \frac{\pi \cdot 1.09^2}{4} \cdot 300 \cdot 9.81 = 3020.8 \text{ N/m.}$$

The distance between temporary metal and ferroconcrete cantledge is as follows:

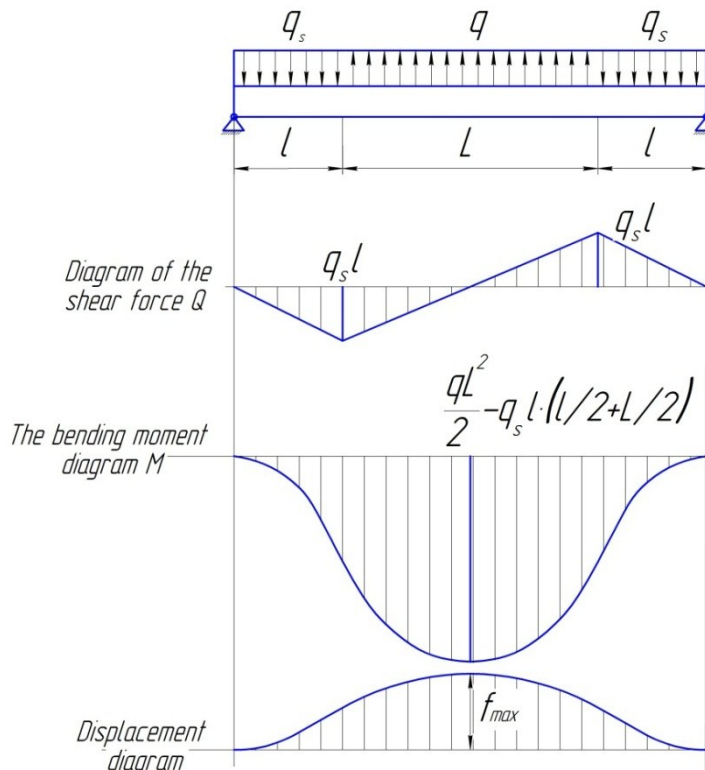
$$k = \sqrt[4]{\frac{384 f_{max} EI}{q}} = \sqrt[4]{\frac{384 \cdot 0.1 \cdot 2.06 \cdot 10^{11} \cdot 559843 \cdot 10^{-8}}{3020.8}} = 61.88 \text{ m.}$$

The mass of the cantledge for cast iron with a density is equal to $\rho_c = 7000 \text{ kg/m}^3$:

$$m_c = \frac{n_p \frac{\pi D_l^2}{4} \Delta \rho_w k}{1 - n_p \frac{\rho_{w,s}}{\rho_c}} = \frac{1.1 \cdot \frac{\pi \cdot 1.09^2}{4} \cdot 300 \cdot \frac{61.88}{2}}{1 - 1.1 \cdot \frac{1400}{7000}} = 12214.3 \text{ kg.}$$

The calculation of parameters of optimized backfill methods with the use of earth cofferdams

The pipeline calculation is conducted according to the model of transversal-loaded beam fixed from both sides with joints as it is indicated in Picture 6. Shearing force diagrams Q are shown in Picture 6, as well as bending moment M and transition diagrams.



Picture 6. Design diagram and shearing force diagrams, bending moment and transition diagrams

For the pipeline to be left in the design position during the backfill, the equation 15 is necessary:

$$2q_s l = qL, \quad (15)$$

where q_s – distributed load from the soil activity (with the record of buoyancy force affecting it), N/m:

$$q_s = (\gamma_s - \gamma_w) D_l h_0, \quad (16)$$

where γ_s – specific weight of soil in the air, N/m³;

γ_w – specific weight of water is assumed equal to $\gamma_w = 11000 \frac{N}{m^3}$;

Kozhaeva K.V. Calculation of optimized methods of the river underwater pipeline backfill with the use of APMWinMachine 9.7. Magazine of Civil Engineering. 2016. No. 5. Pp. 42–66. doi: 10.5862/MCE.65.4

h_0 – pipeline laying depth from the bottom of the basin to the top of the generating line, m.

Hereby, the support reactions equal zero (but in the reality they do not equal zero and they are up-directed, which is explained by negative buoyancy at the expense of reliability coefficient on the loads).

The distributed load "q" affects the entire area of underwater pipeline "L" and is directed upwards. The distributed load acts at the footings on the areas "l".

The maximum bending moment emerges in the midspan and is defined by formula 17:

$$M_{max} = \frac{qL^2}{2} - q_s l \left(\frac{l}{2} + \frac{L}{2} \right). \quad (17)$$

The maximum bending deflection is in the midspan. In the case of bending in the midspan, let us use the universal equations of methods of initial parameters 18, 19:

$$\theta = \theta_0 + \frac{1}{EI} \left[\sum m_i (z - a_i) + \sum F_i \frac{(z - b_i)^2}{2} + \sum q_i \frac{(z - c_i)^3}{6} \right]; \quad (18)$$

$$y = y_0 + \theta_0 z + \frac{1}{EI} \left[\sum m_i \frac{(z - a_i)^2}{2} + \sum F_i \frac{(z - b_i)^3}{6} + \sum q_i \frac{(z - c_i)^4}{24} \right]. \quad (19)$$

In our case the universal equations of the method of initial parameters are presented in formulas 20, 21:

$$\theta = \theta_0 + \frac{1}{EI} \left[q_s \frac{z^3}{6} - (q + q_s) \frac{(z - l)^3}{6} + (q + 2q_s) \frac{(z - l - L)^3}{6} \right]; \quad (20)$$

$$y = y_0 + \theta_0 z + \frac{1}{EI} \left[q_s \frac{z^4}{24} - (q + q_s) \frac{(z - l)^4}{24} + (q + 2q_s) \frac{(z - l - L)^4}{24} \right]. \quad (21)$$

The boundary conditions are as follows:

1) For $z=0, y=0 \Rightarrow y_0=0$ in the usage of (20);

2) For $z=2l+L, y=0 \Rightarrow$ in the usage (21):

$$0 = \theta_0 (2l + L) + \frac{1}{EI} \left[q_s \frac{(2l + L)^4}{24} - (q + q_s) \frac{(l + L)^4}{24} + (q + 2q_s) \frac{l^4}{24} \right];$$

$$\theta_0 = \frac{1}{EI(2l + L)} \left[(q + q_s) \frac{(l + L)^4}{24} - q_s \frac{(2l + L)^4}{24} - (q + 2q_s) \frac{l^4}{24} \right].$$

Consequently, in the midspan for $z = l + L/2$ the deflection is determined by formula 22 as follows:

$$y = \frac{1}{EI(2l + L)} \left[(q + q_s) \frac{(l + L)^4}{24} - q_s \frac{(2l + L)^4}{24} - (q + 2q_s) \frac{l^4}{24} \right] \left(l + \frac{L}{2} \right) + \frac{1}{EI} \left[q_s \frac{\left(l + \frac{L}{2} \right)^4}{24} - (q + q_s) \frac{(L/2)^4}{24} \right]. \quad (22)$$

As it is seen from (22), the deflection depends on the pipeline material characteristics (E), cross-section of pipeline (I) distributed loads (q, q_s) and also distances (l, L). Among the data there are 2 unknown values, to be defined. Proceeding from 15, "L" can be derived from "l" by formula 23:

$$L = \frac{2q_s l}{q}. \quad (23)$$

Considering formula (23) and knowing that the maximum bending deflection in the midspan is $y = f_{max} = 100\text{mm}$, let us substitute it in (22) and get the formula 24:

$$f_{\max} = \frac{1}{E \cdot I \cdot \left(2l + \frac{2q_s \cdot l}{q}\right)} \cdot \left[\left(q+q_s\right) \cdot \frac{\left(l + \frac{2q_s \cdot l}{q}\right)^4}{24} - q_s \cdot \frac{\left(2l + \frac{2q_s \cdot l}{q}\right)^4}{24} - (q+2q_s) \cdot \frac{l^4}{24} \right] \times \\ \times \left(l + \frac{\frac{2q_s \cdot l}{q}}{2}\right) + \frac{1}{E \cdot I} \cdot \left[q_s \cdot \frac{\left(l + \frac{q_s \cdot l}{q}\right)^4}{24} + q_s \cdot \frac{\left(\frac{q_s \cdot l}{q}\right)^4}{24}\right]. \quad (24)$$

Hereby, knowing all the necessary parameters, we can define "l" and then "L".

Let us calculate the parameters for a specific pipeline with the initial data.

The distributed load, affecting the underwater pipeline is as follows:

$$q = n_p \frac{\pi D_l^2}{4} \Delta \rho_w g = 1.1 \cdot \frac{\pi \cdot 1.09^2}{4} \cdot 170 \cdot 9.81 = 1711.8 \text{ N/m}.$$

The distributed load from the soil activity (with the record of buoyancy force affecting it) is follows:

$$q_s = (\gamma_s - \gamma_w) D_l h_0 = (18000 - 11000) \cdot 1.09 \cdot 1 = 7630 \frac{N}{m}$$

$$\text{For } f_{\max} = 100 \text{ mm}, l = 7.76 \text{ mm}, L = \frac{2q_s l}{q} = \frac{2 \cdot 7630 \cdot 7.76}{1711.8} = 69.177 \text{ m},$$

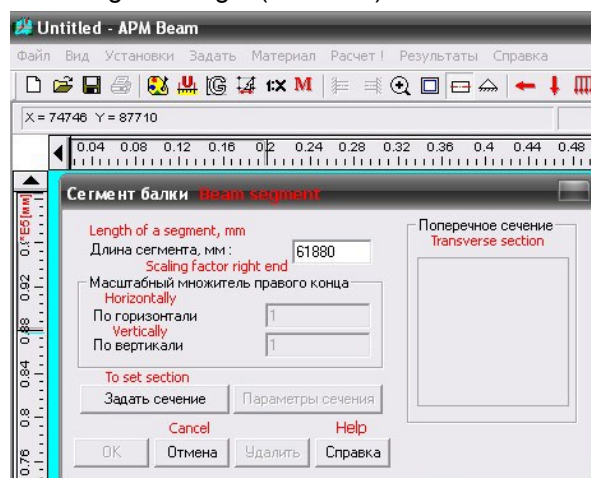
$$\text{for } f = 10 \text{ mm}, l = 4.36 \text{ mm}, L = \frac{2q_s l}{q} = \frac{2 \cdot 7630 \cdot 4.36}{1711.8} = 38.868 \text{ m}.$$

Let us verify the accuracy of the calculation with the help of software engineering program APMWinMachine 9.7. To calculate the parameters of the optimized method of underwater pipeline backfill with the use of reinforced concrete and metal loads, the program APMBeam is used, which can be applied for the calculation and design of braced construction elements by the method of finite elements and also for the calculation of the following parameters:

- 1) reactions in pillow blocks and restraints;
- 2) allocation of bending moments and bending corners;
- 3) allocation of twisting moments and twisting corners;
- 4) allocation of radial and axial forces;
- 5) allocation of movements and tensions.

All calculation should be divided into steps.

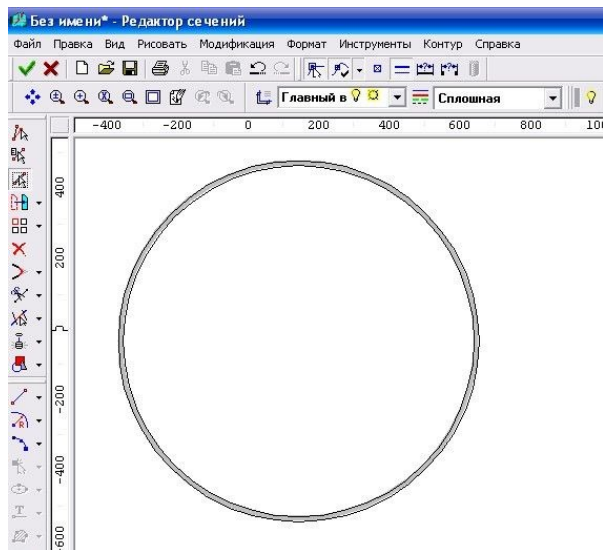
- 1) The created segment and given length (Picture 7):



Picture 7. The creation of a segment

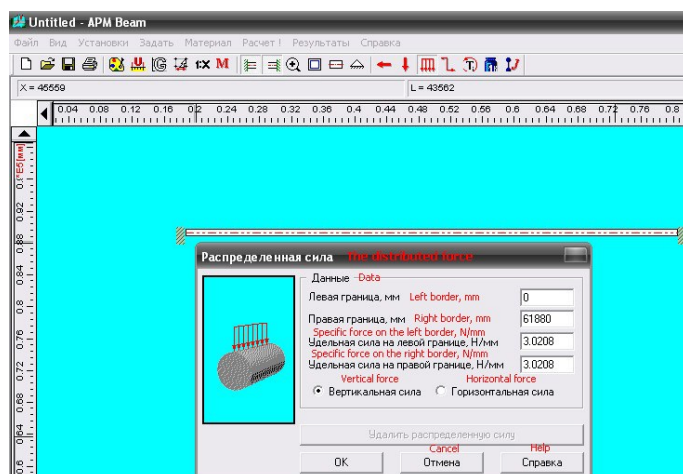
Kozhaeva K.V. Calculation of optimized methods of the river underwater pipeline backfill with the use of APMWinMachine 9.7. Magazine of Civil Engineering. 2016. No. 5. Pp. 42–66. doi: 10.5862/MCE.65.4

2) Set of the section (Picture 8):



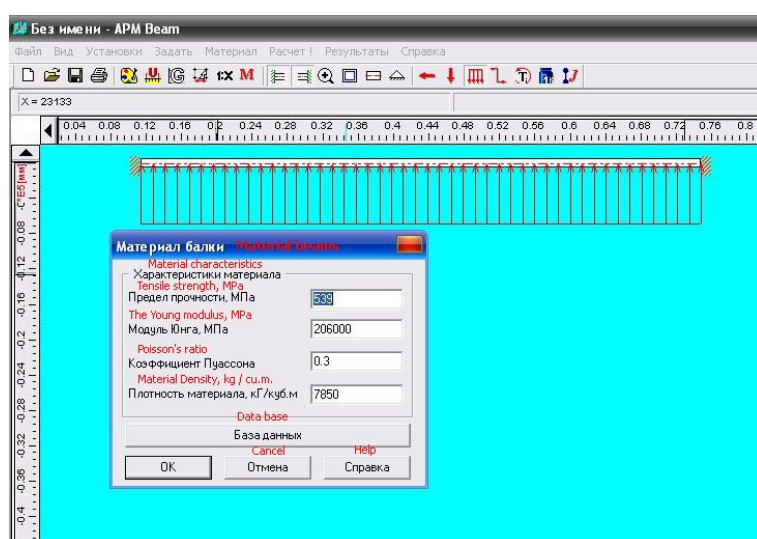
Picture 8. The creation of section

3) Setting of the pillow blocks and restraints and assigned loading q (Picture 9):



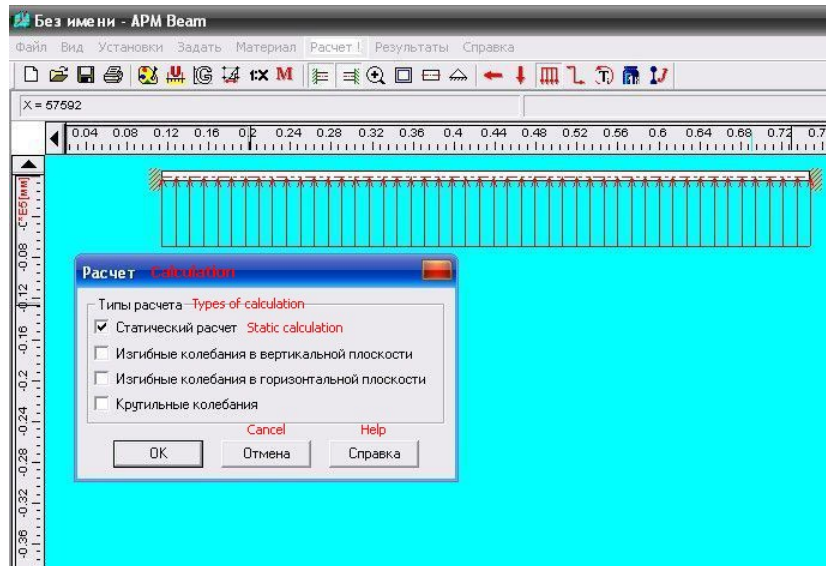
Picture 9. Assigning of pillow blocks and loading

4) Assignment of the material (Picture 10):



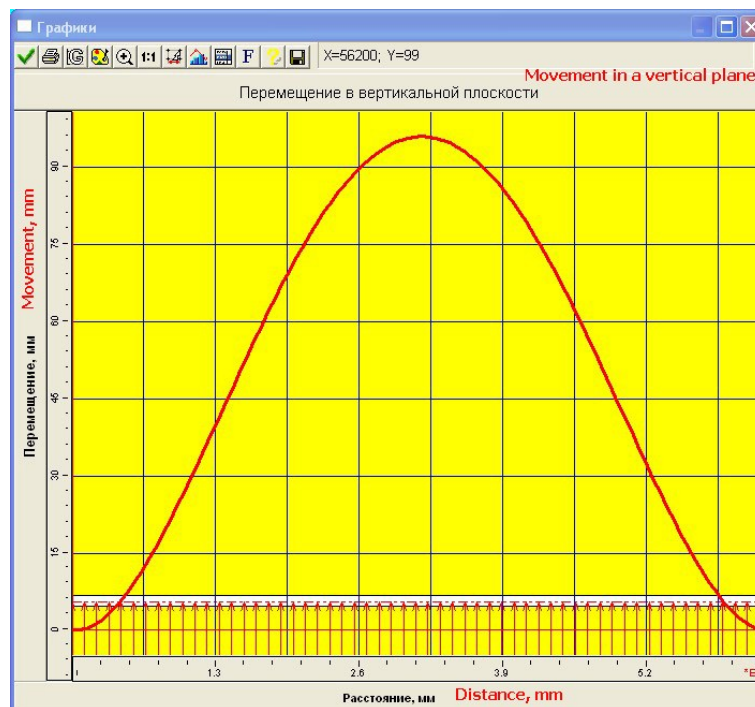
Picture 10. Assignment of material.

5) Choice of “Calculation” insert and assignment of “Static calculation” (Picture 11):



Picture 11. The start of calculation

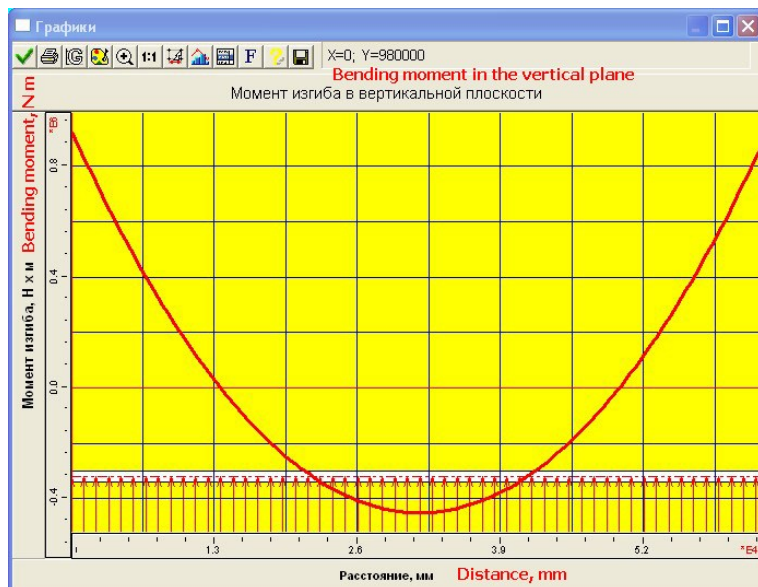
6) Choose the insert “Results” – “Graphical charts”. In the open window choose “Movements” – “Vert.” and analyze results (Picture 12):



Picture 12. Graphical Chart of vertical movements

In the graphical chart you can see that bearable vertical movements of the pipeline are 98 mm, which is acceptable and is approximately equal to rates of 100 mm. Therefore, the analytical calculations are correctly fulfilled [24–26].

Also, we can demonstrate other graphical charts of the obtained calculation: graphical charts of bending moments, tensions, which are chosen in the same window as a graphical chart of vertical movements (Pictures 13, 14).



Picture 13. The graphical chart of the bending moment



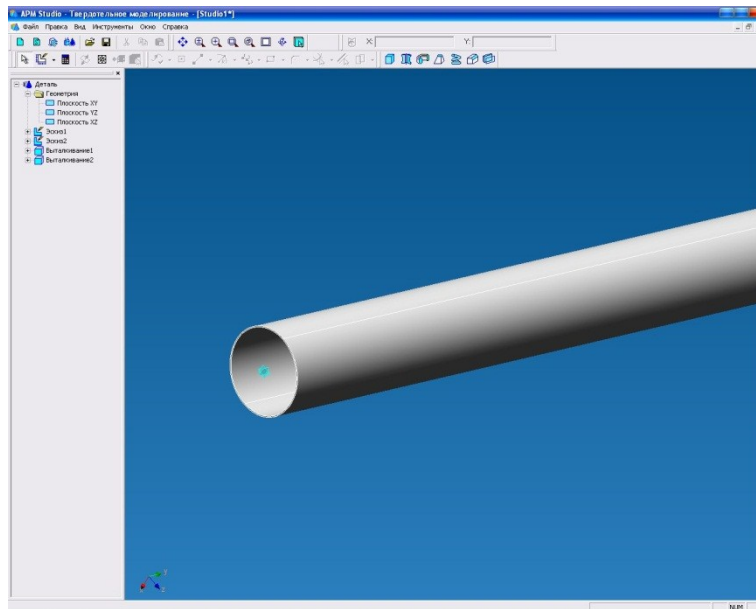
Picture 14. The tension graphical chart

From the tension graphical charts, we can see that maximum stress occurs at the ends of the zone (in the zone of loads mounting) and are approximately equal to 84 MPa, which notably lowers the point of steel fluidity equal to 390 MPa. Therefore, the toughness is provided.

Let us calculate the given example in the APM Structure3D program, which is designed for the calculation and design of spatial constructions and also the calculation of solid state models by the method of finite elements.

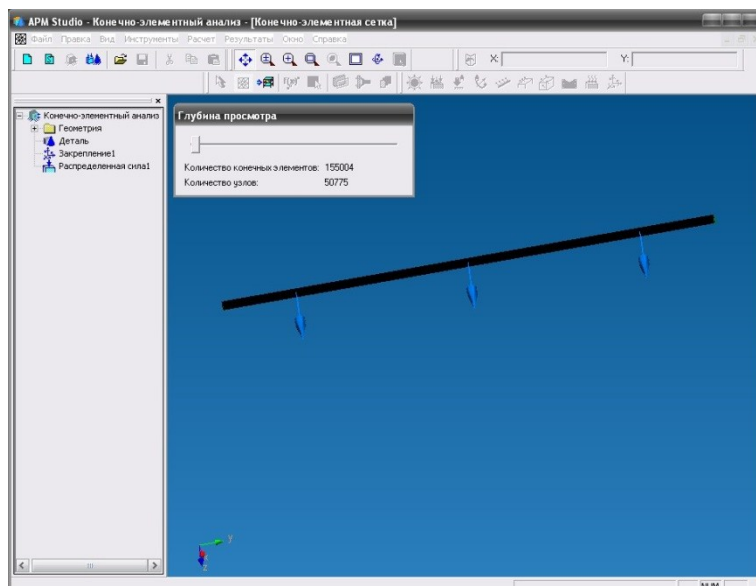
All the process of the calculation is divided into steps:

- 1) Create a solid state model of the pipeline zone with the set-up parameters from initial data and the length $k = 61.88$ m (Picture 15);



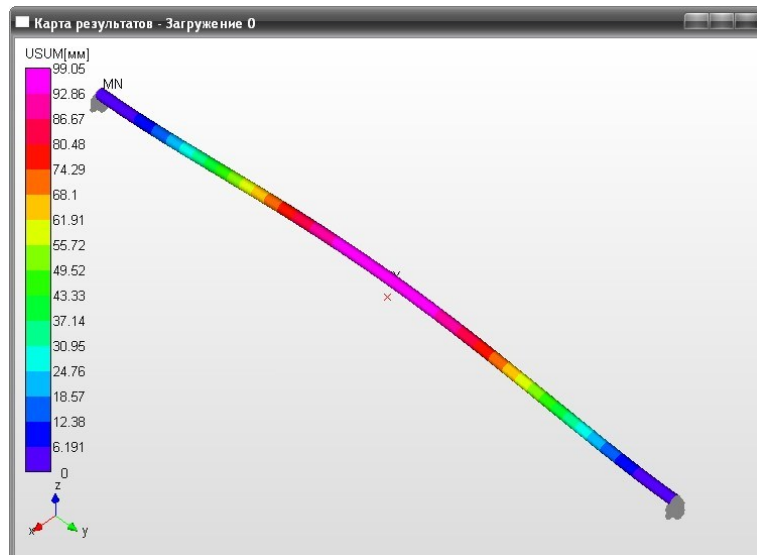
Picture 15. The creation of solid state pipeline model

- 2) Choose the function “The finite-element analysis”, where you can create a pillow block (restraints at the ends of pipeline) and specific weight q , which disrupts it into a finite-element mesh (Picture 16);

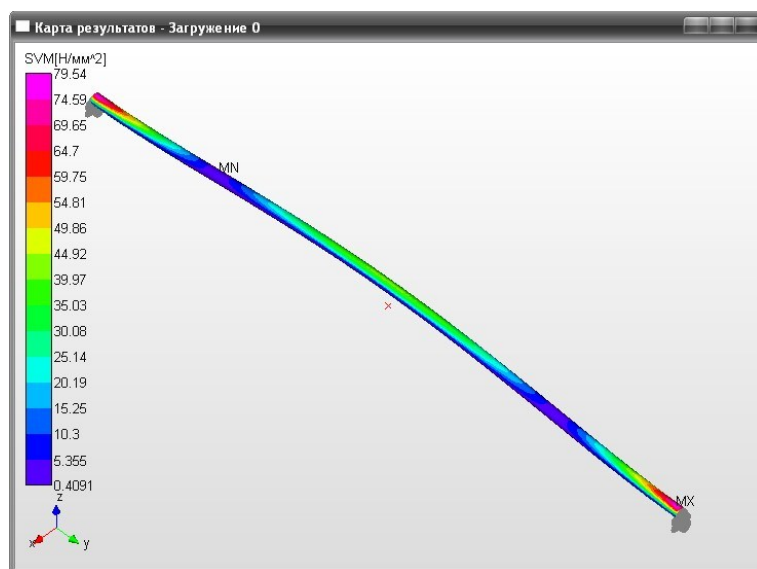


Picture 16. The creation of finite-element mesh

3) Move the given finite-element mesh into APMStructure3D, set up material and choose the insert “Calculation”–“Static calculation”, and after that the calculation the map of movements and tensions (Pictures 17, 18) is obtained.



Picture 17. The displacement map

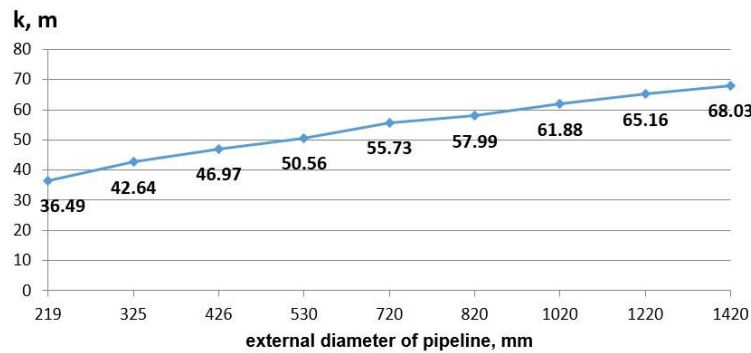


Picture 18. The tension map

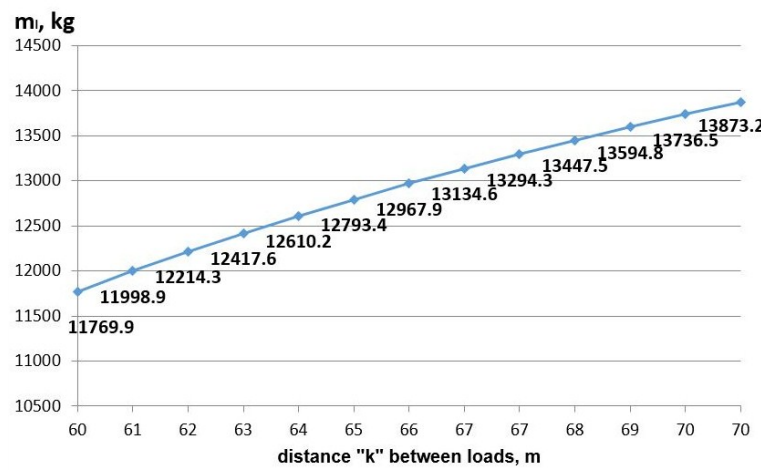
From the tension graphical charts, we can see that bearable tensions occur at the ends of the zone (in the zone of loads mounting), the stress rate reaches 79.54 MPa which is approximately equal to calculated tensions in the program APMBeam. Also, the stress rate reaches 99.05 mm, which is also acceptable and is approximately equally calculated.

Analyzing the results of all 3 calculations, we can draw the conclusion about the right choice of the calculation methods and accuracy of the obtained results for the concrete pipeline.

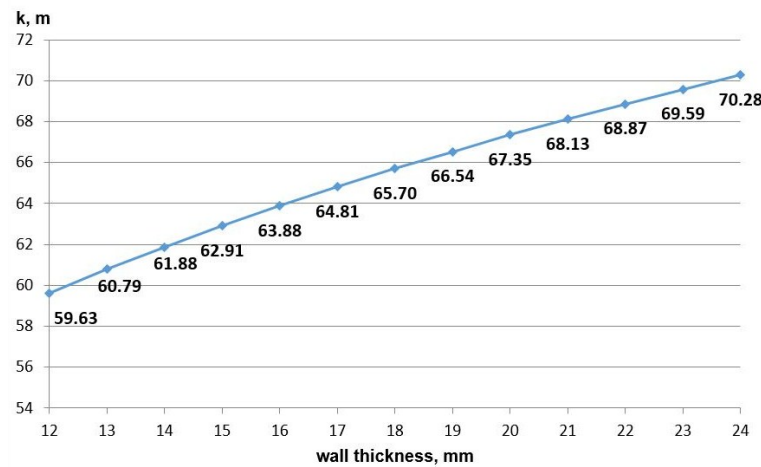
Then we can fulfil calculations by these methods for different cases. They will vary in diameter, in the pipeline wall thickness and the type of backfill soil. The final results will be the distance between metal and reinforced concrete loads “k” and the mass of this load (we will use the cast iron with density as the load material) (Pictures 19–24).



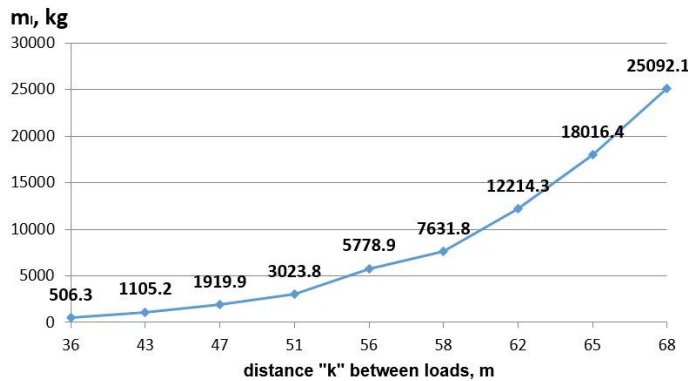
Picture 19. The diagram of distance “ k ” between the loads versus pipeline wall thickness with diameter 1020 mm, with the change of water density of 300 kg/m^3 and pulp specific weight of 1400 kg/m^3



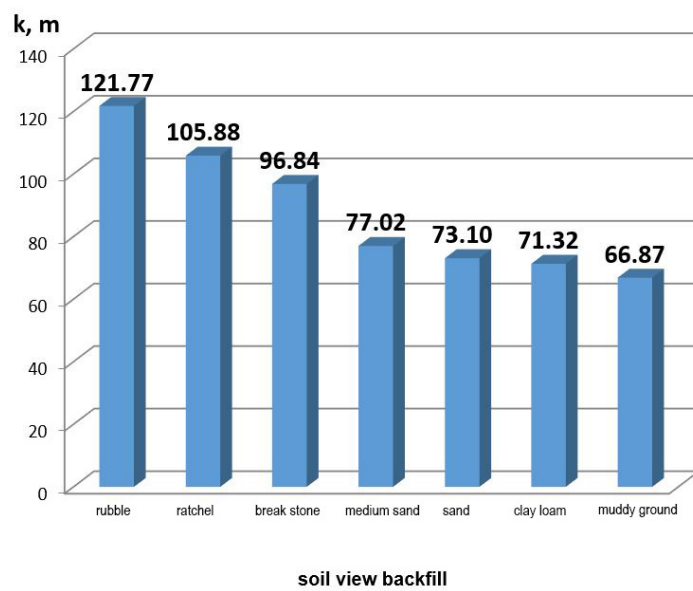
Picture 20. The diagram of load mass versus distance “ k ” between them for the given pipeline with diameter 1020 mm with the relevant walls thickness, with the change of water density of 300 kg/m^3 and pulp specific weight of 1400 kg/m^3



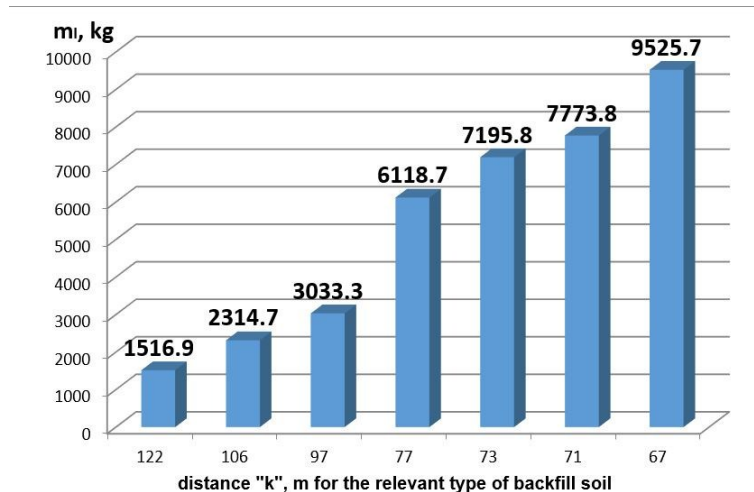
Picture 21. The diagram of the distance between loads “ k ” versus external diameter of the pipeline for the pipelines with the wall thickness of 14 mm, with the change of water density of 300 kg/m^3 and pulp specific weight of 1400 kg/m^3



Picture 22. The diagram of load mass versus distance k between them for the given pipelines of different diameters with the wall thickness 14 mm, with the change of water density of 300 kg/m³ and pulp specific weight of 1400 kg/m³



Picture 23. The diagram of the distance between loads "k" versus soil view backfill for the pipeline with outboard diameter 1020 mm, wall thickness 14 mm, with different values of change of density of water and pulp specific weight



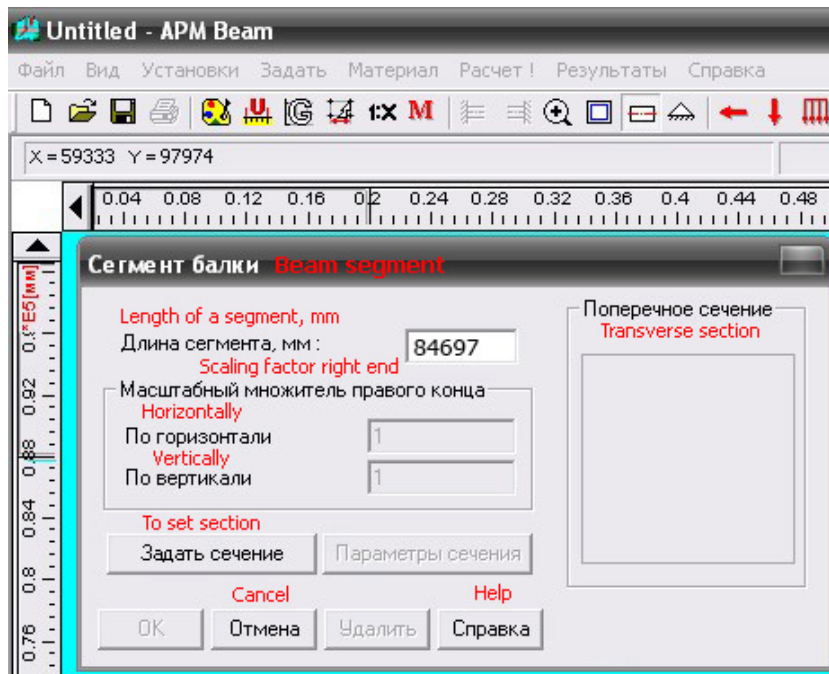
Picture 24. The diagram of load mass versus distance "k" between them for the pipeline with the outboard diameter 1020 mm, wall thickness 14 mm with the backfill of relevant soil sorts

Now we examine the parameters of the optimized way of backfill subaqueous pipeline with the cofferdams for analogous initial data.

We begin the calculation with the help of software engineering programs APMWinMachine 9.7, particularly in APM Beam.

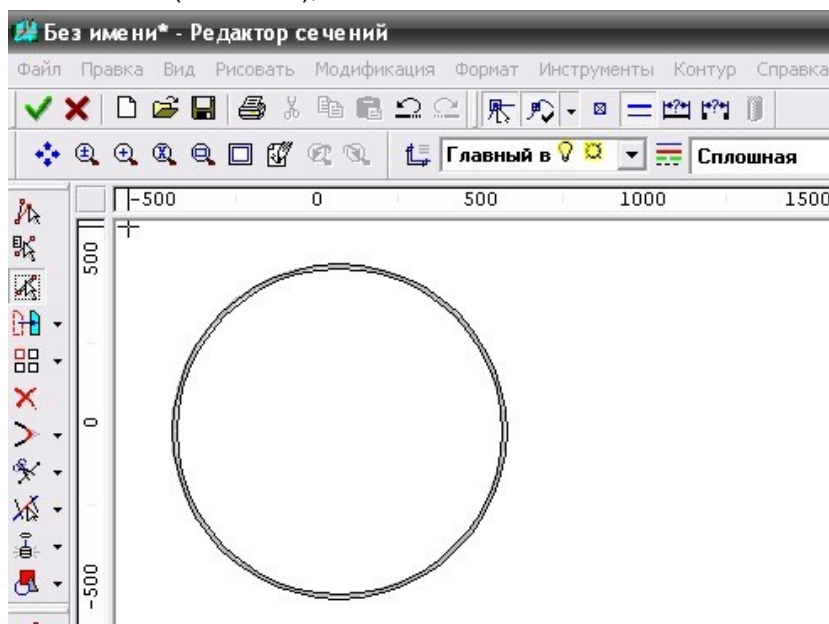
We divide all the calculation into the following steps:

- 1) Create segment with the given length ($2l + L = 2 * 7.76 + 69.177 = 84.697 \text{ m}$) (Picture 25);



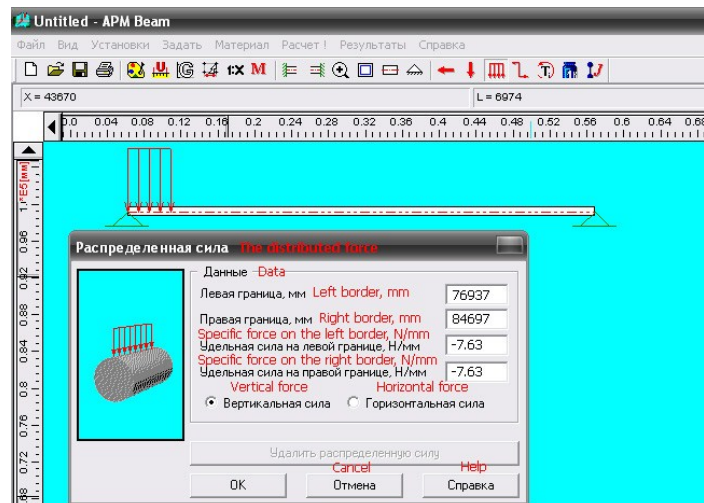
Picture 25. The creation of segment

- 2) Setting of the section (Picture 26);



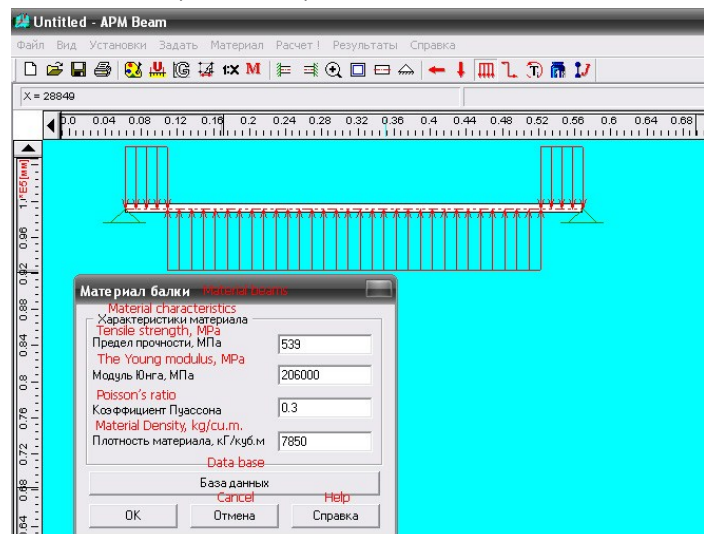
Picture 26. The creation of section

3) Setting of pillow blocks and restraints and assigned loading (Picture 27);



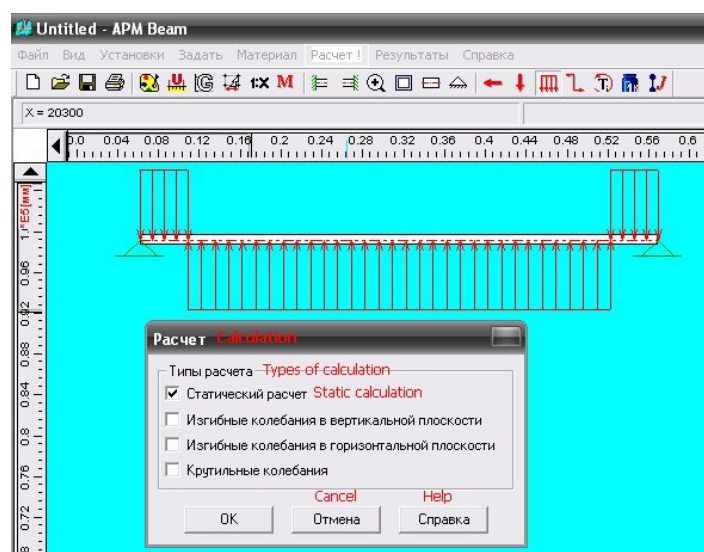
Picture 27. Assigning of pillow blocks and loading

4) Assignment of the material (Picture 28);



Picture 28. Assignment of material

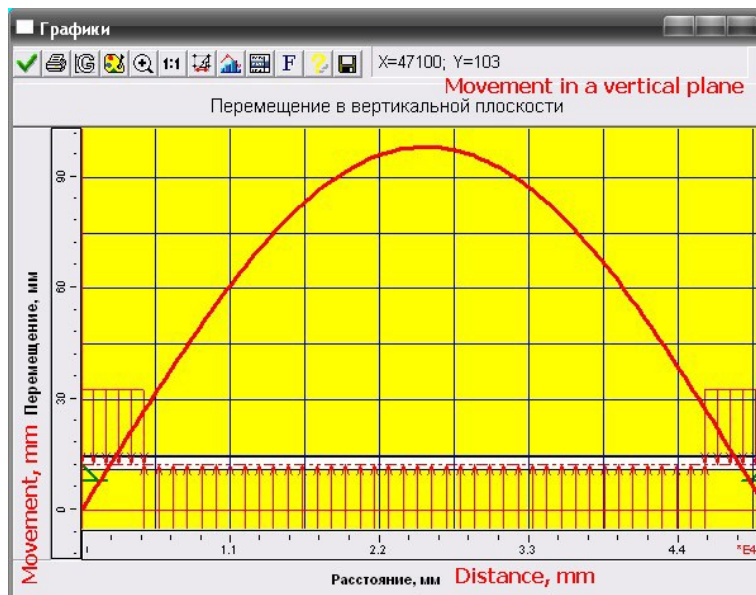
5) Choice of “Calculation” insert and assignment of “Static calculation” (Picture 29);



Picture 29. The start of the calculation

Кожаева К.В. Расчет оптимизированных способов засыпки речного подводного трубопровода с использованием APMWinMachine 9.7 // Инженерно-строительный журнал. 2016. № 5(65). С. 42–66.

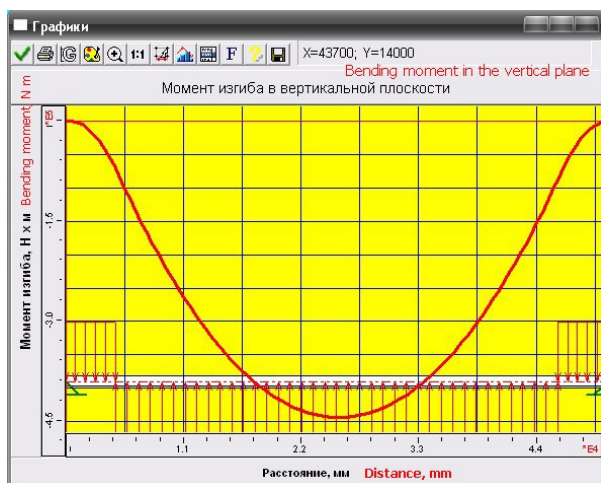
6) Choose the insert "Results"—"Graphical charts". In the open window choose "Movements"—"Vert." and analyze results (Picture 30).



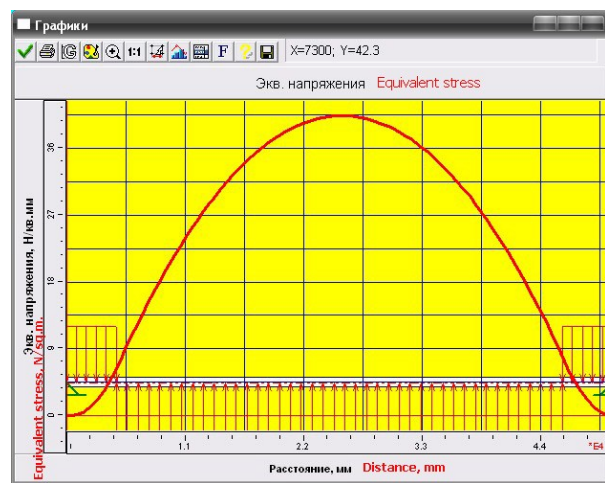
Picture 30. Graphical Chart of vertical movements

In the graphical chart you can see that bearable vertical movements of the pipeline are equal to 98 mm, which is acceptable and is approximately equal to rates 100 mm. Therefore, the analytical calculations are correctly fulfilled.

We can also demonstrate other graphical charts of the obtained calculation results: graphical charts of bending moments, tensions, which are chosen in the same window as a graphical chart of vertical movements (Pictures 31, 32).



Picture 31. The graphical chart of bending moment



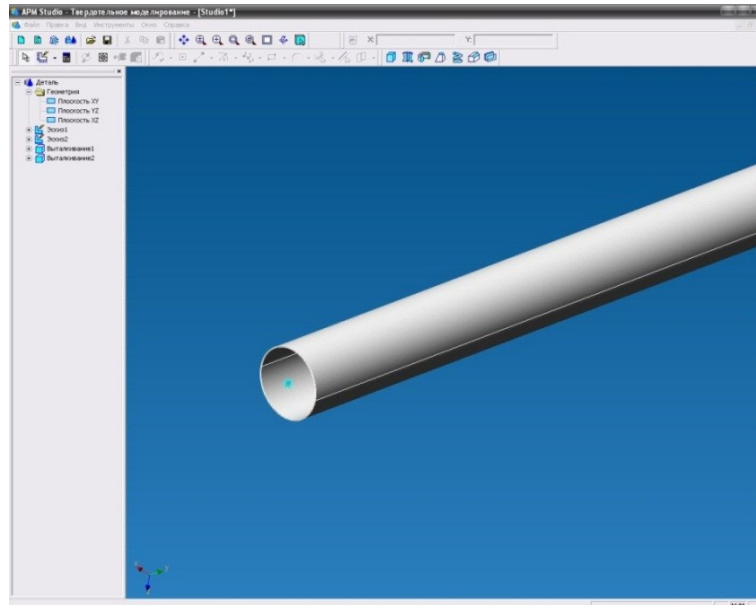
Picture32. The tension graphical chart

From the tension graphical charts, we can see that bearable tensions occur at the midspan zone and they are approximately equal to 40.3 MPa, which notably lowers the point of steel fluidity equal to 390 MPa. Therefore, the toughness is provided.

Let us calculate the given example in the program APM Structure3D.

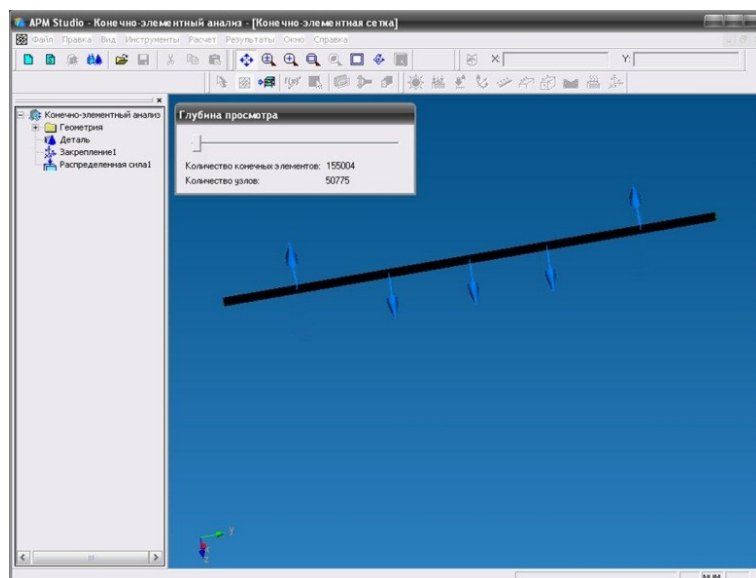
The calculation process is divided into the following steps:

- 1) Create a solid state model of pipeline zone with the set-up parameters from initial data and the length 84.697 m (Picture 33);



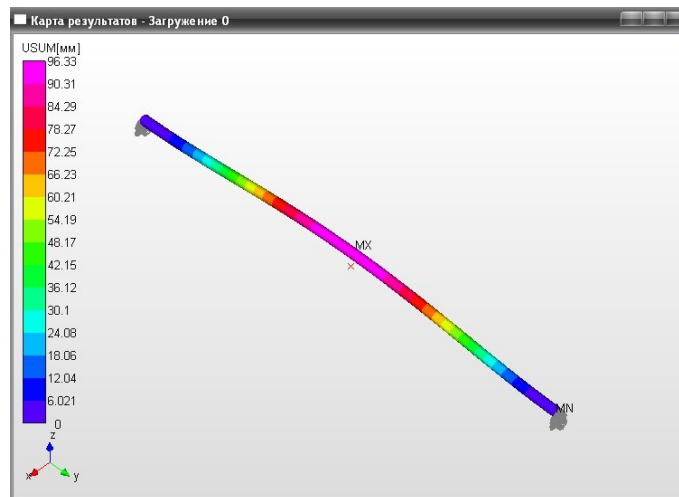
Picture 33. The creation of solid state pipeline model

- 2) Choose function “The finite-element analysis”, where you can create pillow blocks (restraints at the ends of pipeline) and specific weight, which disrupt it into finite-element mesh (Picture 34);

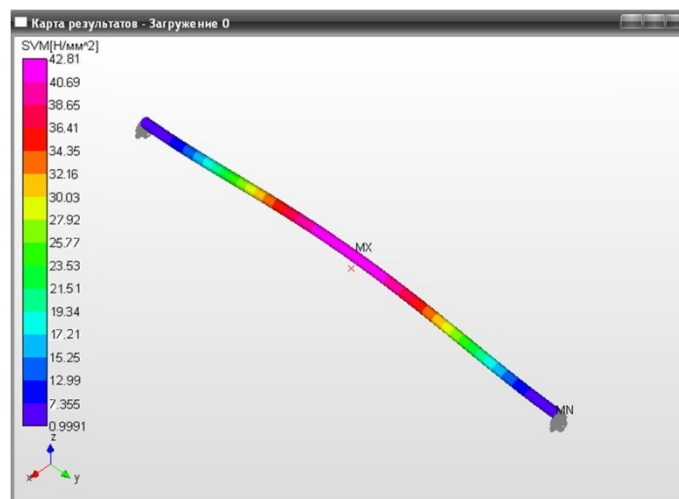


Picture 34. The creation of finite-element mesh

3) Move the given finite-element mesh into APM Structure3D, set up material and choose the insert "Calculation"—"Static calculation", after the calculation the map of movements and tensions (Pictures 35, 36) is obtained.



Picture 35. The displacement map

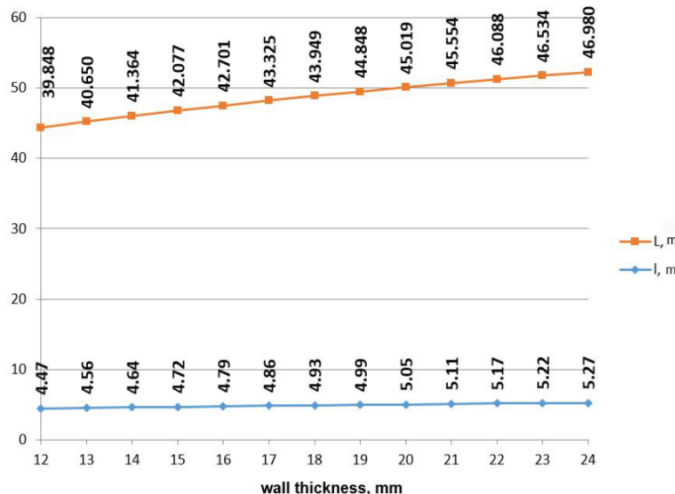


Picture 36. The tension map

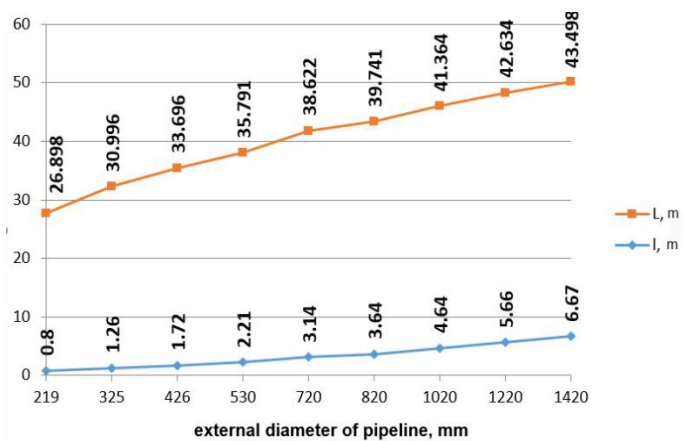
From the tension graphical charts, we can see that bearable tensions occur at the ends of the zone (in the zone of loads mounting), the stress rate reaches 42.81 MPa which is approximately equal to calculated tensions in the program APMBeam. Also, the stress rate reaches 96.33 mm, which is also acceptable and approximately equally calculated.

Analyzing the results of all three calculations, we can draw the conclusion about the right choice of the calculation methods and accuracy of the obtained results for the concrete pipeline.

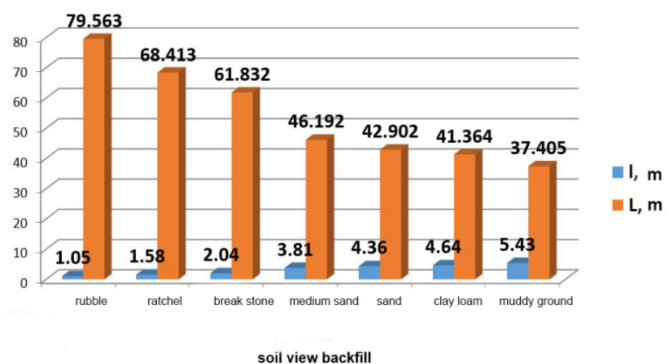
Then we can fulfill calculations by these methods for different cases. They will vary in diameter, in the pipeline wall thickness, also the type of backfill soil. The final results will be the distances "l" and "L" (Pictures 37–39).



Picture 37. The diagram of distance “I” and “L” versus pipeline wall thickness with diameter 1020 mm, with the change of water density of 170 kg/m³ and pulp specific weight of 1270 kg/m³, soil – loamy soil.



Picture 38. Diagram of distance “I” and “L” versus external diameter of the pipeline for pipelines with wall thickness 14 mm, with the change of water density of 170 kg/m³ and pulp specific weight of 1270 kg/m³, soil – loamy soil.



Picture 39. Diagram of distance “I” and “L” versus soil sort backfill for the pipeline with the outboard diameter of 1020 mm, wall thickness 14 mm, with different values of change of water density of and pulp specific weight

On the diagrams, presented in pictures 37–39, it can be seen that the results are significant for “I” from 0.8 to 6.67 m and for “L” from 26.898 to 79.563 m. These results can be explained by the dependence of these values from many parameters, not only inherent to backfill soil, but also to pipeline characteristics. But, despite that, these methods of backfill of subaqueous pipeline are very effective, because, according to all calculations, they provide the design position of subaqueous pipeline after backfill fulfillment. Moreover, the expenses for metal or reinforced loads, for their mounting and

demounting, connected with backfill technology of underwater pipeline backfill by cofferdams, are still much smaller due to the method of execution of works, dredging works, etc.

So far, the similar calculation of existing methods of backfill has not been conducted yet, which proves the innovativeness of the proposed ways of underwater pipeline backfill [27]. However, the method is paid much attention to in such works as [28–42] due to operating reliability of submarine pipelines depending on the methods of construction. The causes of the accidents in underwater pipelines due to imperfection of the construction methods are also examined.

Conclusions

1. The article examines the existing methods of submerged pipelines backfill, and determines their deficiencies. The optimized methods of backfill which were patented are proposed in the article.
2. All optimized methods of backfill have been designed with the help of software engineering programs APM WinMachine 9.7, particularly in APM Beam, APM Studio and APM Structure3D programs. The results of the model calculation by the method of finite elements prove the effectiveness of the proposed methods of submerged pipeline backfill.

References

1. Zabela K.A., Kraskov V.A., Moskvich V.M., Soshchenko A.Ye. *Bezopasnost' pereseceniya truboprovodami vodnykh pregrad* [Safety of crossing by pipelines of water barriers]. Moscow: Nedra, 2001. 194 p. (rus)
2. Borodavkin P.P., Berezin V.L. *Sooruzheniye magistralnykh truboprovodov* [Construction of the main pipelines]. Moscow: OOO "Izdatelstvo "Enerdzhi Press", 2011. 480 p. (rus)
3. Borodavkin P.P., Berezin V.L., Shadrin O.B. *Podvodnyye truboprovody* [Subsea pipelines]. Moscow: Nedra, 1979. 415 p. (rus)
4. Borodavkin P.P. *Podzemnyye magistralnyye truboprovody* [Underground main pipelines]. Moscow: OOO "Izdatelstvo "Enerdzhi Press", 2011. 480 p. (rus)
5. Britanskiy standart BS 8010. *Prakticheskoye rukovodstvo dlya proyektirovaniya, stroytelstva i ukladki truboprovodov, podvodnyye truboprovody* [Practical guidance for design, constructions and laying of pipelines, underwater pipelines]. Part 1, 2, 3. 1993. (rus)
6. VSN 010-88 *Stroytelstvo magistralnykh i promyslovyykh truboprovodov. Podvodnyye perekhody* [Construction of the main and field pipelines. Underwater transitions]. Moscow: Minnefteprovodstroy, 1990. 103 p. (rus)
7. Kukushkin B.M. *Stroytelstvo podvodnykh truboprovodov* [Construction of underwater pipelines]. Moscow: Nedra, 1982. 176 p. (rus)
8. RD 75.200.00-KTN-404-09. *Normy proyektirovaniya perekhodov magistralnykh nefteprovodov i nefteproduktoprovodov cherez vodnyye pregrady* [Norms of design of transitions of the main oil pipelines through water barriers]. Moscow: OAO "AK "Transneft", 2009. 140 p. (rus)
9. Ivanov V.A., Kuzmin S.V., Kramskoy V.F., Toropov S.Yu. *Sooruzheniye podvodnykh perekhodov magistralnykh truboprovodov: Kurs lektsiy* [Construction of underwater transitions of the main pipelines: course of lectures]. Tyumen: TymGNGU, 2003. 217 p. (rus)
10. SP 108-34-97. *Sooruzheniye podvodnykh perekhodov* [Construction of underwater transitions]. Moscow: RAO "Gazprom", 1998. 47 p. (rus)
11. SP 36.13330.2012. *Magistralnyye truboprovody. Aktualizirovannaya redaktsiya SNiP 2.05.06-85** [Main pipelines]. Moscow: Minregion Rossii, 2013. 99 p. (rus)
12. SP 86.13330.2014. *Magistralnyye truboprovody. Aktualizirovannaya redaktsiya SNiP III-42-80** [Main pipelines]. Moscow: Minstroy Rossii, 2014. 223 p. (rus)
13. STO Gazprom 2-2.1-249-2008. *Magistralnyye*

Литература

1. Забела К.А., Красков В.А., Москвич В.М., Сощенко А.Е. Безопасность пересечения трубопроводами водных преград. М.: Недра, 2001. 194 с.
2. Бородавкин П.П., Березин В.Л. Сооружение магистральных трубопроводов. М.: ООО «Издательство «Энерджи Пресс», 2011. 480 с.
3. Бородавкин П.П., Березин В.Л., Шадрин О.Б. Подводные трубопроводы. М.: Недра, 1979. 415 с.
4. Бородавкин П. П. Подземные магистральные трубопроводы. М.: ООО «Издательство «Энерджи Пресс», 2011. 480 с.
5. Британский стандарт BS 8010. Практическое руководство для проектирования, строительства и укладки трубопроводов, подводные трубопроводы. Ч. 1, 2, 3. 1993.
6. ВСН 010-88 Строительство магистральных и промысловых трубопроводов. Подводные переходы. М.: Миннефтепроводстрой, 1990. 103 с.
7. Кукушкин Б.М. Строительство подводных трубопроводов. М.: Недра, 1982. 176 с.
8. РД 75.200.00-КТН-404-09. Нормы проектирования переходов магистральных нефтепроводов и нефтепродуктопроводов через водные преграды. М.: ОАО «АК «Транснефть», 2009. 140 с.
9. Иванов В.А., Кузьмин С.В., Крамской В.Ф., Торопов С.Ю. Сооружение подводных переходов магистральных трубопроводов: Курс лекций. Тюмень: ТюмГНГУ, 2003. 217 с.
10. СП 108-34-97. Сооружение подводных переходов. М.: РАО «Газпром», 1998. 47 с.
11. СП 36.13330.2012. Магистральные трубопроводы. Актуализированная редакция СНиП 2.05.06-85*. М.: Минрегион России, 2013. 99 с.
12. СП 86.13330.2014. Магистральные трубопроводы. Актуализированная редакция СНиП III-42-80*. М.: Минстрой России, 2014. 223 с.
13. СТО Газпром 2-2.1-249-2008. Магистральные газопроводы. М.: ООО «ИРЦ газовой промышленности», 2008. 157 с.
14. Мустафин Ф.М., Быков Л.И. Технология сооружения газонефтепроводов. Т. 1. Уфа: Нефтегазовое дело, 2007. 632 с.
15. Астафьев В.Н. Проектирование подводных трубопроводов в условиях арктических морей. Уфа: Изд-во УГНТУ, 2000. 64 с.
16. Бородавкин П.П. Морские нефтегазовые сооружения. Ч. 1. Конструирование. М.: ООО «Недра-бизнесцентр»,

Kozhaeva K.V. Calculation of optimized methods of the river underwater pipeline backfill with the use of APMWinMachine 9.7. *Magazine of Civil Engineering*. 2016. No. 5. Pp. 42–66. doi: 10.5862/MCE.65.4

- gazoprovody* [Main gas pipelines]. Moscow: ООО "IRTs gazovoy promyshlennosti", 2008. 157 p. (rus)
14. Mustafin F.M., Bykov L.I. *Tekhnologiya sooruzheniya gazonfteprovodov*. T. I [Technology of a construction of gas and oil pipelines. Vol. I]. Ufa: Neftegazovoye delo, 2007. 632 p. (rus)
 15. Astafyev V.N. *Proyektirovaniye podvodnykh truboprovodov v usloviyah arkticheskikh morey* [Design of underwater pipelines in the conditions of the Arctic seas]. Ufa: Izd-vo UGNTU, 2000. 64 p. (rus)
 16. Borodavkin P.P. *Morskiye neftegazovyye sooruzheniya. Ch. 1. Konstruirovaniye* [Sea oil and gas constructions. P.1. Designing]. Moscow: ООО "Nedra-biznestsentr", 2006. 555 p. (rus)
 17. Borodavkin P.P. *Morskiye neftegazovyye sooruzheniya. Ch. 1. Tekhnologiya stroitelstva* [Sea oil and gas constructions. P.1. Technology of construction]. Moscow: ООО "Nedra-biznestsentr", 2007. 408 p. (rus)
 18. VN 39-1.9-005-98. *Normy proyektirovaniya i stroitelstva morskogo gazoprovoda* [Norms of design and construction of the sea gas pipeline]. Moscow: ОАО "Газпром", 1998. 19 p. (rus)
 19. Goryainov Yu.A., Fedorov A.S. *Morskiye truboprovody* [Sea pipelines]. Moscow: ООО "Nedra-Biznestsentr", 2001. 131 p. (rus)
 20. Kapustin K.Ya., Kamyshev M.A. *Stroitelstvo morskikh truboprovodov* [Construction of sea pipelines]. Moscow: Nedra, 1982. 207 p. (rus)
 21. Patent RF № 2515584. 10.05.2014. Mustafin F.M., Kutsenko K.V., Fayruzov V.M., Shammazov A.M., Kotov M.Yu., Mustafin I.G., Mamliyev E.V., Dilimiyev I.N. Sposob zasyipki ulozhennogo v podvodnuyu transheyu truboprovoda [The method of backfilling of the pipeline laid in an underwater trench]. Bulletin "Inventions. Utility Models". 2014, No. 13. (rus)
 22. Zamriy A.A. *Proyektirovaniye i raschet konechnykh elementov trekhmernykh konstruktsiy v srede APM Structure3D* [Design and calculation of final elements of three-dimensional designs in the environment of APM Structure3D]. Moscow: Izdatelstvo APM, 2006. 288 p. (rus)
 23. Belyayev N.M. *Soprotivleniye materialov* [Strength of materials]. Moscow: Glavnaya redaktsiya fiziko-matematicheskoy literatury izd-va «Nauka», 1976. 608 p. (rus)
 24. Aynbinder A. B. *Raschet magistralnykh i promyslovyykh truboprovodov na prochnost i ustoychivost* [Calculation of the main and field pipelines on durability and stability]. Moscow: Nedra, 1991. 287 p. (rus)
 25. Bykov L.I., Mustafin F.M., Rafikov S.K., Nechval A.M., Gamburg I.Sh. *Tipovyye raschety pri proyektirovaniy, stroitelstve i remonte gazonfteprovodov* [Standard calculations at design, construction and repair of gas and oil pipelines]. Saint Petersburg: Nedra, 2011. 748 p. (rus)
 26. Yasin E.M., Chernikin V.I. *Ustoychivost podzemnykh truboprovodov* [Stability of underground pipelines]. Moscow: Nedra, 1968. 120 p. (rus)
 27. Mustafin F.M., Fayruzov V.M., Shestakov I.A. Sposob zasyipki podvodnogo truboprovoda [The method backfill an underwater pipeline]. *Transport i khraneniye nefteproduktov i uglevodordnogo syrya*. 2012. No. 4. Pp. 46–47. (rus)
 28. Nikiforov V.A. *Analiz osnovnykh metodov stroyitelstva podvodnykh perekhodov magistralnykh truboprovodov* [An analysis of the main methods of construction of underwater crossings of main pipelines]. *Nauchnoye obozreniye: teoriya i praktika*. 2012. No. 3. Pp. 10–17. (rus)
 29. Komarov D.N., Korolenok V.A. *Raschet truboprovoda na ustoychivost ot vsplityiya pri stroyitelstve podvodnykh perekhodov* [Calculation of the stability of the pipeline from floating up during the construction of underwater
2006. 555 c.
17. Бородавкин П.П. Морские нефтегазовые сооружения. Ч. 1. Технология строительства. М.: ООО «Недра-Бизнесцентр», 2007. 408 с.
 18. ВН 39-1.9-005-98. Нормы проектирования и строительства морского газопровода. М.: ОАО «Газпром», 1998. 19 с.
 19. Горяинов Ю.А., Федоров А.С. Морские трубопроводы. М.: ООО «Недра-Бизнесцентр», 2001. 131 с.
 20. Капустин К.Я., Камышев М.А. Строительство морских трубопроводов. М.: Недра, 1982. 207 с.
 21. Патент РФ № 2515584, 10.05.2014. Мустафин Ф.М., Кученко К.В., Файрузов В.М., Шаммазов А.М., Котов М.Ю., Мустафин И.Г., Мамлиев Э.В., Дильмиев И.Н. Способ засыпки уложенного в подводную траншею трубопровода. // Официальный бюллетень Федеральной службы интеллектуальной собственности «Изобретение. Полезные модели». 2014, № 13.
 22. Замрий А.А. Проектирование и расчет конечных элементов трехмерных конструкций в среде APM Structure3D. М.: Издательство АПМ, 2006. 288 с.
 23. Беляев Н.М. Сопротивление материалов. М.: Главная редакция физико-математической литературы изд-ва «Наука», 1976. 608 с.
 24. Айнбinder А. Б. Расчет магистральных и промысловых трубопроводов на прочность и устойчивость. М.: Недра, 1991. 287 с.
 25. Быков Л.И., Мустафин Ф.М., Рафиков С.К., Нечваль А.М., Гамбург И.Ш. Типовые расчеты при проектировании, строительстве и ремонте газонефтепроводов. СПб.: Недра, 2011. 748 с.
 26. Ясин Э.М., Черникин В.И. Устойчивость подземных трубопроводов. М.: Недра, 1968. 120 с.
 27. Мустафин Ф.М., Файрузов В.М., Шестаков И.А. Способ засыпки подводного трубопровода // Транспорт и хранение нефтепродуктов и углеводородного сырья. 2012. № 4. С. 46–47.
 28. Никифоров В.А. Анализ основных методов строительства подводных переходов магистральных трубопроводов // Научное обозрение: теория и практика. 2012. № 3. С. 10–17.
 29. Комаров Д.Н., Короленок В.А. Расчет трубопровода на устойчивость от всплытия при строительстве подводных переходов // Труды Российского государственного университета нефти и газа им. И.М. Губкина. 2010. № 1. С. 79–86.
 30. Исламгалеева Л.Ф. Напряженно-деформированное состояние подводных переходов магистральных газопроводов с учетом изменения степени водонасыщенности грунта на прилегающих подземных участках: диссертация ... кандидата технических наук: 25.00.19 / Исламгалеева Лилия Фаритовна; [Место защиты: Уфим. гос. нефтяной техн. ун-т]. – Уфа, 2013. 179 с.
 31. Филатов А.А. Расчетно-экспериментальные исследования напряженно-деформированного состояния подводных переходов магистральных газопроводов: диссертация ... кандидата технических наук: 25.00.19 / Филатов Александр Анатольевич; [Место защиты: Ин-т проблем трансп. энергоресурсов]. – Москва, 2013. 115 с.
 32. Дудников Ю.В. Научные основы проектирования и обеспечения безопасности сложных участков линейной части магистральных нефтепроводов: диссертация ... доктора технических наук: 25.00.19, 05.26.03 / Дудников Юрий Владимирович; [Место защиты: Институт проблем транспорта энергоресурсов]. – Уфа, 2012. 366 с.
 33. Friedmann Y. Sea-bottom forces crucial in pipeline crossings design // Oil & Gas Journal. 1988. Vol. 86.

Кожаева К.В. Расчет оптимизированных способов засыпки речного подводного трубопровода с использованием APMWinMachine 9.7 // Инженерно-строительный журнал. 2016. № 5(65). С. 42–66.

- crossings]. *Trudy Rossiyskogo gosudarstvennogo universiteta nefti i gaza im. I.M. Gubkina*. 2010. No. 1. Pp. 79–86. (rus)
30. Islamgaleyeva L.F. *Napryazhenno-deformirovannoye sostoyaniye podvodnykh perekhodov magistralnykh gazoprovodov s uchetom izmeneniya stepeni vodonasyshchennosti grunta na prilegayushchikh podzemnykh uchastkakh: dissertatsiya ... kandidata tekhnicheskikh nauk*: 25.00.19 [Stress-strain state of underwater crossings of main gas pipelines, taking into account changes in the degree of soil water saturation on the adjacent underground areas]. Islamgaleyeva Liliya Faritovna; [Mesto zashchity: Ufim. gos. neftyanoy tekhn. un-t]. Ufa, 2013. 179 p. (rus)
31. Filatov A.A. *Raschetno-eksperimentalnyye issledovaniya napryazhenno-deformirovannogo sostoyaniya podvodnykh perekhodov magistralnykh gazoprovodov: dissertatsiya ... kandidata tekhnicheskikh nauk*: 25.00.19 [Calculation-experimental research of stress-strain state of underwater crossings of main gas pipelines]. Filatov Aleksandr Anatolyevich; [Mesto zashchity: In-t problem transp. energoresursov]. Moscow, 2013. 115 p. (rus)
32. Dudnikov Yu.V. *Nauchnyye osnovy proektirovaniya i obespecheniya bezopasnosti slozhnykh uchastkov lineynoy chasti magistralnykh nefteprovodov: dissertatsiya ... doktora tekhnicheskikh nauk*: 25.00.19 [Scientific basis for the design and safety of complex sections of a linear part of main oil pipelines]. Dudnikov Yury Vladimirovich; [Mesto zashchity: Institut problem transporta energoresursov]. Ufa, 2012. 366 p. (rus)
33. Friedmann Y. Sea-bottom forces crucial in pipeline crossings design. *Oil & Gas Journal*. 1988. Vol. 86. No. 26. Pp. 47–50, 52–53.
34. Jones D. Inspection: the key to a reliable future. Part 1. *Pipes and Pipelines Internat*. 1997. Vol. 41. No. 2. Pp. 32–43.
35. Konvisar E. Software to diagnose 'stressed out' pipeline. *Oil & Gas Eurasia*. 2006. Pp. 50–59.
36. Rogers C.D.F. The influence of surrounding soil on flexible pipe performance. *Transportation Research Record*. 1987. No. 1129. Pp. 1–11.
37. Gao X.-F., Liu R., Du Z.-F., Tan Z.-D. Overview of Upheaval Buckling Theoretical Studies for Submarine Buried Pipeline. *Chuan Bo Li Xue / Journal of Ship Mechanics*. 2011. Vol. 15. No. 6. Pp. 678–687.
38. Awoshiku K., Tokano M. Analysis of pipelines subjected to different ground settlement. *Nippon Kokan Technical Report*. 1972. No. 14.
39. Elling R.E. The influence of interface friction and tensile debonding on stresses in buried cylinders // *Transportation Research Record*. 1985. No. 1008. Pp. 72–80.
40. Trautmann C.H., O'Rourke T.D. Lateral force-displacement of buried pipe // *Journal of Geotechnical Engineering*. 1985. Vol. 111. No. 9. Pp. 1077–1092.
41. Trautmann C.H., O'Rourfe T.O. Uplift force-displacement response of buried pipe // *Journal of Geotechnical Engineering*. 1985. Vol. 111. No. 9. Pp. 1061–1076.
42. Webb B.C. Here's an update on pipeline anchoring // *Oil & Gas Journal*. Vol. 81. No. 20. Pp. 79–83.
- No. 26. Pp. 47–50, 52–53.

Ksenia Kozhaeva,
+7(917)4702615; msjealous@mail.ru

Ксения Валерьевна Кожаева,
+7(917)4702615; эл.почта: msjealous@mail.ru

© Kozhaeva K.V., 2016

doi: 10.5862/MCE.65.5

Structural sawn timber: resource enhancement

Увеличение ресурсов конструкционных пиломатериалов для строительных конструкций

V.E. Byzov,

St. Petersburg State University of Architecture and Civil Engineering, St. Petersburg, Russia

V.I. Melekhov,

Northern (Arctic) Federal University named after M.V. Lomonosov, Arkhangelsk, Russia

Канд. техн. наук, доцент В.Е. Бызов,

Санкт-Петербургский государственный архитектурно-строительный университет, Санкт-Петербург, Россия

д-р техн. наук, профессор В.И. Мелехов,

Северный (Арктический) федеральный

университет им. М.В. Ломоносова,

г. Архангельск, Россия

Key words: wood; strength and testing of materials; timber structures; quality control

Ключевые слова: древесина; прочностные характеристики; сердцевинные брусья; совокупный объём сучков; прочностные группы; конструкционные пиломатериалы

Abstract. The strength properties of wood have a great variability within the same species and the same growing region. In this regard, defect parameters do not fully characterize the strength and deformability of structural timber. Deterioration of timber quality requires a more reasonable use of resources and accurate assessment of the strength properties of output timber. To evaluate the strength properties of timber planks and beams produced from small size wood assortment, we have adopted a special parameter called "relative aggregate knot volume at destruction section". This paper introduces the regression models demonstrating the correlation between strength properties of timber planks and aggregate knot volume at destruction section. We also provide recommendations for grading timber planks by strength classes and give a comparative analysis of timber output by grades under applicable national standards and regulations, thus demonstrating the possibility of attracting additional sawn timber resources for production of load-bearing engineering structures.

Аннотация. Прочностные характеристики древесины обладают большой изменчивостью в пределах одной породы и региона произрастания. В связи с этим параметры пороков недостаточно полно характеризуют прочность и деформативность конструкционных пиломатериалов. Ухудшение качества лесоматериалов требует более рационального использования ресурсов и точной оценки прочностных характеристик получаемых пиломатериалов. Для этих целей были проведены исследования, направленные на разработку требований к качеству древесины сердцевинных брусьев, выработанных из тонкомерных пиловочных сортаментов, обеспечивающих заданные прочностные характеристики для различных видов напряженно-деформированного состояния конструкционных пиломатериалов. Для оценки прочностных характеристик брусьев принят показатель «относительный совокупный объем сучков участка разрушения», который определяется как отношение суммы объемов сучков, расположенных на участке бруса длиной, равной ширине бруса, к объему этого участка. Приведены регрессионные модели связи прочностных характеристик брусьев с параметром совокупного объема сучков участка разрушения. Установлены нормативы прочностных сортов брусьев. Разработаны рекомендации по сортировке брусьев на прочностные группы. Сравнительный анализ выходов сортов брусьев по действующему национальному стандарту и разработанным нормативам показывает возможность привлечения дополнительных ресурсов пиломатериалов для изготовления несущих строительных конструкций.

Introduction

Coniferous sawn timber is now widely used in construction, and a considerable part of timber is used for making load-bearing structures. Strength is regarded as the most important feature of sawn timber used for construction of load-bearing structures.

Currently, in the Russian Federation, the strength properties of deflected sawn timber determine its attribution to grades 1, 2 and 3 according to Russian State Standard GOST 8486 "Coniferous sawn timber. Specifications". The requirements for timber of the relevant grade are determined by the presence and size of wood defects, such as knots, cracks, wood structure defects and others. The strength properties of grade 1 according to Russian State Standard GOST 8486 approximately corresponds to C30 strength class according to EN 338, whereas grades 2 and 3 correspond to C24 and C16 strength classes, respectively.

However, due to high variability of strength properties of wood, even within the same species and the same site, the strength of sawn timber and modulus of elasticity may vary considerably within the same grade of timber. At the same time, in practice, the standard values of sawn timber of several grades show little difference. Numerous studies conducted by Russian and foreign scientists [1–4] confirm that the parameters used to determine the strength of timber poorly characterize its strength properties.

Modern wood processing industry now faces more and more acute problem related to deterioration of the size and quality of round timber used for manufacturing sawn structural timber. Reduced cross section of blanks results in irrationally high percentage of wood sawing residue due to inadequate assessment of the strength properties under the existing national standards. Some planks with insufficient strength properties are used to manufacture load-bearing structures, while those, characterized by sufficient strength, are prohibited to use by the existing codes and standards. This is due to the fact that the size of defects used to classify timber and attribute it to a certain grade does not fully characterize its strength properties. The grade of sawn timber is largely determined by the sizes of knots it has.

It is obvious that if strength is evaluated according to the size of knots on the faces and edges of a plank, measured according to traditional methods, the requirements of production are no longer met. Thus, since the existing standards for determining the strength of sawn timber fail to meet the modern requirements for energy conservation and rational use of resources, a new standard should be developed for identifying the strength properties of timber. For this purpose, we have developed a method that increases accuracy in assessment of strength properties of sawn timber.

Adaptation of sawing technology to degraded quality of the source material became a key element in the new standard of sawn timber strength. On the one hand, there is need to increase the strength of those grades of timber which in the current system of standards are classified as nonconforming. Such increase could be achieved by changing the sawing technology. On the other hand, there is a high demand for the standards that would reduce the amount of waste and scrap in the course of production. Similar issues were raised in Gradewood project [5], though one of its main objectives was to analyze the old and new destructive tests of the quality of structural wood products. This article is an attempt to prove the existence of correlation between strength properties and appearance of sawn timber, and thus make it possible to develop new standards for non-destructive tests for wood products grading.

Sawing into heartwood beams for increased strength of sawn timber

As it is known, the main type of the deflected mode to which the elements of load-bearing structures are exposed, is lateral bending. In the majority of cases, the cross-section of sawn timber has a wide side, called the "face" and a narrow one, called the "edge". The deflected mode strength of the loaded edge has been considered traditionally as the measure of strength. In order to increase the deflection strength of the elements within a structure, they are arranged in a way that allows them to be exposed to load on the edge [6].

According to the results of research [7], the structure of wood in the trunk of a growing tree, owing to ring-type cross-section of its annual layers, enhances its strength against the bending moment of wind load. In addition, the strength is increased due to the nature of the layered structure of wood, i.e. early wood and latewood alter within the annual layer and thus a capability of additional deflection is created. Additional deflection is possible due to shifts in weak layers of early wood when the trunk is subjected to lateral force.

Increased deflection reduces the bending moment, in particular, under wind loads [8]. These features of the natural structure of the tree trunk should be applied in the manufacture of elements in supporting and load-bearing structures. Thus, it is very important that the maximum number of uncut annual layers is preserved within the timber. For more accurate quantitative and qualitative assessment of relationship between wood structure and strength properties thereof, it seems reasonable to formulate

the objective of the research, which is to examine the wood structure at macro level as a closed system of shells.

Round wood assortment, which is used to produce structural sawn timber, may be schematically represented as a system of thin-walled shells coaxially threaded one over the other to simulate the pattern of annual rings of wood [9]. The core is located in the central part of the assortment cross section. Structural sawn timber of large cross sections made from round assortment retains the ring structure of annual layers of wood to the fullest extent (Figure 1).

Sawn timber of large cross section obtained from small diameter round timber consists of a core and retains the maximum macrostructure of a growing tree trunk, which is a natural structural material with increased strength properties. These are so-called heartwood beams. Thus, the use of square beams made of heartwood allows for expansion of sawn timber resources for the production of load-bearing structures.

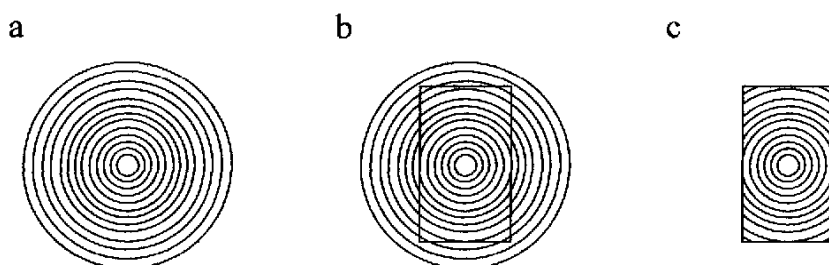


Figure 1. The structure of heartwood sawn timber:
a – roundwood assortment; b – cutting plan for the roundwood assortment;
c – cross section of a heartwood timber plank

Methods

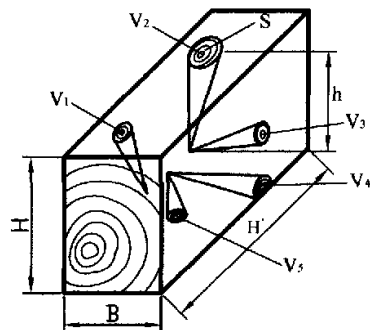
It should be noted that the quantitative evaluation of mechanical characteristics of heartwood timber is still insufficiently studied and not defined. Direct determination of strength parameters is associated with destruction of sawn timber and that does not meet the requirements for resource conservation. In order to reduce the percentage of waste and scrap in production of timber, it is advisable to carry out non-destructive strength testing. To improve the reliability of strength test for timber produced from small saw logs given their macrostructure, it is necessary to define evidence-based criteria for finding out the most relevant parameters and carry out their standardization for assessment of the strength of the sawn timber.

The basis for development of this method is represented by the studies of the relationship between the strength of sawn timber and the parameters determined without destruction of sawn timber, i.e. the so-called indirect parameters of strength. The indirect parameters can only be those present in all samples of sawn timber that undergo strength assessment. These parameters are biological properties of wood, i.e. defects and above all, knots [10–14].

In accordance with that, the task was to change the approach to the assessment of timber strength based on a method of differentiation of defect standards. The defect standards should take into account the deflected mode of timber in load-bearing engineering structures. Increase of reliability of visual assessment of strength properties of timber implies substantiation of efficiency of the new and most significant indirect grading parameter of strength.

As a result of tests aimed at assessment of strength properties of timber, the aggregate knot volume at destruction section was adopted as the key parameter, which is defined as the ratio of total volume of knots located within the section with the length equal to the width of the plank to the volume of this section [15] (Figure 2). This parameter reflects, in the best way, the reduction in strength due to the presence of knots in heartwood. Foreign companies are familiar with the use of standards for visual grading of sawn timber according to the parameters of knots. In particular, the UK applies BS 4978:2007 + A1:2011 "Visual strength grading of softwood. Specification". This standard specifies the requirements for two grades of visual grading of softwood timber, namely general structural grade (GS) and special structural grade (SS). Grading of sawn timber is performed in accordance with the KAR and MKAR standard parameters of knots. The KAR (knot area ratio) is the ratio of knot projections area of a sawn timber section to the area of their cross section. The MKAR (margin knot area ratio) is the ratio of the area of knot projections, present in the margin zone, to the margin zone area of sawn timber. In order

to improve the rules for softwood grading, the European standard EN 1912-2012 "Structural timber. Strength classes. Assignment of visual grades and species" came into force in 2012.



$$V_{agr} = (V_1 + V_2 + V_3 + \dots + V_n) / B * H * H'$$

Figure 2. The aggregate knot volume at destruction section:

V_{agr} – aggregate knot volume at destruction section;

V_1, V_2, \dots, V_n – knot volumes at destruction section; S – knot section area; h – knot height;

B – sawn timber width; H – sawn timber height; H' – destruction section length

Results and Discussion

We have carried out comprehensive research in order to develop quality requirements for heartwood timber and provide the desired strength properties for different types of deflected mode. We have obtained quantitative assessments of the strength properties of softwood timber through testing the samples of timber planks for bending load on the edge and compression along the grain. The test samples of timber were obtained from logs harvested in the forests of the Northern European part of Russia.

According to the results of the sawn timber certification, the values of the relative aggregate knot volume in destruction sections were identified, and tests were conducted to determine the strength properties of sawn timber. The cross-sectional dimensions of the samples tested for bending load on the edge and compression along the grain were 100 x 150 mm. These dimensions were chosen in accordance with Russian State Standard GOST 24454, which determines the sizes of construction materials.

The depth of the samples used in deflection tests was 150 mm. Their length was 20 times the depth, i.e. 3000 mm. We used 4-point bending, as in EN 408. The beam span was 18 times the depth. The span between the points of loading was 6 times the depth, i.e. 900 mm. The sample tested was symmetrically loaded at two points over the span (Figure 3). The tests were performed on a hydraulic testing machine R-20 with the use of a special device ensuring the necessary loading regime.

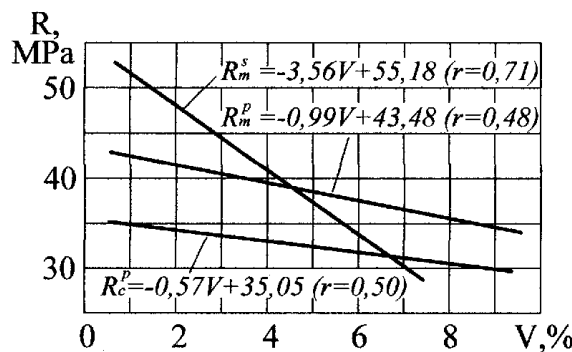
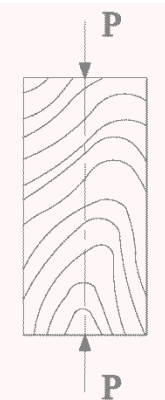


Figure 3. Bending test

The length of the samples used in compression tests was 400 mm, not 6 times the smaller cross-sectional dimension, as in EN 408. The specimen was loaded along the axis by using spherically sealed loading heads, ensuring application of the compressive load without inducing bending (Figure 4). The tests were performed using hydraulic press with the accuracy of $\pm 2\%$ of the applied load.

**Figure 4. Compression test**

We obtained data on a totality of distributions of ultimate strength parameters for beams for the cases involving bending through loading the edge and compression along the grain, as well as distribution of values for the relative aggregate knot volume at destruction sections. The conformance test aimed to check the empirical distributions against the general distribution law confirmed that there is possibility for approximation of experimental distributions in relation to this theoretical law. Table 1 shows the results of the statistical analysis of strength parameters and aggregate knot volume parameters.

Table 1. Statistical parameters of distribution

Type of stress-strain state	Species	Parameters ¹⁾	Number of specimens tested	Statistics ²⁾ of empirical distribution			
				\bar{X}	σ_x	$X_{0.95}$	ω^2
Bending through loading the edge	spruce	R , MPa	54	45.8	8.8	31.3	0.27
Bending through loading the edge	pine	R , MPa	52	35.9	9.5	20.2	0.36
Compression along the grain	pine	R , MPa	42	31.7	4.9	23.6	0.91
Bending through loading the edge	spruce	V , %	54	2.7	1.7	—	0.81
Bending through loading the edge	pine	V , %	52	7.6	4.8	—	1.04
Compression along the grain	pine	V , %	42	7.1	4.7	—	0.49

Note:

¹⁾Parameters:

R – ultimate stress;

V – aggregate knot volume in the destruction section.

²⁾Statistics:

\bar{X} – arithmetical average (mean);

σ_x – root-mean-square deviation;

$X_{0.95}$ – permissible limit (lower tolerable) with probability of 0.95;

ω^2 – test for concordance of experimental distribution with theoretical distribution law (if $\omega^2 \leq 1.94$, then the hypothesis of concordance is adopted with significance value of 0.1).

b – regression equation ratio;

a – absolute term of regression equation;

r – correlation coefficient;

S_{yx} – standard error of estimation.

The table clearly shows the point estimations of distribution of ultimate strength values and relative aggregate knot volume in the destruction sections, which were determined by a test involving bending

through loading the edges of test samples made of spruce and pine, as well as compression along the grain of pinewood samples.

In order to carry out non-destructive testing of timber strength parameters, it is necessary to establish standards for an indirect strength parameter, which allows predicting the strength of the material without its destruction. In order to find the standards for aggregate knot volume, which correspond to the given strength properties of heartwood, regression analysis of the relationship of the ultimate strength parameter to the aggregate knot volume parameter was conducted in accordance with the existing methods [16].

The parameters of regression equations of coupling ultimate strength with the parameters of relative aggregate knot volume in the destruction section in deflected modes of bending through loading the edge and of compression along the grain are shown in Table 2.

Table 2. The parameters of regression equations

Type of stress-strain state	Species	Regression parameters			
		b	a	r	S _{jx}
Bending through loading the edge	spruce	-3.565	55.182	0.707	5.843
Bending through loading the edge	pine	-0.988	43.480	0.485	7.889
Compression along the grain	pine	-0.574	35.051	0.496	4.468

The analysis of regression models of coupling the ultimate strength with the parameters of aggregate knot volume in the destruction sections allowed us to establish quantitative relationship, which became the basis for calculating the standards for the aggregate volume of knots, which maintain the given level of strength in deflected modes of bending through loading the edge and compression along the grain. On the basis of these standards, the regulations were developed to test the strength of timber in building structures, and a system of characteristic strength of timber was also adopted for production of components for load-bearing structures exposed to different types of deflected mode. We managed to calculate the characteristic values of the aggregate volume of knots, which provide for the strength of timber with sufficient reliability.

The regression models of coupling strength properties were established for spruce and pine timber under bending through loading the edge and compression along the grain of pinewood with aggregate knot volume parameter (Figure 5).

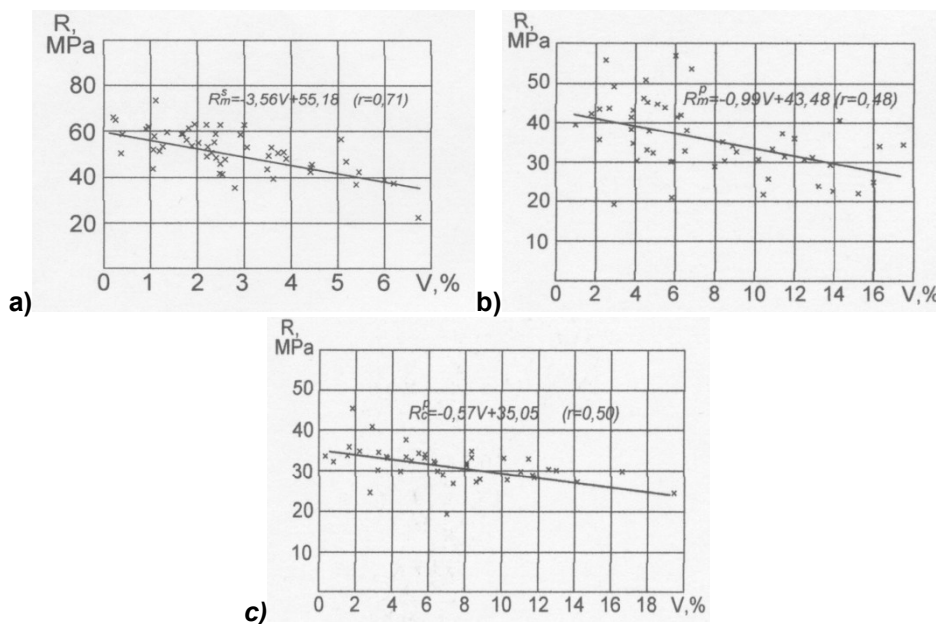


Figure 5. Regression models of coupling ultimate strength properties of samples with aggregate knot volume parameters:

**a – bending through loading the edge (spruce); b – bending through loading the edge (pine);
c – compression along the grain (pine)**

New standard for determination of strength properties

When developing the guidelines for testing the strength parameter, the following conditions were met:

1. parameters of strength of beam grades;
2. practical solutions for strength testing;
3. beams output for various classes of strength.

The first condition implies that the strength parameters of timber corresponding to different types of deflected mode and strength grades must be linked to each other [17–19]. In addition, they must meet the actual needs for the production of components for load-bearing structures. The second condition implies cost efficiency and the need for adequate reliability of timber strength assessment. The third condition suggests that the need for production of timber of various grades of strength in terms of quantity should correspond to the production potential. There are various gradations of sawn timber strength [20, 21].

We adopted the following standards of grading the strength of sawn timber exposed to bending through edge loading and compression along the grain, i.e. 30, 24 and 15 MPa. These strength grades were identified, respectively, as 1K, 2K and 3K. The test limits for ultimate strength for grades of sawn timber, as well as the limits of parameters of aggregate knot volume for strength grades that ensure the above-mentioned ultimate strength, were identified. Test limits for separation of sawn timber by grades were set using the method proposed by V.V. Ogurtsov, which provides for dependencies for separating the sawn timber by strength grades with the necessary level of probability [22]. This method is used, because it allows determining the standards for other parameters of mechanical properties, e.g. compression of timber along the grain with the necessary level of probability upon finding the standard for the most important parameter of mechanical properties, such as the ultimate strength under bending on the edge.

In order to test the requirements elaborated for forecasting the strength properties of timber according to the aggregate knot volume parameters, we carried out tests involving a frame with parallel belts and a triangular lattice of beams graded by the relevant strength grades of 1K, 2K and 3K. The span of the frame was 18 m, the height – 2.25 m. The design load $Q = 17.2$ kN with the step of 6 m. The tests were based on the worst possible loading scenario. In calculation of the frame strength, which was made based on the traditional technology, we established that the frame can sustain the total load of 310 kN. Destruction of the frame made of heartwood graded by strength grades occurred under the total load of 640 kN. The safety factor of the frame equaled 2.0.

Classification of knots for visual evaluation of strength properties at production site

Since at present there is lack of automated equipment allowing evaluating the aggregate size of knots, calculations were made based on the dependence of the sizes of knots on the faces and edges of heartwood timber from the aggregate volume of knots. All knots are divided into three categories, including edge knots, margin knots and axial knots (the used terminology as proposed by the author) (Figure 6). The edge knots appear on the edge of beams, whereas the margin knots appear on the face of a beam at a distance not exceeding two thirds of the diameter of the knot from the beam arise. The remaining knots on the face of a beam are axial knots. The size of the edge knot is defined as the distance between the tangents of the knot boundary, which are drawn in parallel to the beam arise. The size of a margin knot is determined by its smaller diameter. The size of a arise knot is determined by the smallest diameter or in the same way as the size of an edge knot is defined. The size of an axial knot is defined as arithmetical average (mean) between its largest and smallest diameters on the face of the beam. The allowable sizes are defined for edge, margin and axial knots and for knots present on the radial axis of the plank, provided that the proposed standard parameter of the relative aggregate size of knots per each strength grade is followed. The values of visually determined allowable sizes of knots are provided in Table 3.

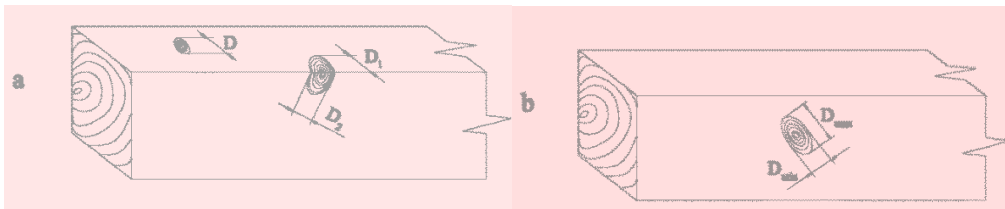


Figure 6. Classification and measurement of knots in the timber:
a – including edge knots and margin knots; b – axial knots;
D, D₁, D₂ – the size of knots on the face side and edges of the boards;
D_{max}, D_{min} – the maximum and minimum diameters of knots

Table 3. Visually allowable knot sizes for strength grades

Name of species	Strength grade	Knot sizes in ratio to side width		
		edge	margin	axial
Spruce	1K	1/3	1/5	1/5
Pine	1K	1/3	1/6	1/6
	2K	1/2	1/3	1/3

Comparison with the current standard

The comparative analysis of timber yield as per grades according to Russian State Standard GOST 8486 and upon grading by aggregate knot volume parameter (see Table 4) has shown that the yield of timber from heartwood graded in accordance with the developed standards and characterized by similar strength parameters, is greater.

The comparative analysis of timber yield as per grades under Russian State Standard GOST 8486 and strength grades has shown that the strength of all the types of spruce timber graded in accordance with the developed standards with the probability value of 0.95 makes up no less than 30 MPa under bending through edge loading. At the same time, only 37 % of spruce timber volume meets the requirements of grade 1 as per Russian State Standard GOST 8486. The characteristic strength of timber planks for grade 1 equals 26 MPa.

Table 4. Comparative analysis of timber yield

Grading method	Wood species	Grade	Strength value, MPa	Yield, %
GOST	spruce	1	26	37
		2	24	26
		3	16	33
		“natural pruning”		4
		1K	30	100
Aggregate knot volume	pine	2	24	40
		3	16	38
		“natural pruning”		22
		2K	24	83
		3K	15	17

83 % of pinewood timber corresponds to 2K strength grade with characteristic strength under bending through loading on the edge with 24 MPa. 40 % of pinewood timber meets the requirements of grade 2 as per GOST 8486. Thus, in comparison with Russian State Standard GOST 8486, the output of timber with similar strength values is much greater when graded by the aggregate knot volume parameter.

100 % of spruce timber has strength of no less than 30 MPa, when graded by the aggregate knot volume parameter, whereas 83 % of pinewood timber has strength of no less than 24 MPa. When graded by Russian State Standard GOST 8486, the output of grade 2 timber planks, with strength under bending

through loading on the edge of no less than 24 MPa, equals 63 % for spruce timber and 40 % for pinewood.

Conclusions

1. Theoretical and empirical data demonstrate that visual grading may ensure the predetermined characteristic strength of beams with required confidential probability.
2. When grading according to the substantiated standards of aggregate knot volume with account to the deflected mode of beams in load-bearing structures, the accuracy of beam strength assessment is higher than when timber grading is based on the current standard.
3. Distribution of strength properties of beams graded in accordance with the developed standards qualitatively outperforms the distribution of strength properties graded under GOST 8486. This allows us to use shaped timber elements with a small cross section produced from small logs in construction, use additional raw material resources, and contribute to solving the problems related to resource conservation.
4. Higher values of characteristic strength of timber allow compensating the decrease in load-bearing capacity resulting from the decreased cross section of load-bearing structure components due to the lack of saw log of the desired diameter.
5. The flat framing structure made from beams, which strength is evaluated pursuant to the developed standards, is characterized by increased structural stiffness and a double standard strength reserve.
6. If the developed requirements are included into the standards of timber grading, additional timber can be allocated for production of load-bearing engineering structures.
7. The technology of structural timber production technology will be simplified due to production of sawn timber for specific purposes.

References

1. Borovikov A.M. *Kachestvo pilomaterialov* [Quality of sawn timber]. Moscow: Lesnaya promyshlennost, 1990. 256 p. (rus)
2. Savkov Ye.I. *Prochnost pilomaterialov* [Strength of sawn timber]. Moscow: Goslesbumizdat, 1962. 88 p. (rus)
3. Miller D.G. Selective efficiencies of nondestructive strength test. *Forest Products Journal*. 1962. Vol.5. No.8: Pp. 87–92.
4. Dean M.A., Kaiserlik Y.H. Nondestructive screening of hardwood specialty blanks. *Forest Products Journal*. 1984. Vol. 34. No. 3. Pp. 51–56.
5. VVT Technical Research Centre of Finland Ltd. *Grading of timber for engineered wood products* (Gradewood). Final report. 2006. 34 p.
6. Ugolev B.N. Wood as natural smart material. *Wood Science and Technology*. 2014. Vol. 48. No. 3. Pp. 553–568.
7. Ylinen A. *Über den mechanische Schaffformtheorie der Bäume*. Techn. Hochschule in Finnland, Wiss. Forschungen. Helsinki, 1952. 51 p.
8. Ashkenazi Ye.K. *Anizotropiya drevesiny i drevesnykh materialov* [Anisotropy of timber and timber-based materials]. Moskow: Lesnaya promyshlennost, 1978. 224 p. (rus)
9. Melekhov V.I., Byzov V.Ye. Rasshireniye resursov pilomaterialov dlya nesushchikh stroitelnykh konstruktsiy [The expansion of resources for load-bearing structures]. *Izvestiya Sankt-Peterburgskoy lesotekhnicheskoy akademii*. 2015. No. 213. Pp. 204–211. (rus)
10. Miller D.G. Effect of Tolerance on Selection Efficiency of Wood. *Forest Products Journal*. 1964. No. 4(14). Pp. 179–183.
11. Karel'skiy A.V., Zhuravleva T.P., Labudin B.V. Ispytaniye na izgib derevyanых sostavnnykh balok, soyedinenyykh metallicheskimi zubchatymi plastinami, razrushayushchey nagruzkoj [Load-to-failure test of wood composite beams connected by gang nail]. *Magazine of Civil Engineering*. 2015. No. 2(54). Pp. 125–127. (rus)
12. Neklyudova Ye.A., Semenov A.S., Melnikov B.Ye., Semenov S.G. Eksperimentalnye issledovaniya i analiz

Литература

1. Боровиков А.М. Качество пиломатериалов. М.: Лесная промышленность, 1990. 256 с.
2. Савков Е.И. Прочность пиломатериалов. М.: Гослесбумиздат, 1962. 88с.
3. Miller D.G. Selective Efficiencies of Nondestructive Strength Test // Forest Products Journal. 1962. Vol. 5. № 8. Pp. 87–92.
4. Dean M.A., Kaiserlik Y.H. Nondestructive Screening of Hardwood Specialty Blanks // Forest Products Journal. 1984. Vol. 34. № 3. Pp. 51–56.
5. VVT Technical Research Centre of Finland Ltd. Grading of timber for engineered wood products (Gradewood). Final report. 2006. 34 p.
6. Ugolev B.N. Wood as natural smart material // Wood science and technology. 2014. Vol. 48. № 3. Pp. 553–568.
7. Ylinen A. Über den mechanische Schaffformtheorie der Bäume. Techn. Hochschule in Finnland, Wiss. Forschungen. Helsinki, 1952. 51 p.
8. Ашкенази Е.К. Анизотропия древесины и древесных материалов. М.: Лесная промышленность, 1978. 224 с.
9. Мелехов В.И., Бызов В.Е. Расширение ресурсов пиломатериалов для несущих строительных конструкций // Известия Санкт-Петербургской лесотехнической академии. 2015. № 213. С. 204–211.
10. Miller D.G. Effect of Tolerance on Selection Efficiency of Wood // Forest Products Journal. 1964. № 4(14). Pp. 179–183.
11. Карельский А.В., Журавлева Т.П., Лабудин Б.В. Испытание на изгиб деревянных составных балок, соединенных металлическими зубчатыми пластинами, разрушающей нагрузкой // Инженерно-строительный журнал. 2015. № 2(54). С. 77–127.
12. Неклюдова Е.А., Семёнов А.С., Мельников Б.Е., Семёнов С.Г. Экспериментальные исследования и анализ методом конечных элементов прочностных и упругих характеристик композитного материала из стеклопластика // Инженерно-строительный журнал. 2014. № 3(47). С. 25–39.

Бызов В.Е., Мелехов В.И. Увеличение ресурсов конструкционных пиломатериалов для строительных конструкций // Инженерно-строительный журнал. 2016. № 5(65). С. 67–76.

- metodom konechnykh elementov prochnostnykh i uprugikh kharakteristik kompozitnogo materiala iz stekloplastika [Experimental research and finite element analysis of elastic and strength properties of fibreglass composite material]. *Magazine of Civil Engineering*. 2014. No. 3(47). Pp. 25–39. (rus)
13. Chubinskii A.N. Phisical Nondestructive Methods for linkthe Testing and Evalustion of the Structure of Wood Based Materials [Phisical Nondestructive Metods for linkhe Testing and Evalustion of the Structure of Wood Based Materials]. *Russian Journal of Nondestructive Testing*. 2014. No. 11. Pp. 693–700. (rus)
 14. Wei Q., Leblon B., La Rocque A. On the use of X-ray computed tomography for determining wood properties: a review. *Canadian Journal of Forest Research*. 2011. No. 41. Pp. 2120–2140.
 15. Tambi A.A. Prognozirovaniye prochnostnykh kharakteristik pilomaterialov [Prediction of the strength characteristics of lumber]. *Materialy nauchno-prakticheskoy konferentsii (Sovremennyye problemy pererabotki drevesiny)* [Materials of scientific-practical conference (Modern problems of wood processing)]. Saint-Petersburg.: Izd-vo Politekhn. un-ta, 2013. Pp. 40–45. (rus)
 16. Melekhov V.I., Byzov V.Ye. Vliyanije serdtsevinnykh vklucheniij na prochnostnye kharakteristiki konstruktionsionnykh pilomaterialov [Influence of pith inclusions on strength properties of structural timber]. *Construction materials*. 2010. No. 12. Pp. 80–81. (rus)
 17. Kendall M.G. *Rank correlation methods*. 4th ed. Griffin. London, 1975.
 18. Piao C., Groom L. Residual strength and stiffness of lumber from decommisioned chromate copper arsenate-treated southern pine utility poles. *Forest Products Journal*. 2010. Vol. 60. No. 2. Pp. 166–172.
 19. Horvath B., Peszen I., Perolta P., Horvath L., Kasal B., Li L. Elastic modulus determination of transgenic aspen using a dynamic mechanical analyzer in static bending mode // *Forest Products Journal*. 2010. Vol.60. No. 3. Pp. 296–300.
 20. Chauzov K.V., Koltunova T.V., Tambi A.A. K voprosu o soroobrazovanii pilomaterialov na osnove trebovaniy, predyavlyayemykh k konechnoy produktii [To the question of sortable lumber on the basis of the requirements for the final product]. *Sbornik nauchnykh trudov III Mezhdunarozhnoy nauchno-tehnicheskoy konferentsii (Aktualnye problemy i perspektivy razvitiya lesopromyshlennogo kompleksa)* [Collection of scientific proceedings of the 3 international scientific-technical conference (Actual problems and prospects of development of timber industrial complex)]. Kostroma: KGTU, 2015. Pp. 40–42. (rus)
 21. Rykunin S.N., Vladimirova Ye.G. Sortirovaniye pilomaterialov na gruppy kachestva [Sawn timber grading on quality groups]. *Lesnoy vestnik*. 2012. No. 3. Pp. 89–91. (rus)
 22. Ogurtsov V.V. Printsipy opredeleniya dopuskov pri avtomaticheskoy sortirovke pilomaterialov po mekhanicheskim svoystvam [Principles of determination of tolerance for automatic grading of sawn timber according to its mechanical properties]. *Forestry magazine*. 1980. No. 1. Pp. 98–102.(rus)

Viktor Byzov,
+7(981)1220539; mapana@inbox.ru

Vladimir Melekhov,
88182216149; lti@narfu.ru

Виктор Евгеньевич Бызов,
+7(981)1220539; эл. почта: mapana@inbox.ru

Владимир Иванович Мелехов,
88182216149; эл. почта: lti@narfu.ru

© Byzov V.E., Melekhov V.I., 2016



ПОЛИТЕХ

Санкт-Петербургский
политехнический университет
Петра Великого

Инженерно-строительный институт

Центр дополнительных профессиональных программ

195251, г. Санкт-Петербург, Политехническая ул., 29,
тел/факс: 552-94-60, www.stroikursi.spbstu.ru,
stroikursi@mail.ru

Приглашает специалистов проектных и строительных организаций,
не имеющих базового профильного высшего образования
на курсы профессиональной переподготовки (от 500 часов)
по направлению «Строительство» по программам:

П-01 «Промышленное и гражданское строительство»

Программа включает учебные разделы:

- Основы строительного дела
- Инженерное оборудование зданий и сооружений
- Технология и контроль качества строительства
- Основы проектирования зданий и сооружений
- Автоматизация проектных работ с использованием AutoCAD
- Автоматизация сметного дела в строительстве
- Управление строительной организацией
- Управление инвестиционно-строительными проектами. Выполнение функций технического заказчика

П-02 «Экономика и управление в строительстве»

Программа включает учебные разделы:

- Основы строительного дела
- Инженерное оборудование зданий и сооружений
- Технология и контроль качества строительства
- Управление инвестиционно-строительными проектами. Выполнение функций технического заказчика и генерального подрядчика
- Управление строительной организацией
- Экономика и ценообразование в строительстве
- Управление строительной организацией
- Организация, управление и планирование в строительстве
- Автоматизация сметного дела в строительстве

П-03 «Инженерные системы зданий и сооружений»

Программа включает учебные разделы:

- Основы механики жидкости и газа
- Инженерное оборудование зданий и сооружений
- Проектирование, монтаж и эксплуатация систем вентиляции и кондиционирования
- Проектирование, монтаж и эксплуатация систем отопления и теплоснабжения
- Проектирование, монтаж и эксплуатация систем водоснабжения и водоотведения
- Автоматизация проектных работ с использованием AutoCAD
- Электроснабжение и электрооборудование объектов

П-04 «Проектирование и конструирование зданий и сооружений»

Программа включает учебные разделы:

- Основы сопротивления материалов и механики стержневых систем
- Проектирование и расчет оснований и фундаментов зданий и сооружений
- Проектирование и расчет железобетонных конструкций
- Проектирование и расчет металлических конструкций
- Проектирование зданий и сооружений с использованием AutoCAD
- Расчет строительных конструкций с использованием SCAD Office

П-05 «Контроль качества строительства»

Программа включает учебные разделы:

- Основы строительного дела
- Инженерное оборудование зданий и сооружений
- Технология и контроль качества строительства
- Проектирование и расчет железобетонных конструкций
- Проектирование и расчет металлических конструкций
- Обследование строительных конструкций зданий и сооружений
- Выполнение функций технического заказчика и генерального подрядчика

По окончании курса слушателю выдается диплом о профессиональной переподготовке установленного образца, дающий право на ведение профессиональной деятельности

